(97)

Genetic and molecular analysis of *C. elegans* vulval invagination

by Tory Herman

A.B. Music, Harvard-Radcliffe College 1989

Submitted to the Department of Biology in partial fulfillment of the requirements for the degree of Doctor of Philosophy at the Massachusetts Institute of Technology

February 1998

Signature of author: _____

Department of Biology
February 1998

Certified by: _____

H. Robert Horvitz
Professor of Biology
Thesis Supervisor

Accepted by: _____

Frank Solomon
Chairman of the Graduate Committee, Department of Biology

Genetic and Molecular Analysis of *C.elegans* Vulval Invagination

Tory Herman

ABSTRACT

Epithelial invagination is a fundamental component of gastrulation, neurulation, and many other examples of organogenesis. To identify molecules involved in this process, we have analyzed the invagination of the *C. elegans* hermaphrodite vulva, a tube that connects the outer epithelium to the uterine epithelium. We screened for and isolated 25 mutations that perturb vulval invagination and found that they define eight genes, which we have named *sqv-1* to *8* (squashed vulva). Mutations in these genes appear to cause identical vulval defects: a partial collapse of the invagination and elongation of the central invaginating cells. All but the weakest mutations also cause hermaphrodite sterility, implicating the *sqv* genes in additional developmental events. We have molecularly analyzed *sqv-3*, *sqv-7*, and *sqv-8*. The predicted SQV-3 protein is similar to members of a glycosyltransferase family consisting of vertebrate β(1,4)-galactosyltransferases, which add galactose (Gal) to N-acetylglucosamine (GlcNAc), and an invertebrate β(1,4)-N-acetylglucosaminyltransferase, which adds GlcNAc to GlcNAc. SQV-8 is similar to a β(1,3)-glucuronyltransferase, which adds glucuronic acid (GlcA) to Gal-β(1,4)-GlcNAc and hence may use a SQV-3 product as a substrate. SQV-7 is similar to members of a family of nucleotide-sugar transporters. The *sqv* genes are therefore likely to encode components of a conserved glycosylation pathway that assembles a *C. elegans* carbohydrate moiety the absence of which perturbs vulval invagination.

Thesis Supervisor: H. Robert Horvitz
Title: Professor of Biology

Acknowledgments

I would like to thank Bob Horvitz for the training and fun I've had for the past seven years and for the fun I anticipate having in Larry Zipursky's lab. I would also like to thank the members of my thesis committee for their help and Saechin Kim for encouraging me to do a mutant hunt, Michael Koelle for teaching me molecular biology and for introducing me to Pearl Jam, Nirvana, the Rustavi Choir, and Manitas de Plata, Mark Metzstein and Gillian Stanfield for xeroxing the NY Times crossword puzzles for me, Ho-Yon Hwang for his photographs both of humans and of a certain cactus, Na An for tirelessly cooking me sticky rice cakes, Erika Hartwieg for her critical eye and invaluable saliva, Beth James for her cheerful and professional dissection of G's, A's, T's, and C's, and Nancy Tsung for naming me honorary piglet. I must also thank Sumati Murli for sharing massaman curry, the best tape of Indian movie music ever, a love of movies not called "Orlando," and her calming influence in times of crisis. And finally, I would like to thank Allison MacKay, idol and friend, Lisa Stifelman for sharing the experience of moving from left to center, Cynara Wu for worshipping Tara Mounsey as much as I do, Christina Gehrke for teaching me her moves, and Katia Pashkevitch for her wisdom and beauty on and off the ice. Oh, and my parents, sister, and grandparents too.

Table of Contents

Chapter one

Introduction and overview

Properties of epithelia

Epithelia in their simplest form are single layers of cells bound laterally to one another by means of specialized junctions. These layers are polarized, with the basal side secreting and adhering to a basal lamina and the apical side often facing a lumen or the outside environment. Because of these characteristics, epithelia perform important barrier and structural functions in developing and mature animals (reviewed by Eaton and Simons, 1995; Davies and Garrod, 1997). Animals are surrounded by an outer epithelium, which chemically and mechanically separates their internal and external environments. In addition, epithelia create barriers between internal tissues, preventing inappropriate interactions and also providing structural support. One important way in which epithelia create structure is by surrounding and thereby maintaining lumenal spaces, such as the hollow tubes of circulatory systems (e.g. blood vessels), respiratory systems (e.g. tracheae, lungs), digestive and excretory systems (e.g. digestive tracts, kidneys), and reproductive systems (e.g. uteri, passages through which eggs or sperm are released), as well as the primordial lumina of some sensory organs such as the vertebrate eye and ear. To achieve these complex structures, epithelia undergo major changes in topology during development (Bard, 1990; Gumbiner, 1992; Gumbiner, 1996; Fristrom, 1988). Sheets of epithelial cells fold inward (invaginate) or outward (evaginate), spread uniformly or extend in a particular direction, move relative to underlying tissues, and break and make connections with one another. Such topological changes in an epithelium require coordinated changes in the individual cells within it, whether in their shape, rigidity, cell-cell contacts, cell-matrix contacts, or other parameters. We have been begun a genetic and molecular analysis of an example of this process, the invagination of the hermaphrodite vulva in the nematode *Caenorhabditis elegans.*

***C. elegans* vulval development**

C. elegans is surrounded by an outer epithelium that consists of a single layer of cells connected to one another by desmosomes (White, 1988). The basal side of this layer lies along a basal lamina, and the apical side faces outward and secretes a protective cuticle. The adult vulva is an epithelial tube that connects the uterine and outer epithelia and allows the adult hermaphrodite to release eggs from its uterus into the external environment and to receive sperm from males (Sulston and Horvitz, 1977). The vulva is formed from the descendants of three cells, P5.p, P6.p, and P7.p, which, during the third larval (L3) stage, lie along the ventral side of

the hermaphrodite in a sheet with and connected by desmosomes to the rest of the outer epithelium (Appendix 1, Figure 1) . In this region the basal lamina of the outer epithelium is adjacent to cells of the developing uterus, including the anchor cell. During the second half of the L3 stage the anchor cell signals P5.p, P6.p, and P7.p to undergo two rounds of division (Sulston and Horvitz, 1977). Genes required for the specification, timing, execution, and precise pattern of these divisions have been extensively analyzed; the anchor cell signals the vulval precursors by means of an EGF/Ras pathway (reviewed by Horvitz and Sternberg, 1991).

During the final round of cell divisions, the central subset of descendants detaches from the cuticle, allowing this region of the epithelium to bend inward and the cells within it to rearrange their cell-cell contacts (Chapter 2, Figure 3; Appendix 1, Figure 1 (see Chapter 1, Figure 1 legend for a correction of the latter); and Chapter 1, Figure 1). Because invagination can take place in the absence of other cells in the region (see Appendix 1 for a brief discussion), it is likely to be an intrinsic property of the epithelial cells themselves or of their extracellular matrix. The vulval invagination increases in dorsal-ventral height as the anterior vulval cells move posteriorly and the posterior vulval cells move anteriorly: the bunching of cells results in their gradual dorsal displacement as vulval cell-cell contacts are reorganized and the cells are in effect stacked one on top of another. A series of vulval cell fusions takes place, culminating by the late L4 stage in a stack of seven syncytial toroids. This invagination process can be observed in part by Nomarski DIC microscopy (e.g., Chapter 2, Figure 3), but the boundaries between cells, and hence their precise shapes, contacts, and fusions are not visible by these means. John White has analyzed vulval invagination by electron microscopy, and Benjamin Podbilewicz has done the same by MH27 antibody staining of the desmosomal connections between the vulval cells, but neither of these studies has been published (the source of the error in the description of vulval development in Appendix 1). Figure 1 of this chapter is based on a schematic drawing by B. Podbilewicz (pers. comm., Worm Breeder's Gazette, October 1997) of the desmosomal connections between vulval cells during the late L3 and early L4 stages, as viewed either from the dorsal (top) or ventral (bottom) side (this was not made explicit in his drawing). This diagram therefore shows some of the changes in vulval cell shapes and contacts and the order in which vulval cell fusion occurs.

In this thesis are described the results of a genetic screen for mutants having abnormal vulval invaginations (Chapter 2). Three of the eight genes so identified were molecularly analyzed and are predicted to encode proteins with sequence

similarities to proteins involved in protein and lipid glycosylation (Chapter 3). This work therefore draws together two topics in biology that remain somewhat mysterious: the cellular and molecular mechanisms by which epithelia undergo complex topological changes (for a brief review of epithelial invagination see Appendix 1) and the precise roles of the many and varied carbohydrates that modify components of the cell surface and extracellular matrix.

Possible roles of glycosylation in epithelial morphogenesis

Carbohydrates perform important nutritional and structural functions in all organisms. When covalently linked to protein or lipid they can also affect or directly mediate such functions as intracellular trafficking, protein folding and stability, extracellular matrix (ECM) organization and properties, as well as cell-cell and cell-matrix signaling, recognition and adhesion. Despite the complexity and apparent specificity of carbohydrate modifications, the carbohydrate composition of even closely related species can differ widely (Varki, 1993). However, it is likely that many general functions of carbohydrates are conserved.

Glycosaminoglycans

Glycosaminoglycans (GAGs) are linear polysaccharides consisting of up to several hundred (several thousand, in the case of hyaluronan) repeating disaccharide units, each containing a GlcA or epimerized GlcA (IdA) and a GlcNAc or GalNAc (an exception is keratan sulfate, which contains Gal-GlcNAc disaccharides) (GlcA = glucuronic acid, IdA = iduronic acid, GalNAc = N-acetylgalactosamine, GlcNAc = N-acetylglucosamine, and Gal = galactose). All except hyaluronan are sulfated. In general, GAGs are synthesized on specific proteins in the endoplasmic reticulum and Golgi apparatus, the same subcellular compartments in which other glycoproteins and glycolipids in the secretory pathway receive their carbohydrate modifications. The resulting proteoglycans may be secreted and form part of the ECM or may remain on the cell surface, attached either by a GPI anchor or by a membrane-spanning region in the protein. An exception to this is hyaluronan, which is synthesized at the plasma membrane and secreted directly without attachment to protein (reviewed by Esko, 1991; Hardingham and Fosang, 1992; Lander, 1993; Weigel et al., 1996, although see Varki, 1996).

Because of their size and charge, GAGs can have considerable effects on the structural properties of ECMs and on interactions that take place at the cell surface. In addition, they can specifically bind certain components of the ECM and cell

surface as well as specifically concentrate certain extracellular proteins, including growth factors (reviewed by Toole, 1991).

Hyaluronan, because of its enormous size and hydrophilicity, is thought to facilitate the expansion of extracellular spaces and consequently also the migration of cells. It may also mediate cell-cell and cell-matrix interactions by binding to specific receptors, CD44 in particular (reviewed by Laurent and Fraser, 1992; Sherman et al, 1994). For example, during inner ear development in *Xenopus*, the opposite sides of an epithelium surrounding a lumen protrude toward one another and eventually fuse, resulting in a circular tube. Because hyaluronan is apparently secreted basally by the protruding regions of the epithelium and because enzymatic removal of the hyaluronan results in collapse of the protrusion, it has been proposed that the secreted hyaluronan in effect propels the epithelia away from the basal lamina (Haddon and Lewis, 1991). An example of hyaluronan receptor activity likely occurs during the formation of the prostate gland in mouse, when the epithelium is induced by mesenchyme to undergo branching morphogenesis. In organ culture, treatment of the developing prostate with hyaluronan hexasaccharides, the degradatory enzyme hyaluronidase, or anti-CD44 antibodies inhibits this branching (Gakunga et al., 1997).

Proteoglycans and, consequently, their covalently attached GAGs have also been implicated in cell-cell and cell-matrix interactions, including adhesion, as well as in the organization and structural properties of ECM (reviewed by Toole, 1991; Hardingham and Fosang, 1992; Lander, 1993; Rapraeger, 1993), and so may also play a role in epithelial morphogenesis. For example, E-cadherin-mediated adhesion between epithelial cells may depend on syndecan (Leppä et al., 1992), during kidney development the growth and branching morphogenesis of the uretic bud is inhibited by enzymes that degrade heparan and chondroitin/dermatan sulfates as well as by inhibitors of GAG sulfation (Davies et al., 1995), and it has been proposed that apical secretion of a proteoglycan drives the invagination of the vegetal plate during sea urchin gastrulation (Lane et al., 1993).

Other carbohydrate moieties

The more modest carbohydrate modifications of N- and O-glycosylated glycoproteins have also been shown to affect cell-cell and cell-matrix interactions, suggesting they could affect epithelial morphogenesis. Most cell adhesion receptors and components of the ECM are glycoproteins (reviewed by Hynes and Lander, 1992; Gumbiner, 1996); there is some evidence that, for example, the oligosaccharides on

members of the integrin superfamily (Zheng et al., 1994; Chammas et al., 1993), laminin (e.g., Dean et al., 1990), and fibronectin (e.g., Jones et al., 1986) can affect cell-matrix interactions such as adhesion, cell spreading and neurite outgrowth. There is also some direct evidence for the involvement of N-linked carbohydrates in examples of epithelial morphogenesis such as the cell rearrangements that occur during elongation of the sea urchin archenteron after primary invagination (Ingersoll and Ettensohn, 1994) and the formation of a bronchial epithelium in mouse (Ioffe et al., 1996).

Several special carbohydrate structures on glycoproteins and glycolipids may directly mediate cell-cell and cell-matrix adhesion. These include the carbohydrate moieties that bind the selectins and mediate the initial adhesion of leukocytes to endothelial cells, allowing leukocytes to invade the endothelial layer (Brandley et al., 1990; Rosen and Bertozzi, 1994), and polysialic acid moieties, which when covalently modifying N-CAM, decrease the latter's ability to mediate cell-cell adhesion either directly, by homophilic binding, or indirectly, by affecting the interactions between other adhesion molecules (Rutishauser, 1996). The HNK-1 epitope, of which the important component is thought to be a terminal sulfated GlcA residue, has also been implicated in mediating adhesion: vertebrate N-CAM, L1, myelin-associated glycoprotein and other cell adhesion proteins carry the HNK-1 epitope (Kruse et al., 1984; Schachner and Martini, 1995), antibodies against the HNK-1 epitope can disrupt cell-cell adhesion (Keilhauer et al., 1985), cell-substratum adhesion (Lallier and Bronner-Fraser, 1991) and neurite outgrowth (Riopelle et al., 1986), the isolated carbohydrate SO4-3-GlcA-β1,3-Gal-β(1,4)-GlcNAc-β(1,3)-Gal also disrupts cell migration and neurite outgrowth (Künemund et al., 1988), and COS-1 cells transfected with GlcAT-P express the HNK-1 epitope and extend long and branched processes, suggesting that their interaction with the substratum may be altered (Terayama et al., 1997).

Cell surface glycosyltransferases

There is some evidence that glycosyltransferases may be located not only in the endoplasmic reticulum and Golgi apparatus, where they catalyze the addition of sugars to glycoconjugates in the secretory pathway, but also on the plasma membrane, where it has been proposed they may directly bind extracellular carbohydrate residues, either catalytically or in a lectin-like capacity, and thereby mediate cell-cell and cell-matrix adhesion (Shur, 1993). For example, mammalian β(1,4)-galactosyltransferase appears to be on the surface of mouse sperm where it can

bind oligosaccharides of the ZP3 glycoprotein on the mouse egg coat, facilitating sperm-egg binding (Miller et al., 1992; Lu and Shur, 1997). However, mutants lacking the cell surface β(1,4)-galactosyltransferase do not have obvious defects in epithelial morphogenesis (Lu et al., 1997; Asano et al., 1997).

Finally, at least one class of pattern formation molecule, Fringe and related molecules, may be secreted glycosyltransferases (Yuan et al., 1997). This type of molecule could also in principle affect epithelial morphogenesis by directly modifying extracellular and/or cell surface carbohydrates.

Overview and directions for future experiments

Most analyses of epithelial invagination have been limited to manipulating epithelia *in vitro*, either mechanically or by the addition of chemical reagents, and to defining the expression patterns of molecules proposed to be involved; the *in vivo* relevance of models derived from such experiments remains to be tested. Recently, the analysis of *Drosophila* mutants defective in gastrulation has identified an *in vivo* role for G-protein signaling (Parks and Wieschaus, 1991; Costa et al., 1994) and Rho-dependent cytoskeletal changes (Barrett et al., 1997) in this process and suggests that *Drosophila* gastrulation depends on cell shape changes coordinated by extracellular signaling. To identify additional molecules involved *in vivo* in epithelial invagination, we have begun a genetic analysis of *C. elegans* vulval invagination. We have identified mutations that define eight genes, *sqv-1* to *sqv-8*, and cause a partial collapse of the invaginating vulva and elongation of the central invaginating cells as well as defects in oocyte and embryonic development. SQV-3 is similar to vertebrate β(1,4)-galactosyltransferases and an invertebrate β(1,4)-N-acetylglucosaminyltransferase, SQV-8 is similar to a β(1,3)-glucuronyltransferase, and SQV-7 is similar to members of a family of nucleotide-sugar transporters, suggesting that the absence of a particular carbohydrate moiety perturbs normal vulval invagination.

Like the analysis of epithelial invagination, the analysis of carbohydrate function in multicellular animals has until recently been limited to *in vitro* experiments. Most cell-surface and secreted proteins and some lipids are modified by the covalent addition of carbohydrate moieties which can have considerable variety and complexity, suggesting that they may be important encoders of information. However, mutant mammalian cell lines with only minimal carbohydrate modifications are viable (Stanley and Ioffe, 1995). While *in vitro* experiments, including the use of inhibitors of glycosylation, competitive

oligosaccarides, lectins, carbohydrate-specific antibodies, enzymatic modifiers of carbohydrates, and somatic cell mutants, as well as analyses of the expression patterns and biochemical properties of glycoconjugates, implicate the carbohydrate components of proteoglycans, glycoproteins, and glycolipids in cell-cell and cell-matrix adhesion, recognition, and signaling as well as in extracellular matrix structure and properties (Varki, 1993), surprisingly, few mutations isolated in multicellular animals have been found to cause defects in glycosylation. Recently, several glycosyltransferases have been genetically eliminated from mice, and the resulting phenotypes confirm the importance of carbohydrate modifications in normal mouse development (Ioffe and Stanley, 1994; Lu et al., 1997; Asano et al., 1997) and the role of fucosylated carbohydrates as ligands for members of the selectin family (Maly et al., 1996). The identification of the *sqv* genes directly implicates a conserved glycosylation pathway in *C. elegans* development and, since the *sqv* genes are likely to affect only a small number of terminal glycosylation steps, provides further evidence that, although sufficient for the viability of mammalian cell lines (Stanley and Ioffe, 1995), minimal carbohydrate moieties are not sufficient for the normal development and function of multicellular animals. Clearly it will be of interest to identify the precise structure of the SQV-dependent carbohydrate likely to be involved as well as the nature of the glycoconjugate(s) it modifies. In particular, is this SQV-dependent carbohydrate acting indirectly to affect vulval invagination and other developmental events, for example by affecting the stability or modulating the activity of the glycoconjugate(s) it modifies, or does it simply modify and thereby mask one or more carbohydrates or glycoconjugates that can otherwise perturb these processes, or, as in the case of GAGs and the O-linked carbohydrates on mucins, does it exert its effects largely by virtue of its size and charge, or, as in the case of the selectin ligands, does it directly and specifically bind other molecules?

One obvious way to begin to address these questions is by defining the biochemical activities of SQV-3, SQV-7, and SQV-8, as well as the remaining SQV proteins, including whether they modify proteoglycans, glycoproteins and/or glycolipids. Defining their biochemical activities may also be of interest because the *sqv* genes are likely to encode many or all components of a conserved glycosylation pathway and may include new components not yet identified by purely biochemical means in other systems.

It might also be possible, particularly once the sugar linkage of the SQV-dependent carbohydrate is known, to find reagents such as lectins or anti-carbohydrate antibodies that can detect the presumed difference in sugar

composition between wild-type and *sqv* mutant animals. Such reagents might allow the SQV-dependent carbohydrate to be visualized in intact animals, for example yielding information as to its localization during vulval invagination, and allow the glycoconjugates to which it is attached to be identified, for example by western blot analysis. The cellular and subcellular expression pattern of the SQV proteins, as assessed by antibodies, and the cells in which the *sqv* genes are required, as assessed by genetic mosaic analysis, should also yield information on how they are involved in vulval invagination and early development.

While the use of *C. elegans* genetics has provided direct evidence that glycosylation affects vulval invagination as well as other aspects of development, it would be nice in addition to manipulate this system by the addition of chemicals that inhibit glycosylation, enzymes that modify carbohydrates, or oligosaccharides, lectins or antibodies that might interfere with carbohydrate function. For example, one might inject such inhibitors or modifiers directly into the invagination space during vulval invagination and observe the consequence. Unfortunately, puncturing the cuticle that bounds this space during the mid-L4 stage results in itself in collapse of the invagination at some frequency (P. Sternberg, pers. comm.; T. Herman, observation). However, it remains possible that puncturing the cuticle at earlier stages of invagination may not result in collapse and may therefore allow the injection and testing of such reagents. An alternative would be to use such reagents to analyze the involvement of SQV-dependent glycosylation in oocyte and embryonic development. Injection of the gonad is a routine procedure in *C. elegans* and allows multiple oocytes to receive injected material. Determining which reagents can phenocopy the Sqv phenotype may allow the identification of the SQV-dependent carbohydrate and the type of glycoconjugate(s) it modifies.

C. elegans is a powerful system in which to explore more generally the function of carbohydrate modifications. The *C. elegans* genome sequencing project has identified many putative open reading frames predicted to encode proteins with similarity to various glycosyltransferases, including some related to SQV-8 and SQV-3. It is a straightforward matter to perform antisense experiments or to select mutants in which these genes have been deleted to learn how they may be involved in *C. elegans* development: for instance, one might expect that removing glycosyltransferases that act earlier than SQV-3 and SQV-8 and therefore modify a larger set of glycoconjugates would cause phenotypes more severe than the Sqv phenotype. On the other hand, what sort of phenotype might result from removing the *sqv-3*-related ORF or any of the five *sqv-8*-related ORFs? For example, is there

some redundancy among the functions of carbohydrate modifications, particularly among those that are somewhat related, or does the variety and complexity of carbohydrate modifications reflect specific functions for each?

Finally, while the identification of the *sqv* genes is likely to provide insight into some aspects of vulval invagination, they are unlikely to be the only genes involved, since none of the mutations isolated entirely blocks invagination. There are several obvious technical reasons why other genes required for invagination might not have been identified in our screen: for example, if their loss has only maternal effects on vulval invagination or also causes vulval lineage defects or zygotic lethality at a stage before vulval development. New genetic screens might therefore identify additional genes: in fact, a screen in which animals were shifted to 25°C (high, non-permissive temperature) after embryonic development, examined for a defect in laying eggs, and then their progeny checked for a temperature-sensitive defect in vulval invagination, has yielded mutants with new invagination defects (M. Han, pers. comm.). It is also possible that several mechanisms may cooperate to drive vulval invagination and that loss-of-function mutations in a single gene might not completely disrupt the process. In this case, the *sqv* mutants may provide a sensitized background in which to isolate new classes of mutation and identify further genes required for vulval invagination.

References

Asano, M., Furukawa, K., Kido, M., Matsumoto, S., Umesaki, Y., Kochibe, N., and Iwakura, Y. (1997). Growth retardation and early death of β-1,4-galactosytransferase knockout mice with augmented proliferation and abnormal differentiation of epithelial cells. *EMBO J.* **16**: 1850-1857.

Bard, J. (1990). *Morphogenesis: the cellular and molecular basis of developmental anatomy*. Cambridge University Press, Cambridge, England.

Barrett, K., Leptin, M., and Settleman, J. (1997). The Rho GTPase and a putative RhoGEF mediate a signaling pathway for the cell shape changes in *Drosophila* gastrulation. *Cell* **91**: 905-915.

Brandley, B.K., Swiedler, S.J., and Robbins, P.W. (1990). Carbohydrate ligands of the LEC cell adhesion molecules. *Cell* **63**: 861-863.

Chammas, R., Veiga, S.S., Travassos, L.R., and Brentani, R.R. (1993). Functionally distinct roles for glycosylation of α and β integrin chains in cell-matrix interactions. *Proc. Natl. Acad. Sci. USA* **90**: 1795-1799.

Costa, M., Wilson, E.T., and Wieschaus, E. (1994). A putative cell signal encoded by the *folded gastrulation* gene coordinates cell shape changes during *Drosophila* gastrulation. *Cell* **76**: 1075-1089.

Davies, J.A. and Garrod, D.R. (1997). Molecular aspects of the epithelial phenotype. *BioEssays* **19**: 699-704.

Davies, J., Lyon, M., Gallagher, J., and Garrod, D. (1995). Sulphated proteoglycan is required for collecting duct growth and branching morphogenesis but not nephron formation during kidney development. *Development* **121**: 1507-1517.

Dean, J.W., Chandrasekaran, S., and Tanzer, M.L. (1990). A biological role of the carbohydrate moieties of laminin. *J. Biol. Chem.* **265**: 12553-12562.

Eaton, S. and Simons, K. (1995). Apical, basal, and lateral cues for epithelial polarization. *Cell* **82**: 5-8.

Erickson, C.A. and Perris, R. (1993). The role of cell-cell and cell-matrix interactions in the morphogenesis of the neural crest. *Dev. Biol.* **159**: 60-74.

Esko, J.D. (1991). Genetic analysis of proteoglycan structure, function and metabolism. *Curr. Opin. Cell Biol.* **3**: 805-816.

Fristrom, D. (1988). The cellular basis of epithelial morphogenesis. A review. *Tissue Cell* **20**: 645-690.

Gakunga, P., Frost, G., Shuster, S, Cunha, G., Formby, B., and Stern, R. (1997). Hyaluronan is a prerequisite for ductal branching morphogenesis. *Development* **124**: 3987-3997.

Greenwald, I. (1997). In *C. elegans II* (ed. D.L. Riddle, T. Blumenthal, B.J. Meyer, and J.R. Priess), pp.519-541. Cold Spring Harbor Laboratory Press, Cold Spring Harbor, New York.

Gumbiner, B.M. (1992). Epithelial morphogenesis. *Cell* **69**: 385-387.

Gumbiner, B.M. (1996). Cell adhesion: the molecular basis of tissue architecture and morphogenesis. *Cell* **84**: 345-357.

Haddon, C.M. and Lewis, J.H. (1991). Hyaluronan as a propellant for epithelial movement: the development of semicircular canals in the inner ear of *Xenopus*. *Development* **112**: 541-550.

Hardingham, T.E. and Fosang, A.J. (1992). Proteoglycans: many forms and many functions. *FASEB J.* **6**: 861-870.

Horvitz, H.R. and Sternberg, P. W. (1991). Multiple intercellular signaling systems control the development of the *Caenorhabditis elegans* vulva. *Nature* **351**: 535-541.

Hynes, R.O. and Lander, A.D. (1992). Contact and adhesive specificities in the associations, migrations, and targeting of cells and axons. *Cell* **68**:303-322.

Ingersoll, E.P. and Ettensohn, C.A. (1994). An N-linked carbohydrate-containing extracellular matrix determinant plays a key role in sea urchin gastrulation. *Dev. Biol.* **163**: 351-366.

Ioffe, E. and Stanley, P. (1994). Mice lacking N-acetylglucosaminyltransferase I activity die at mid-gestation, revealing an essential role for complex or hybrid N-linked carbohydrates. *Proc. Natl. Acad. Sci. USA* **91**: 728-732.

Ioffe, E., Liu, Y., and Stanley, P. (1996). Essential role for complex N-glycans in forming an organized layer of bronchial epithelium. *Proc. Natl. Acad. Sci. USA* **93**: 11041-11046.

Jones, F.S., Arumugham, R.G., and Tanzer, M.L. (1986). Fibronectin glycosylation modulates fibroblast adhesion and spreading. *J. Cell. Biol.* **103**: 1663-1670.

Keilhauer, G., Faissner, A., and Schachner, M. (1985). Differential inhibition of neurone-neurone, neurone-astrocyte and astrocyte-astrocyte adhesion by L1, L2 and N-CAM antibodies. *Nature* **316**: 728-730.

Kruse, J., Mailhammer, R., Wernecke, H., Faissner, A., Sommer, I., Goridis, C., and Schachner, M. (1984). Neural cell adhesion molecules and myelin-associated glycoprotein share a common carbohydrate moiety recognized by monoclonal antibodies L2 and HNK-1. *Nature* **311**: 153-155.

Künemund, V., Jungalwala, F.B., Fischer, G., Chou, D.K., Keilhauer, G., and Schachner, M. (1988). The L2/HNK-1 carbohydrate of neural cell adhesion molecules is involved in cell interactions. *J. Cell. Biol.* **106**: 213-223.

Lallier, T., and Bronner-Fraser, M. (1991). Avian neural crest cell attachment to laminin: involvement of divalent cation dependent and independent integrins. *Development* **113**: 1069-1084.

Lander, A.D. (1993). Proteoglycans in the nervous system. *Curr. Opin. Neurobiol.* **3**: 716-723.

Lane, M.C., Koehl, M.A.R., Wilt, F., and Keller, R. (1993). A role for regulated secretion of apical extracellular matrix during epithelial invagination in the sea urchin. *Development* **117**: 1049-1060.

Laurent, T.C. and Fraser, J.R. (1992). Hyaluronan. *FASEB J.* **6**: 2397.

Leppä, S., Mali, M., Miettinen, H.M., and Jalkanen, M. (1992). Syndecan expression regulates cell morphology and growth of mouse mammary epithelial tumor cells. *Proc. Natl. Acad. Sci. USA* **89**: 932-936.

Lu, Q., and Shur, B.D. (1997). Sperm from beta-1,4-galactosyltransferase-null mice are refractory to ZP3-induced acrosome reactions and penetrate the zona pellucida poorly. *Development* **124**: 4121-4131.

Lu, Q., Hasty, P., and Shur, B.D. (1997). Targeted mutation in β1,4-galactosyltransferase leads to pituitary insufficiency and neonatal lethality. *Dev. Biol.* **181**: 257-267.

Maly, P., Thall, A., Petryniak, B., Rogers, C.E., Smith, P.L., Marks, R.M., Kelly, R.J., Gersten, K.M., Cheng, G., Saunders, T.L., Camper, S.A., Camphausen, R.T., Sullivan, F.X., Isogai, Y., Hindsgaul, O., von Andrian, U.H., Lowe, J.B. (1996). The alpha(1,3)fucosyltransferase Fuc-TVII controls leukocyte trafficking through an essential role in L-, E-, and P-selectin ligand biosynthesis. *Cell* **86**: 643-653.

Miller, D.J., Macek, M.B., and Shur, B.D. (1992). Complementarity between sperm surface beta-1,4-galactosyltransferase and egg-coat ZP3 mediates sperm-egg binding. *Nature* **357**: 589-593.

Parks, S. and Wieschaus, E. (1991). The *Drosophila* gastrulation gene *concertina* encodes a G alpha-like protein. *Cell* **64**: 447-458.

Rapraeger, A.C. (1993). The coordinated regulation of heparan sulfate, syndecans and cell behavior. *Curr. Opin. Cell Biol.* **5**: 844-853.

Riopelle, R.J., McGarry, R.C., Roder, J.C. (1986). Adhesion properties of a neuronal epitope recognized by the monoclonal antibody HNK-1. *Brain Res.* **367**: 20-25.

Rosen, S.D. and Bertozzi, C.R. (1994). The selectins and their ligands. *Curr. Opin. Cell Biol.* **6**: 663-673.

Rutishauser, U. (1996). Polysialic acid and the regulation of cell interactions. *Curr. Opin. Cell Biol.* **8**: 679-684.

Schachner M. and Martini, R. (1995). Glycans and the modulation of neural-recognition molecule function. *Trends Neurosci.* **18**: 183-191.

Sherman, L., Sleeman, J., Herrlich, P., and Ponta, H. (1994). Hyaluronate receptors: key players in growth, differentiation, migration and tumor progression. *Curr. Opin. Cell Biol.* **6**: 726-733.

Shur, B.D. (1993). Glycosyltransferases as cell adhesion molecules. *Curr. Opin. Cell Biol.* **5**: 854-863.

Stanley, P. and Ioffe, E. (1995). Glycosyltransferase mutants: key to new insights in glycobiology. *FASEB J.* **9**: 1436-1444.

Sulston, J.E. and Horvitz, H.R. (1977). Post-embryonic cell lineages of the nematode, *Caenorhabditis elegans*. *Dev. Biol.* **56**: 110-156.

Terayama, K., Oka, S., Seiki, T., Miki, Y., Nakamura, A., Kozutsumi, Y., Takio, K., and Kawasaki, T. (1997). Cloning and functional expression of a novel glucuronyltransferase involved in the biosynthesis of the carbohydrate epitope HNK-1. *Proc. Natl. Acad. Sci. USA* **94**: 6093-6098.

Toole, B.P. (1991). Proteoglycans and hyaluronan in morphogenesis and differentiation. In *Cell Biology of Extracellular Matrix* (ed. E.D. Hay), pp. 305-341 Plenum Press, New York.

Varki, A. (1996). Does DG42 synthesize hyaluronan or chitin?: A controversy about oligosaccharides in vertebrate development. *Proc. Natl. Acad. Sci. USA* **93**: 4523-4525.

Varki, A. (1993). Biological roles of oligosaccharides: all of the theories are correct. *Glycobiology* **3**: 97-130.

Weigel, P.H., Hascall, V.C., and Tammi, M. (1997). Hyaluronan synthases. *J. Biol. Chem.* **272**: 13997-14000.

White, J. (1988). The Anatomy. In *The Nematode* Caenorhabditis elegans (ed. W.B. Wood and the community of *C. elegans* researchers), pp. 81-122. Cold Spring Harbor Laboratory Press, Cold Spring Harbor, New York.

Yuan, Y.P., Schultz, J., Mlodzik, M. and Bork, P. (1997). Secreted Fringe-like signaling molecules may be glycosyltransferases. *Cell* **88**: 9-11.

Zheng, M., Fang, H., and Hakomori, S. (1994). Functional role of N-glycosylation in alpha 5 beta 1 integrin receptor. De-N-glycosylation induces dissociation or altered

association of alpha 5 and beta 1 subunits and concomitant loss of fibronectin binding activity. *J. Biol. Chem.* **269**: 12325-12331.

Figure 1. Schematic of vulval development showing the desmosomal connections between vulval cells during the late L3 and early L4 stages, as viewed either from the dorsal (top) or ventral (bottom) side (the orientation was not specified; B. Podbilewicz, pers. comm.) and labeled according to Greenwald (1997). (A) P5.p, P6.p, and P7.p have each given rise to four cells (labeled ABCD, EFFE, and DCBA, respectively) that remain in the plane of the surrounding epithelium. (B) just before the final round of divisions the six central descendants undergo a slight change in shape. (C) each of the A cells from (B) has given rise to a binucleate A cell, each B cell has given rise to a B1 and B2, and the remaining cells in (B) have divided to yield two cells of the same name in (C). Note that the D, E, and F cells are already beginning to form rings. Although Podbilewicz does not explain this, I assume (D) and (E) are not actual but instead flattened depictions of the stack of rings that are formed by rearrangement of the cells in (C). (D) the remaining cells have now formed rings. (E) fusions have occurred, resulting in a stack of seven toroids. While, according to this diagram, the A, B, C, and D cells behave as described in Appendix 1, the order in which the E and F cells fuse is apparently not as sequential as Appendix 1 implied, nor, according to this diagram, do F, and possibly E, appear to extend lateral arms as described in Appendix 1.

A


A B C D E F F E D C B A

B


A B C D E F F E D C B A

C

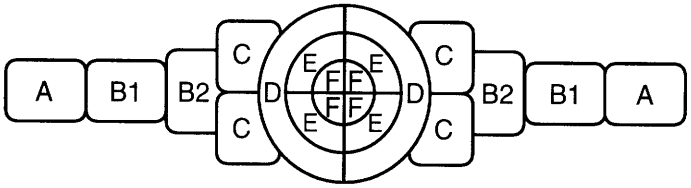
A
B1
B2
C
D
E
F
F
F
F
E
E
D
C
C
B2
B1
A

D

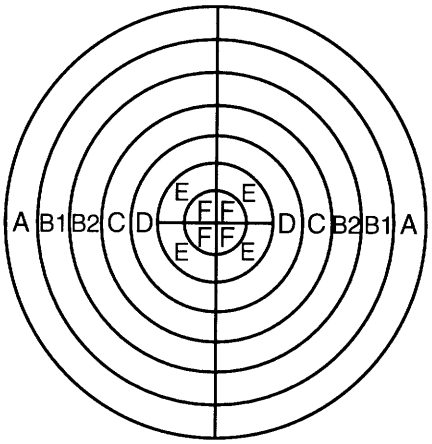
A B1 B2 C D E F F F F E E D C B2 B1 A

E

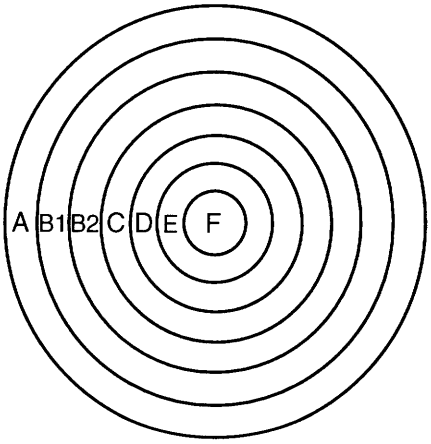
A B1 B2 C D E F

Chapter two

Identification of eight genes required for wild-type vulval invagination in *C. elegans*

To be submitted to *Development*

Summary

We have isolated 25 mutations that perturb the invagination of the *C. elegans* hermaphrodite vulva, a tube that connects the uterus to the outer epithelium. All 25 mutations cause the same vulval defect, an apparent partial collapse of the vulval invagination and elongation of the central vulval cells. The 25 mutations define eight genes, which we have named *sqv-1* to *sqv-8* (squashed vulva). All but the weakest *sqv* mutations also cause hermaphrodite sterility, implicating the *sqv* genes in additional developmental events.

Introduction

The three-dimensional structure of an animal and its organs is shaped in part by the movement and folding of epithelial cell layers (Bard, 1990). For example, amphibian gastrulation is initiated by the invagination of endodermal cells (Keller, 1985), during neurulation ectodermal cells fold inward and pinch off to form a tube that will become the spinal cord and brain (Schoenwolf and Smith, 1990), and during the development of the vertebrate eye the optic vesicle bends inward to form a cup that will ultimately become the retina (Jacobson and Sater, 1988). There are several general models of how an epithelium might initiate inward folding or invagination (reviewed by Ettensohn, 1985; Fristrom, 1988; and Davidson et al., 1995). In models for sea urchin gastrulation (Burke et al., 1991), *Drosophila* gastrulation (Sweeton et al., 1991; Parks and Wieschaus, 1991; Costa et al., 1994; Barrett et al., 1997), and vertebrate neurulation (Clausi and Brodland, 1993), cells in the invaginating epithelium individually undergo cytoskeletal changes that result in constriction of their apical surface relative to their basal surface. Other models (Gustafson and Wolpert, 1963; Nardi, 1981; Mittenthal and Mazo, 1983) propose that changes in cell-cell adhesion drive invagination. In the simplest such, that of Gustafson and Wolpert (1963), an increase in adhesiveness between cells in the invaginating epithelium favors an increase in the extent of contact between them and, consequently, an increase in their height. If the basal surfaces of the cells remain adherent to a substrate, causing the basal surface area to remain the same, this increase in cell height is accommodated by a decrease in apical surface area and consequent inward folding of the epithelium. A third type of model, for sea urchin gastrulation, proposes that changes in the extracellular matrix drive invagination (Lane et al., 1993). Cells that are to invaginate deposit a new hygroscopic layer of extracellular matrix between their apices and an older less hygroscopic matrix. The greater hydration of the new matrix layer causes it to swell and increase in surface area relative to the old matrix, driving the bilayer to bend inward and causing the underlying epithelial sheet to bend as well. Although each of these models of invagination is based on a single cellular mechanism, it is also possible that multiple mechanisms may be coordinated during invagination and that the relative importance of each individual mechanism may differ among different examples of invagination.

Most analyses of epithelial invagination have been limited to manipulating epithelia *in vitro*, either mechanically or by the addition of chemical reagents, and to defining the expression patterns of molecules proposed to be involved. More

recently, the analysis of *Drosophila* mutants defective in gastrulation has identified an *in vivo* role for G-protein signaling (Parks and Wieschaus, 1991; Costa et al., 1994) and Rho-dependent cytoskeletal changes (Barrett et al., 1997) in this process. To identify additional molecules involved *in vivo* in epithelial invagination, we have begun a genetic analysis of an example of this process in the nematode *C. elegans*.

The *C. elegans* body is enclosed by a single layer of epithelial cells which underlie a collagenous cuticle (White, 1988). During the third (L3) and fourth (L4) larval stages, the descendants of the vulval precursors P5.p, P6.p, and P7.p, a specialized set of outer epithelial cells, invaginate and create a tube that connects the outer epithelium to the layer of epithelial cells that enclose the uterus (Sulston and Horvitz, 1977). This vulval tube allows the adult hermaphrodite both to lay eggs and to receive sperm from males. The signaling pathways that direct P6.p to undergo a so-called primary pattern of cell division and P5.p and P7.p to undergo secondary patterns of division have been extensively studied (reviewed by Horvitz and Sternberg, 1991; Kornfeld, 1997). During the final round of vulval cell divisions, the primary descendants and some secondary descendants detach from the cuticle, allowing the vulval sheet to bend inward and the cells within it to rearrange their cell-cell contacts. Because vulval invagination can occur in the absence of most other nearby cells, including the vulval muscles (T. Herman, observation of *sem-4* mutants) and the somatic gonad (Kimble, 1981), it is likely that the mechanical force required is intrinsic to the epithelium or its extracellular matrix, consistent with models of other invaginations (see above), although the primary descendants must be in contact with a cell in the gonad, the anchor cell, for the invagination to have the correct shape and to attach to the uterus (Kimble, 1981; Thomas et al., 1990; Newman and Sternberg, 1996). In this paper we describe the results of a screen for mutations that affect vulval invagination.

Materials and Methods

Strains

Strains were cultured as described by Brenner (1974) and, unless indicated otherwise, were grown at 20°C. Most mutations and chromosomal rearrangements mentioned are described by Hodgkin et al. (1988) or Hodgkin (1997). Exceptions are *tra-2(q122*dm*)* (Schedl and Kimble, 1988), *let-253(n2412)* (M. Labouesse, personal communication), *eDf21* (Shen and Hodgkin, 1988), *lin-12(n302n865)* (Greenwald et al., 1983), *nDf40* (Hengartner et al., 1992), *qC1 dpy-19(e1259) glp-1(q339)* (Austin and Kimble, 1989; J. Austin and J. Kimble, personal communication), *hT2* (McKim et al., 1993), *h661* (A. Rose, personal communication), and *n754* (E. Ferguson and H. Horvitz, personal communication). Tc1 polymorphisms between the N2 and RW7000 strains are described by Williams et al. (1992). *mn63* was isolated by Sigurdson et al. (1984), and the gene it defined was originally named *spe-2*; we have received permission to rename this gene *sqv-8*.

The *lin-12(n302n865) sqv-3(n2841)* chromosome was constructed as follows. *+/eT1; lin-12(n302n865) unc-50(e306)/eT1 n886; him-5(e1467*ts*)* males were mated to *dpy-19(e1259*ts,mat*) sqv-3(n2841)/qC1* hermaphrodites and the resulting male progeny mated singly to *dpy-19(e1259*ts,mat*) unc-50(e306)* hermaphrodites. Wild-type (nonUnc nonDpy) progeny were transferred, one per plate, from plates on which they were rare, and their progeny were examined. In some cases, all Lin progeny were also Sqv, and the parental genotype was therefore judged to have been *lin-12(n302n865) sqv-3(n2841)/dpy-19(e1259*ts,mat*) unc-50(e306)*.

The *dpy-19(e1259*ts,mat*) lin-12(n137*sd*) sqv-3(n2841)* chromosome was constructed as follows. *dpy-19(e1259*ts,mat*) lin-12(n137*sd*) unc-69(e587*am*)/sqv-3(n2842) unc-69(e587*am*)* hermaphrodites were mated to *sqv-3(n2841)/eT1* males and the resulting nonUnc hermaphrodite progeny transferred one per plate. Three hundred Muv nonUnc progeny of those animals judged to be *dpy-19(e1259*ts,mat*) lin-12(n137*sd*) unc-69(e587*am*)/sqv-3(n2841)* were then transferred one per plate. Of these plates, those that contained only Muv progeny were further examined for Sqv animals. Those few that contained Muv Sqv animals were judged to have had a parent of genotype *dpy-19(e1259*ts,mat*) lin-12(n137*sd*) sqv-3(n2841)/dpy-19(e1259*ts,mat*) lin-12(n137*sd*) unc-69(e587*am*)*.

Isolation of mutations that affect vulval invagination

Unstarved hermaphrodites of the wild-type strain N2 were mutagenized with ethylmethane sulfonate as described by Brenner (1974) and grown on individual

plates. Up to 40 hermaphrodite progeny from each mutagenized P0 animal were transferred one to a plate. The F2 progeny of these F1 animals were examined with a dissecting microscope, and F2 animals with abnormal vulval invaginations were examined further with Nomarski differential interference contrast (DIC) microscopy to determine the number of vulval nuclei present. If this differed from the wild-type number, indicating that the lineage of the vulval cells was abnormal, then the mutant was discarded. Otherwise, the mutant was transferred to a plate so as to propagate the mutation. If the mutant had no viable progeny, several of its wild-type siblings were transferred to individual plates and their progeny examined for the presence of mutant animals. In all such cases, it was possible to find wild-type siblings that had a proportion of mutant progeny, suggesting that these mutations could be propagated heterozygously. In this way we examined just over 12,000 independent mutagenized haploid genomes for recesssive and dominant mutations and isolated 25 mutations that affect vulval invagination.

Genetic mapping and complementation tests

Newly isolated mutant strains were backcrossed at least four times to N2. In the course of backcrossing, we examined whether any of the mutations caused a dominant vulval phenotype. No vulval abnormalities were ever observed in the progeny of N2 hermaphrodites mated with heterozygous mutant males; the mutant phenotypes therefore appear to be completely recessive.

All mutations were genetically mapped to linkage groups (LG) by the method of Williams et al. (1992) (data not shown), and nearly all mutations were mapped within each linkage group by standard three-factor methods (Brenner, 1974). Exceptions were the four *sqv-2* alleles: while each of these alleles demonstrated linkage to the *stP100* polymorphism on the left arm of LG *II* (data not shown), only *n2826* was tested in three-factor mapping experiments, and the further positional information obtained from the latter was minimal (Table 1).

Since each of the mutations isolated caused a recessive vulval phenotype, standard complementation tests were performed. The following pairs of mutations failed to complement: alleles of *sqv-1*: *n2820* and *n2819*, *n2820* and *n2828*, *n2820* and *n2848*, *n2820* and *n2824*, *n2820* and *n2849*; alleles of *sqv-2*: *n2826* and *n2821*, *n2826* and *n3037*, *n2826* and *n3038*; alleles of *sqv-3*: *n2842* and *n2841*, *n2842* and *n2823*; alleles of *sqv-4*: *n2827* and *n2840*; alleles of *sqv-7*: *n2844* and *n2839*; and alleles of *sqv-8*: *mn63* and *n2822*, *mn63* and *n2825*, *n2825* and *n2822*, *n2825* and *n2843*, *n2825* and *n2847*, *n2825* and *n2850*, *n2825* and *n2851*.

The following pairs of mutations were shown to complement: *sqv-2(n2826)* and *sqv-7(n2839)*; *sqv-7(n2839)* and *sqv-8(n2825)*; *sqv-7(n2844)* and *sqv-8(n2825)*; *sqv-4(n2840)* and *sqv-6(n2845)*; *sqv-4(n2827)* and *sqv-6(n2845)*; *sqv-4(n2827)* and *spe-10(hc104*ts*)*. (*n2827/spe-10(hc104*ts*)* animals are wild-type at the non-permissive temperature, and *spe-10(hc104*ts*)* homozygotes have no vulval defect at any temperature. We therefore conclude that *n2827* is not an allele of *spe-10*.)

Alleles of *sqv-3* failed to complement the deficiency *nDf40*, alleles of *sqv-7* failed to complement the deficiency *mnDf30*, and alleles of *sqv-8* failed to complement the deficiency *mnDf29* but did complement *eDf21*.

Lineage analysis of mutant animals

L3 Unc hermaphrodites from the strains *sqv-3(n2841) unc-69(e587)/qC1*, *sqv-5(n3039) unc-75(e950)/hT2 bli-4(e937); +/hT2 h661*, *sqv-7(n2844) unc-4(e120)/mnC1*, and *sqv-8(mn63) unc-4(e120)/mnC1*, and non-Unc L3 hermaphrodites from the strains *sqv-1(n2819)/nT1 n754; +/nT1*, *sqv-2(n2826)*, *+/nT1 n754; sqv-4(n2840)/nT1*, and *+/nT1 n754; sqv-6(n2845)/nT1 n754* were mounted for Nomarski DIC microscopy, and the divisions of the P3.p, P4.p, P5.p, P6.p, P7.p, and P8.p cells and their descendants were observed (Sulston and Horvitz, 1977).

Electron microscopy, MH27 antibody staining, assays of egg laying

Animals to be analyzed by electron microscopy were fixed for 1 hour (on ice, in the dark) in 0.1M sodium cacodylate buffer containing 0.8% glutaraldehyde and 0.7% osmium tetroxide and then post-fixed overnight (again at 4°C in the dark) in 0.1M sodium cacodylate containing 1% osmium tetroxide. The animals were then embedded into agar blocks, dehydrated, and further embedded into an Epon-Araldite mixture. Serial thin sections (50nm) were cut and contrasted with uranylacetate and lead citrate. Micrographs were taken at 80 kV with a Jeol JEM 1200 EX II.

Wild-type and mutant larvae were stained with MH27 antibodies (Waterston, 1988) by the method of Podbilewicz and White (1994), and the immunofluorescence was examined with a Bio-Rad MRC-500 confocal microscope.

To assess the ability of wild-type and mutant animals to lay eggs, 15 mid-L4 stage hermaphrodites of each genotype were picked to a plate and aged for 41 hours. They were then picked individually to small pools of M9 on glass slides and dissected with a syringe needle, allowing all the eggs in the uterus to be released and counted. *sqv-1(n2849)*, *sqv-2(n3027)*, *sqv-3(n2841)*, *sqv-4(n2840)*, *sqv-5(n3039)*, *sqv-*

6(n2845), *sqv-7(n2844)*, and *sqv-8(n2822)* mutants were examined by Nomarski DIC at the L4 stage for the presence of HSN neurons and at the adult stage for vulval muscle contractions; in each case HSNs and vulval contractions were observed, although no observed contractions resulted in the release of eggs.

Characterization of hermaphrodite fertility

To determine the brood sizes of wild-type and homozygous viable mutant strains, five N2 or mutant L4 larvae were transferred to individual plates and then transferred to new plates on each of seven consecutive days. Hatched progeny (larvae) on each plate were counted three days after the parent had been removed and the total number of hatched progeny determined for each parental animal. To determine the brood sizes of all other homozygous mutants, 100 mutant L4 larvae were transferred five per plate and the hatched progeny on each plate counted five days and rechecked seven days afterward.

To assess the stage at which progeny of mutant hermaphrodites arrest, L4 animals were picked to a plate, aged for approximately 18 to 24 hours, and then transferred to small pools of M9 on glass slides where they were dissected with a syringe needle, allowing all the eggs in the uterus to be released. These eggs were transferred to a plate, aged for 12 to 18 hours and examined with Nomarski DIC optics to estimate their stage of developmental arrest. This estimate was complicated by abnormalities in the shape of arrested embryos, but the groupings used (one-cell, bean/comma, two-/three-fold, hatched larvae) are likely to have been sufficiently distinct for accuracy (these names are derived from the gross appearance of embryos by Nomarski DIC microscopy).

Artificial insemination was carried out by the method of LaMunyon and Ward (1994). Recipients of injected sperm were transferred to individual plates, which were examined four days after injection for the presence of cross-progeny. The viability of sperm was tested by injecting sperm removed from hermaphrodites into homozygous *eT1* hermaphrodites (approximately five to ten sperm per recipient) and looking for non-Unc progeny. Five *eT1* hermaphrodites were injected with *sqv-1(n2819)* sperm and produced eight cross-progeny, four injected with *sqv-2(n3037)* sperm produced seven, twelve injected with *sqv-3(n2842)* sperm produced eighteen, ten injected with *sqv-4(n2840)* produced sixteen, ten injected with *sqv-5(n3039)* produced five, eleven injected with *sqv-6(n2845)* produced sixteen, six injected with *sqv-7(n2844)* produced thirteen, and twelve injected with *sqv-8(n2822)* produced nineteen. The viability of oocytes (and, necessarily, the

somatic gonad that contained them) was tested first by mating at least ten N2 males to at least ten mutant hermaphrodites and then, if this failed, by injecting sperm removed from wild-type males into homozygous mutant hermaphrodites (approximately 20 to 30 sperm per recipient). Nine *sqv-1(n2819)*, eight *sqv-3(n2842)*, seven *sqv-4(n2840)*, seven *sqv-5(n3039)*, eight *sqv-6(n2845)*, and six *sqv-7(n2844)* injected hermaphrodites produced no progeny, while seven *sqv-8(n2822)* hermaphrodites produced 54 cross-progeny.

To test whether *sqv-8(n2822)* exhibited a paternal effect like that reported for the *mn63* allele (Sigurson et al., 1984), we mated N2 males to *sqv-8(n2822)* hermaphrodites, mated the resulting male cross-progeny to *sqv-8(n2822)* hermaphrodites, and examined whether any progeny from the latter were Sqv. Since none was Sqv, we retested the *sqv-8(mn63)* allele in the same way but were again unable to reproduce the previous Sigurdson et al. (1984) result: N2 males were mated to *sqv-8(mn63) unc-4(e120)* homozygous hermaphrodites and the cross-progeny males mated to *sqv-8(mn63) unc-4(e120)* homozygous hermaphrodites. We obtained just over 80 cross-progeny, all of which were nonUnc-4 and nonSqv. In a second experiment, *sqv-8(mn63) unc-4(e120)/mnC1* males were mated to *sqv-8(mn63) unc-4(e120)* homozygous hermaphrodites. Again we obtained just over 80 progeny, all of which were nonUnc-4 and nonSqv.

Results

Isolation of mutations that perturb vulval invagination

To identify genes involved in vulval invagination, we undertook a genetic screen (Fig. 1). We mutagenized the wild-type strain N2, transferred the F1 progeny to individual plates, and, using a dissecting microscope, examined the F2 broods for animals with vulval defects. F2 hermaphrodites were examined at the mid-L4 stage, after the vulval cells have normally invaginated and during a period when the space between the invaginating vulval cells and the cuticle is largest (see Fig. 3E). We sought animals in which this space was absent or abnormal, indicating that the vulval cells had not invaginated or had invaginated incorrectly. The appearance of the invagination space is also affected by abnormalities in vulval cell lineage: animals with too many or too few vulval cells can have multiple, misshapen or absent invaginations. Because we were interested in identifying genes specifically required for the invagination process, we therefore demanded that candidate mutants possess the wild-type number of vulval nuclei, as assessed by Nomarski DIC microscopy and, in some cases, later confirmed that they had wild-type vulval lineages (see below).

In this way, we examined hermaphrodites representing just over 12,000 mutagenized haploid genomes and isolated 25 mutations that perturb vulval invagination.

The 25 mutations isolated correspond to eight genes, *sqv-1* to *sqv-8*

We located each of the 25 mutations on the genetic map by standard methods, and, since all the mutations caused a recessive vulval phenotype, those that mapped to similar regions of the genetic map were tested for their ability to complement (see Materials and Methods; Table 1 and Fig. 2). The 25 mutations define eight complementation groups, of which seven appear to be new. We have named the latter genes *sqv-1* to *sqv-7* (squashed vulva) because of the gross appearance of their mutant vulval phenotype. Mutations in the eighth complementation group failed to complement a previously identified mutation, *spe-2(mn63)* (Sigurdson et al., 1984), which we found also causes a defect in vulval invagination. Although *spe-2(mn63)* hermaphrodites were previously reported to have a sperm defect (Sigurdson et al., 1984), we were unable to reproduce these results either with the *mn63* allele or a new allele, *n2822* (see Materials and Methods), and found additionally that sperm from an *n2822* homozygous hermaphrodite are viable (see

below). With the permission of R. Herman we have therefore renamed this gene *sqv-8*.

Because the *sqv* mutations were not rare, because the phenotypes they cause are recessive to wild-type, and because the phenotypes caused by those tested (all alleles of *sqv-3*, *sqv-7*, and *sqv-8*) are similar whether the mutations are homozygous or hemizygous, it is likely that these mutations cause a loss of gene function.

Mutations in *sqv-1* to *sqv-8* cause a partial collapse of the vulval invagination

All 25 newly isolated mutations and *mn63* appear to cause identical vulval phenotypes, as judged by Nomarski DIC microscopy. Before the final round of vulval cell divisions, both wild-type and *sqv* mutant vulval cells lie along the ventral cuticle in a plane with the surrounding outer epithelium, hyp7 (Figs 3A,B). In the wild type, during the final round of vulval cell divisions, a defined subset of the vulval cells detaches from the cuticle and begins to invaginate, leaving the plane of the surrounding epithelium and creating a space between the apices of these vulval cells and the cuticle (Fig. 3C). In the *sqv* mutants, however, while the appropriate cells appear to detach from the cuticle, the resulting invagination space is considerably reduced in size (Fig. 3D). This abnormality persists through the mid-L4 stage, when it also becomes more evident that the height of the mutant vulval invagination is slightly decreased relative to that of the wild-type, suggesting that the mutant invagination may be partially collapsed (Figs 3E,F). Three alleles isolated, *sqv-2(n2821)*, *sqv-2(n2826)*, and *sqv-7(n2839)*, cause a slightly weaker vulval defect than that depicted in Figure 3 (i.e., a smaller reduction in the size of the invagination space) and may therefore cause only a partial loss of gene function.

To confirm that the Sqv vulval phenotype was not somehow the result of abnormal vulval cell lineages, we directly observed the pattern of vulval cell divisions in at least one hermaphrodite of each of the following genotypes: *sqv-1(n2819)*, *sqv-2(n2826)*, *sqv-3(n2841) unc-69(e587)*, *sqv-4(n2840)*, *sqv-5(n3039) unc-75(e950)*, *sqv-6(n2845)*, *sqv-7(n2844) unc-4(e120)*, and *sqv-8(mn63) unc-4(e120)*. In every case this pattern was wild-type (data not shown). In addition, we have observed that these and the remaining 17 *sqv* mutations do not appear to affect the number and gross arrangement of the vulval nuclei at the mid- to late-L4 stage (data not shown).

Both primary and secondary vulval cell descendants display the Sqv phenotype

To determine whether all invaginating vulval cells are affected by the Sqv mutant phenotype or only a specific subset derived from the primary or from the secondary lineage, we took advantage of the lineage transformations caused by loss-of-function (lf) and gain-of-function (gf) mutations in the gene *lin-12*. In animals homozygous for the *lin-12* lf allele, *n302n865*, no vulval precursor cells undergo a secondary pattern of divisions and instead P5.p, P6.p and, often, P7.p undergo primary patterns of divisions (Greenwald et al., 1983). By the mid-L4 stage these primary descendants have formed a single large invagination (Fig. 4A), which is considerably reduced in size in *lin-12(n302n865) sqv-3(n2841)* animals (Fig. 4B). In animals homozygous for the *lin-12* gf allele, *n137*, no vulval precursor cells undergo a primary pattern of divisions, and instead P3.p to P8.p undergo secondary patterns of divisions (Greenwald et al., 1983). By the mid-L4 stage, *lin-12(n137*sd*)* animals have multiple small vulval invaginations (Fig. 4C), which are reduced in size in *lin-12(n137*sd*) sqv-3(n2841)* animals (Fig. 4D). These results suggest that most or all invaginating vulval cells may be affected by the Sqv mutant phenotype, although it is also possible that only particular descendants from each type of lineage are affected.

The vulval invagination space is more electron-dense, and the central invaginating vulval cells are more elongated in the *sqv* mutant than in the wild type

To directly examine the invaginating vulval cells at the early L4 stage, when the difference between wild-type and *sqv* mutant vulvas is first detectable by Nomarski DIC, we prepared serial sections of N2 and *sqv-3(n2842)* hermaphrodites for electron microscopy (EM). At this stage, the central wild-type vulval cells have detached from the cuticle and surround an invagination space of minimal electron-density (Fig. 5A). The central vulval cells of the *sqv-3(n2842)* mutant have also detached properly from the cuticle but surround an invagination space that is not only considerably reduced in size but also more electron-dense than that of the wild type (Fig. 5B), a difference that was observed in several N2 and *sqv-3(n2842)* animals. The increased electron density may reflect a qualitative difference in the composition of the mutant extracellular space or may simply be the result of concentrating wild-type material into a smaller volume.

To compare the arrangement and shapes of the wild-type and *sqv-3* vulval cells, we traced their plasma and nuclear membranes as well as the cuticle in electron micrographs of our serial sections; four such tracings are shown in Figs

5C,D,E,F. Cell identifications were made on the basis of the known arrangement of vulval nuclei as judged by Nomarski DIC microscopy, and it was possible in this way to assign cell identities in the *sqv-3* vulva that were consistent with its having a grossly normal arrangement of cells. However, a comparison of roughly equivalent wild-type and *sqv-3* sections shows that the central mutant vulval cells (in particular, those labeled F, E, and D) are abnormally elongated, extending into and reducing the size of the invagination space. This general difference was also observed in other N2 and *sqv-3(n2842)* animals examined, although in these cases we did not follow the three-dimensional shapes of the cells through EM sections.

Because the precise stage of a Sqv vulval invagination cannot be accurately gauged by the size of its invagination space, the *sqv-3* animal analyzed by EM may be at a somewhat later stage than the wild-type animal, which was selected by the size of its invagination space to be at a stage soon after vulval divisions were completed. Such a difference in stage would be unlikely to substantially affect the results presented. However, it may mask another possible difference. By Nomarski DIC microscopy the Sqv vulval invagination appears to be slightly shorter (that is, to extend less dorsally) than the wild-type, suggesting that the the arch of invaginating cells is partially collapsed (see above). The EM tracings do not obviously show such a difference; it is possible that this is because the wild-type invagination is at an earlier and consequently shorter stage.

The *sqv* mutant vulval cells form a partially functional adult vulval tube

As wild-type vulval cells invaginate they reorganize their cell-cell contacts around the invagination space and fuse in a specific pattern that results in a stack of seven toroidal cells (B. Podbilewicz and J. White, pers. comm.; Podbilewicz and White, 1994; Newman et al., 1996.). The dorsalmost toroid is attached to the uterine epithelium, the ventralmost toroid remains attached to the outer epithelium, and the central hole of the stack becomes the vulval tube of the adult. To test whether, despite the abnormal appearance of the L4 vulva, the *sqv* mutant vulval cells are still forming toroids, we stained mid-to late-L4 stage wild-type and mutant animals with a monoclonal antibody, MH27, that recognizes the desmosomal connections between epithelial cells in *C. elegans* (Waterston, 1988). In the wild type, this antibody decorates each ring of contact between adjacent vulval toroids, as well as the vulval attachments to the uterus and outer epithelium and the connections between epithelial cells in the uterus (Fig. 6A). The MH27 antibody also recognizes a pattern of rings in *sqv-3(n2841)* animals (Fig. 6B), indicating that despite their

abnormal invagination, the *sqv* vulval cells can form toroids, although we did not ascertain whether the precisely correct number of toroids were formed nor whether the connection between vulva and uterus was precisely wild-type.

By the adult stage, the wild-type and *sqv* mutant vulvae appear similar by Nomarski DIC microscopy (Figs 3G,H). However, while adult Sqv hermaphrodites can occasionally lay some eggs, and *sqv-8* hermaphrodites can receive sperm from mating males (see below), the strongest mutant alleles of most *sqv* genes cause a defect in laying eggs (Table 2), resulting in older adult animals that are visibly bloated with unlaid eggs and often have protruding vulvae. Because the other cells required for egg-laying, the HSN neurons and vulval muscles, appear to be present and functional in these mutants (see Materials and Methods), their egg-laying defect may be the result of the *sqv* vulval defect. Support for this idea comes from an observation made during the artificial insemination of *sqv* hermaphrodites with wild-type sperm (see below): some force is required to propel a glass needle (wide enough to contain sperm) through *sqv* mutant vulvae, which occasionally rupture, while little force is required to inseminate wild-type hermaphrodites. Although *sqv-5* hermaphrodites were not defective in the assay of egg-laying in Table 2, they do not appear to lay eggs, suggesting that they may simply produce few oocytes (see below); they also required some force to be artificially inseminated.

The *sqv* mutations cause hermaphrodite sterility

Nearly all the mutations we isolated, including at least one allele each of *sqv-1* to *sqv-8*, cause a severe reduction in hermaphrodite fertility (Table 3). (The three mutations that have a weak or no effect on brood size are those that also cause weaker vulval defects (see above).) We determined the stages at which progeny of mutant hermaphrodites arrest and found that the strongest *sqv-1* to *sqv-8* mutants produce at least some eggs that fail to undergo cytokinesis. We did not determine whether these one-cell eggs have undergone fertilization; they may be unfertilized, since, like unfertilized oocytes from *spe-1(mn47) unc-4(e120)* hermaphrodites, they are dissolved by bleach, but they appear to retain their shape better than *spe-1* oocytes and so may have a partial eggshell.

While animals homozygous for the strongest alleles of *sqv-1* to *sqv-7* produce mostly or entirely one-cell eggs, none of the seven *sqv-8* alleles causes such a distribution of arrest phenotypes (Table 3). Instead, the strongest *sqv-8* homozygotes produce a small number of one-cell eggs and a much larger number of embryos arrested at the bean and comma stage. It is possible that this difference is caused by a

difference in allele strength and that the null phenotype of *sqv-8* might resemble that of *sqv-1* to *sqv-7*. However, *sqv-8(n2822)* behaves genetically like a strong loss of *sqv-8* function (Table 4).

The *sqv* hermaphrodite sterility is due to oocyte or somatic gonad defects

Because *sqv* mutant hermaphrodites produced possibly unfertilized, one-cell eggs, we used artificial insemination to test whether their sterility was due to a sperm or an oocyte defect (see Materials and Methods). Sperm from *sqv-1(n2819)*, *sqv-2(n3038)*, *sqv-3(n2842)*, *sqv-4(n2840)*, *sqv-5(n3039)*, *sqv-6(n2845)*, *sqv-7(n2844)*, and *sqv-8(n2822)* hermaphrodites were able to produce adult cross-progeny when injected into *eT1* hermaphrodites, indicating that *sqv-1* to *sqv-8* sperm are viable and suggesting that the sterility is caused by a defect in the mutant oocytes or somatic gonad. Indeed, *sqv-1(n2819)*, *sqv-3(n2842)*, *sqv-4(n2840)*, *sqv-5(n3039)*, *sqv-6(n2845)*, and *sqv-7(n2844)* hermaphrodites were unable to produce hatching progeny when provided with wild-type sperm, either by mating or by artificial insemination. And while *sqv-2(n3038)* hermaphrodites did produce a small number of cross-progeny when mated into (eleven from ten hermaphrodites and no self-progeny), this number is not significantly different from the number of hatching self-progeny expected (see Table 3).

By contrast, *sqv-8(n2822)* and *sqv-8(n2850)* hermaphrodites produced a significant number of adult cross-progeny (21 from ten *n2822* hermaphrodites and 18 from ten *n2850* as compared with zero self-progeny expected (see Table 3)); Sigurdson et al. (1984) had previously observed that *sqv-8(mn63)* hermaphrodites also produce cross-progeny. Because *sqv-8* hermaphrodite sperm is viable, these results indicate that *sqv-8(n2822)*, *sqv-8(n2850)*, and *sqv-8(mn63)* cause a maternal-effect lethality that can be partially rescued by providing a wild-type *sqv-8* gene in the zygote. When these matings (N2 males with *sqv-8(n2822)* and *sqv-8(n2850)* hermaphrodites) were repeated on a larger scale, we found a small number (<10%) of hatching progeny are dumpyish, often twisted or rolling, and irregular in body shape, most often bulging at the tail or mid-body (data not shown), suggesting that the *sqv-8* defect was only partially rescued by zygotic expression. Most such animals die as larvae, but those that survived to the L4 stage had normal vulvas, and those that survived to adulthood were fertile and had wild-type and *sqv-8* progeny, indicating they were indeed cross-progeny.

In the course of assaying egg-laying ability (see above), the hermaphrodite uterus was dissected, releasing the contents of the uterus. Along with oocytes/eggs

of normal size, *sqv-1* to *sqv-8* mutants released a number of small oocyte-like cells, indicating that they may have a defect in oocyte formation. Such a defect would be consistent with the failure of *sqv-5(n3039)* and *sqv-1(n2819)* to appear egg-laying defective in the assay, since they may simply produce few normal oocytes. The gross appearance of the *sqv-5(n3039)* hermaphrodite somatic gonad is also often abnormal as judged by Nomarski DIC microscopy (data not shown).

Discussion

Several models could explain the *sqv* mutant defect in vulval invagination

We have isolated probable loss-of-function mutations that define eight genes, which we have named *sqv-1* to *sqv-8*. These mutations appear to cause a partial collapse of the vulval invagination and elongation of the central invaginating cells, but do not prevent the formation of vulval toroids and a partially functional adult vulva. While the precise cellular mechanism of wild-type vulval invagination is unknown, any of several simple models could explain the *sqv* mutant phenotype.

One possibility is that the loss of the *sqv* genes decreases the rigidity of the vulval cell layer, reducing its ability to support itself over a large invagination space and causing it instead to form a collapsed invagination over a smaller space. Such a decrease in the layer's rigidity could result from a defect in the vulval cells themselves, for instance in their cytoskeleton or in the strength of the adhesion among them. Or such a decrease could also result from a decrease in the rigidity of the apical extracellular matrix. Indeed, the vulval invagination of mid-L4 animals has been observed to collapse when the adjacent cuticle is punctured, presumably because the invagination alone is not rigid enough to support the internal hydrostatic pressure of the worm (P. Sternberg, pers. comm.); this also suggests that a leaky cuticle might be capable of causing the Sqv vulval defect, although no obvious cuticular defect was observed in the *sqv* mutants.

A second possibility is that the expansion of the invagination space, presumably by the accumulation of water, is an active process that is blocked by the loss of the *sqv* genes.

A third possibility is that the *sqv* vulval phenotype results from an inappropriate or increased adhesion between the vulval cell apices and the electron-dense material observed in the mutant invagination space. Such adhesion might be accommodated during invagination partly by an elongation of the vulval cells and partly by a collapse of the invagination itself, and the invagination space would be reduced in size as a consequence.

A fourth possibility is that the *sqv* phenotype results from an increased adhesiveness among the mutant vulval cells themselves. Such an increase would favor a vulval conformation that increased the extent of vulval cell-cell contact, causing at least some cells to become abnormally elongated, but might not interfere with the bending inward of the vulval sheet and subsequent formation of the vulval toroids. In fact, Gustafson and Wolpert (1963) proposed that such an increase in adhesiveness could itself drive invagination (see Introduction).

In all of these models the *sqv* genes are required to execute invagination efficiently, but other, intact mechanisms can still cause the changes in cell-cell contacts and the cell fusions required for the formation of vulval toroids.

Why were *sqv* mutations the only type isolated in this screen?

All the mutations isolated in our genetic screen cause a single type of defect in vulval invagination, and none entirely blocks invagination, indicating that there must be other as yet unidentified genes involved in this process. Although mutants with subtle defects in the appearance of the mid-L4 invagination could have been missed (for example, no Class II or Class III *evl* mutants were isolated (Seydoux et al., 1993)), our screen should have identified any mutants in which vulval invagination failed to occur. There are several obvious technical reasons why the loss of genes required for invagination might not result in mutants identifiable by our screen: for example, if their loss has only maternal effects on vulval invagination or also causes vulval lineage defects or zygotic lethality at a stage before vulval development. It is also possible that several mechanisms may cooperate to drive vulval invagination and that loss-of-function mutations in a single gene might not completely disrupt the process. In this case, the *sqv* mutants may provide a sensitized background in which to isolate new classes of mutations to identify further genes required for vulval invagination.

The *sqv* genes are required for other developmental events in addition to vulval invagination

In addition to causing a defect in vulval invagination, loss of *sqv* gene function results in a severe reduction in hermaphrodite fertility, indicating that these genes are involved in other developmental events. The strongest *sqv-1* to *sqv-8* mutants appear to produce some abnormally small oocytes and also produce at least some eggs that fail to undergo cytokinesis and may not be fertilized. These genes may therefore be required for aspects of oocyte development and/or fertilization. In addition, we isolated many weaker alleles, particularly of *sqv-8*, that result in embryonic arrest at later stages, suggesting that at least some of the *sqv* genes may also be involved in later embryonic development (Table 3). Such arrested animals are often abnormally shaped: for instance, embryos with well-developed pharynxes are often less elongated and lumpier than wild-type embryos at a similar stage of pharyngeal development, and in several cases hatched embryos were also observed to be lumpy and poorly elongated (the "misshapen" embryos in

Table 3). Because an elongated body shape is derived in part from cell shape changes in the outer epithelium during embryogenesis, it is therefore possible that at least some of the *sqv* genes may affect other events of epithelial morphogenesis in addition to vulval invagination.

Acknowledgments

We thank Robert K. Herman for, among other things, allowing us to rename the *spe-2* gene and we thank the *Caenorhabditis* Genetics Center for providing strains containing the *sqv-8(mn63)* and *spe-10(hc104*ts*)* mutations. This work was supported by United States Public Health Service research grant GM24663. H.R.H. is an Investigator of the Howard Hughes Medical Institute.

References

Austin, J., and Kimble, J. (1989). Transcript analysis of *glp-1* and *lin-12*, homologous genes required for cell interactions during development of *C. elegans*. *Cell* **58**, 565-571.

Bard, J. (1990). *Morphogenesis: the cellular and molecular basis of developmental anatomy*. Cambridge University Press, Cambridge, England.

Barrett, K., Leptin, M., and Settleman, J. (1997). The Rho GTPase and a putative RhoGEF mediate a signaling pathway for the cell shape changes in *Drosophila* gastrulation. *Cell* **91**, 905-915.

Brenner, S. (1974). The genetics of *Caenorhabditis elegans*. *Genetics* **77**, 71-94.

Burke, R.D., Myers, R.L., Sexton, T.L., and Jackson, C. (1991). Cell movements during the initial phase of gastrulation in the sea urchin embryo. *Dev. Biol.* **146**, 542-557.

Clausi, D.A. and Brodland, G.W. (1993). Mechanical evaluation of theories of neurulation using computer simulations. *Development* **118**, 1013-1023.

Costa, M., Wilson, E.T., and Wieschaus, E. (1994). A putative cell signal encoded by the *folded gastrulation* gene coordinates cell shape changes during *Drosophila* gastrulation. *Cell* **76**, 1075-1089.

Davidson, L.A., Koehl, M.A., Keller, R., and Oster, G.F. (1995). How do sea urchins invaginate? Using biomechanics to distinguish between mechanisms of primary invagination. *Development* **121**, 2005-2018.

Ettensohn, C.A. (1985). Mechanisms of epithelial invagination. *Q. Rev. Biol.* **60**, 289-307.

Fristrom, D. (1988). The cellular basis of epithelial morphogenesis. A review. *Tissue Cell* **20**, 645-690.

Greenwald, I. (1997). In *C. elegans II* (ed. D.L. Riddle, T. Blumenthal, B.J. Meyer, and J.R. Priess), pp.519-541. Cold Spring Harbor Laboratory Press, Cold Spring Harbor, New York.

Greenwald, I.S., Sternberg, P.W., and Horvitz, H.R. (1983). The *lin-12* locus specifies cell fates in *C. elegans*. *Cell* **34**, 435-444.

Gustafson, T. and Wolpert, L. (1963). The cellular basis of morphogenesis and sea urchin development. *Int. Rev. Cytol.* **15**, 139-214

Hengartner, M.O., Ellis, R.E., and Horvitz, H.R. (1992). *Caenorhabditis elegans* gene *ced-9* protects cells from programmed cell death. *Nature* **356**, 494-499.

Hodgkin, J. (1997). Appendix 1: Genetics. In C. elegans *II* (ed. D.L. Riddle, T. Blumenthal, B.J. Meyer, and J.R. Priess), pp. 881-1047. Cold Spring Harbor Laboratory Press, Cold Spring Harbor, New York.

Hodgkin, J., Edgley, M., Riddle, D.L., and Albertson, D.G. (1988). Appendix 4: Genetics. In *The Nematode* Caenorhabditis elegans (ed. W.B. Wood and the Community of *C. elegans* Researchers), pp. 491-586. Cold Spring Harbor Laboratory Press, Cold Spring Harbor, New York.

Horvitz, H.R. and Sternberg, P. W. (1991). Multiple intercellular signaling systems control the development of the *Caenorhabditis elegans* vulva. *Nature* **351**, 535-541.

Jacobson, A.G. and Sater, A.K. (1988). Features of embryonic induction. *Development* **104**, 341-359.

Keller, R.E. (1985). The cellular basis of amphibian gastrulation. In *Developmental Biology: A Comprehensive Synthesis*, Vol. 2 (ed. L. Browder), pp. 241-327. Plenum Press, New York.

Kimble, J. (1981). Alterations in cell lineage following laser ablation of cells in the somatic gonad of *Caenorhabditis elegans*. *Dev. Biol.* **87**, 286-300.

Kornfeld, K. (1997). Vulval development in *Caenorhabditis elegans*. *Trends Genet.* **13**, 55-61.

LaMunyon, C.W. and Ward, S. (1994). Assessing the viability of mutant and manipulated sperm by artificial insemination of *Caenorhabditis elegans*. *Genetics* **138**, 689-692.

Lane, M.C., Koehl, M.A., Wilt, F., and Keller, R. (1993). A role for regulated secretion of extracellular matrix during epithelial invagination in the sea urchin. *Development* **117**, 1049-1060.

McKim, K.S., Peters, K., and Rose, A. (1993). Two types of sites required for meiotic chromosome pairing in *Caenorhabditis elegans*. *Genetics* **134**, 749-768.

Mittenthal, J.E. and Mazo, R.M. (1983). A model for cell shape generation by strain and cell-cell adhesion in the epithelium of an arthropod leg segment. *J. Theor. Biol.* **100**, 443-483.

Nardi, J.B. (1981). Induction of invagination in insect epithelium: paradigm for embryonic invagination. *Science* **214**, 564-566.

Newman A.P., and Sternberg, P.W. (1996). Coordinated morphogenesis of epithelia during development of the *Caenorhabditis elegans* uterine-vulval connection. *Proc. Natl. Acad. Sci. USA* **93**, 9329-9333.

Newman A.P., White J.G., and Sternberg P.W. (1996). Morphogenesis of the *C. elegans* hermaphrodite uterus. *Development* **122**, 3617-3626.

Parks, S. and Wieschaus, E. (1991). The *Drosophila* gastrulation gene *concertina* encodes a G alpha-like protein. *Cell* **64**, 447-458.

Podbilewicz, B. and White, J.G. (1994). Cell fusions in the developing epithelia of *C. elegans*. *Dev. Biol.* **161**, 408-424.

Schedl , T. and Kimble, J. (1988). *fog-2*, a germ-line-specific sex determination gene required for hermaphrodite spermatogenesis in *Caenorhabditis elegans*. *Genetics* **119**, 43-61.

Schoenwolf, G. and Smith, J.L. (1990). Mechanisms of neurulation: traditional viewpoint and recent advances. *Development* **109**,243-270.

Seydoux, G., Savage, C., and Greenwald, I. (1993). Isolation and characterization of mutations causing abnormal eversion of the vulva in *Caenorhabditis elegans*. *Dev. Biol.* **157**, 423-436.

Shen, M.M. and Hodgkin, J. (1988). *mab-3*, a gene required for sex-specific yolk protein expression and a male-specific lineage in *C. elegans*. *Cell* **54**, 1019-1031.

Sigurdson, D.C., Spanier, G.J., and Herman, R.K. (1984). *Caenorhabditis elegans* deficiency mapping. *Genetics* **108**, 331-345.

Sulston, J.E. and Horvitz, H.R. (1977). Post-embryonic cell lineages of the nematode, *Caenorhabditis elegans*. *Dev. Biol.* **56**, 110-156.

Sweeton, D., Parks, S., Costa, M., and Wieschaus, E. (1991). Gastrulation in *Drosophila*: the formation of the ventral furrow and posterior midgut invaginations. *Development* **112**, 775-789.

Thomas, J.H., Stern, M.J., and Horvitz, H.R. (1990). Cell interactions coordinate the development of the *C. elegans* egg-laying system. *Cell* **62**, 1041-1052.

Waterston, R.H. (1988). Muscle. In *The Nematode* Caenorhabditis elegans (ed. W.B. Wood and the Community of *C. elegans* Researchers), pp. 281-335. Cold Spring Harbor Laboratory Press, Cold Spring Harbor, New York.

White, J. (1988). The Anatomy. In *The Nematode* Caenorhabditis elegans (ed. W.B. Wood and the community of *C. elegans* researchers), pp. 81-122. Cold Spring Harbor Laboratory Press, Cold Spring Harbor, New York.

Williams, B.D., Schrank, B., Huynh, C., Shownkeen, R., and Waterston, R.H. (1992). A genetic mapping system in *Caenorhabditis elegans* based on polymorphic sequence-tagged sites. *Genetics* **131**, 609-624.

Figure 1. A screen for *C. elegans* mutants with defects in vulval invagination. Hermaphrodites were mutagenized with EMS, their F1 progeny placed on individual plates, and the resulting F2 broods examined for mutants defective in vulval invagination. In this diagram a grey semicircle on the ventral side of mid-body indicates a normal L4-stage invagination space. Candidate mutants were further examined using Nomarski DIC microscopy to ensure the correct number of vulval nuclei were present.

Mutagenize P0s

Put F1s on individual plates

Examine F2 broods for animals with an abnormal or absent vulval invagination

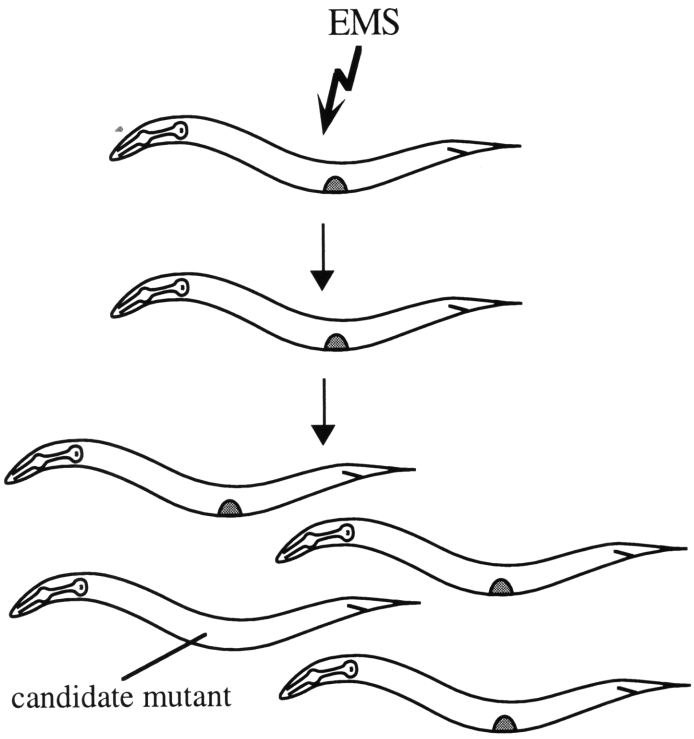

Figure 2. Locations of *sqv-1* to *sqv-8* on the genetic map. The likely positions of *sqv-1* to *sqv-7* are based on the three-factor data in Table 1 and on linkage analysis. The position of *sqv-8* was determined by Sigurdson et al. (1984) who identified its original mutant allele (the "1 old" allele).

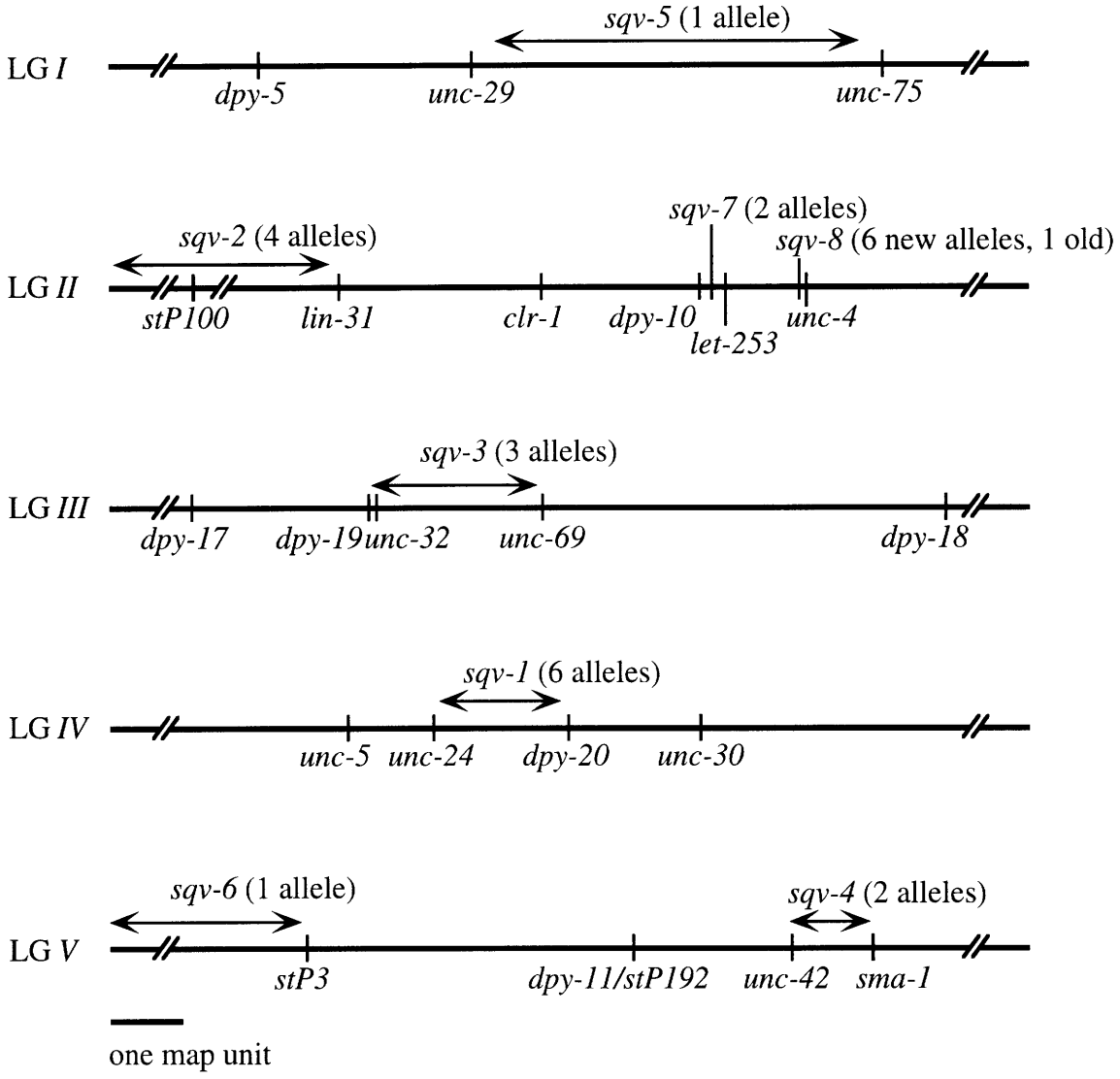
LG I
sqv-5 (1 allele)
dpy-5
unc-29
unc-75
LG II
sqv-2 (4 alleles)
sqv-7 (2 alleles)
sqv-8 (6 new alleles, 1 old)
stP100
lin-31
clr-1
dpy-10
let-253
unc-4
LG III
sqv-3 (3 alleles)
dpy-17
dpy-19
unc-32
unc-69
dpy-18
LG IV
sqv-1 (6 alleles)
unc-5
unc-24
dpy-20
unc-30
LG V
sqv-6 (1 allele)
sqv-4 (2 alleles)
stP3
dpy-11/stP192
unc-42
sma-1
one map unit

Figure 3. The *sqv* mutations result in a partially collapsed vulval invagination. Nomarski micrographs of wild-type (A, C, E, G) and *sqv-3(n2841)* (B, D, F, H) vulvae before, during, and after vulval invagination. (A, B) Late L3 stage. In both wild-type and *sqv* mutant vulvae the vulval precursors P5.p, P6.p, and P7.p have each given rise to four cells, which lie in a plane with the surrounding epithelium, hyp7. The arrowhead points to the center of the vulva, between cells P6.pap and P6.ppa. In the wild type, the gonadal anchor cell eventually takes a position directly above and between these cells, as it does in A. The anchor cell in the *sqv-3(n2841)* animal in B has not yet taken this position and lies slightly posterior. The animal in B is also homozygous for *unc-69(e587*am*)*. (C, D) Early L4 stage. Vulval cell division is complete. In both wild type and *sqv* mutant the appropriate cells have detached from the cuticle and left the plane of of the surrounding epithelium, but the space between the vulval cells and cuticle is considerably smaller in the *sqv* mutant than in the wild type. Again, the arrowhead points the center of the vulva. (E, F) Mid-L4 stage. The *sqv* mutant invagination appears to extend less dorsally than the wild-type, suggesting that the former is partially collapsed and that the space between the vulval cells and cuticle is reduced at least in part as a consequence of this. (G, H) Adult. The wild-type and *sqv* mutant vulvae do not obviously differ in appearance, although in later adulthood, when *sqv* mutants become bloated with eggs, their vulvae often protrude abnormally. In these Nomarski micrographs as in all following, the bar at the lower right is 10μm, and the animals are oriented such that anterior is to the left, and ventral is down.

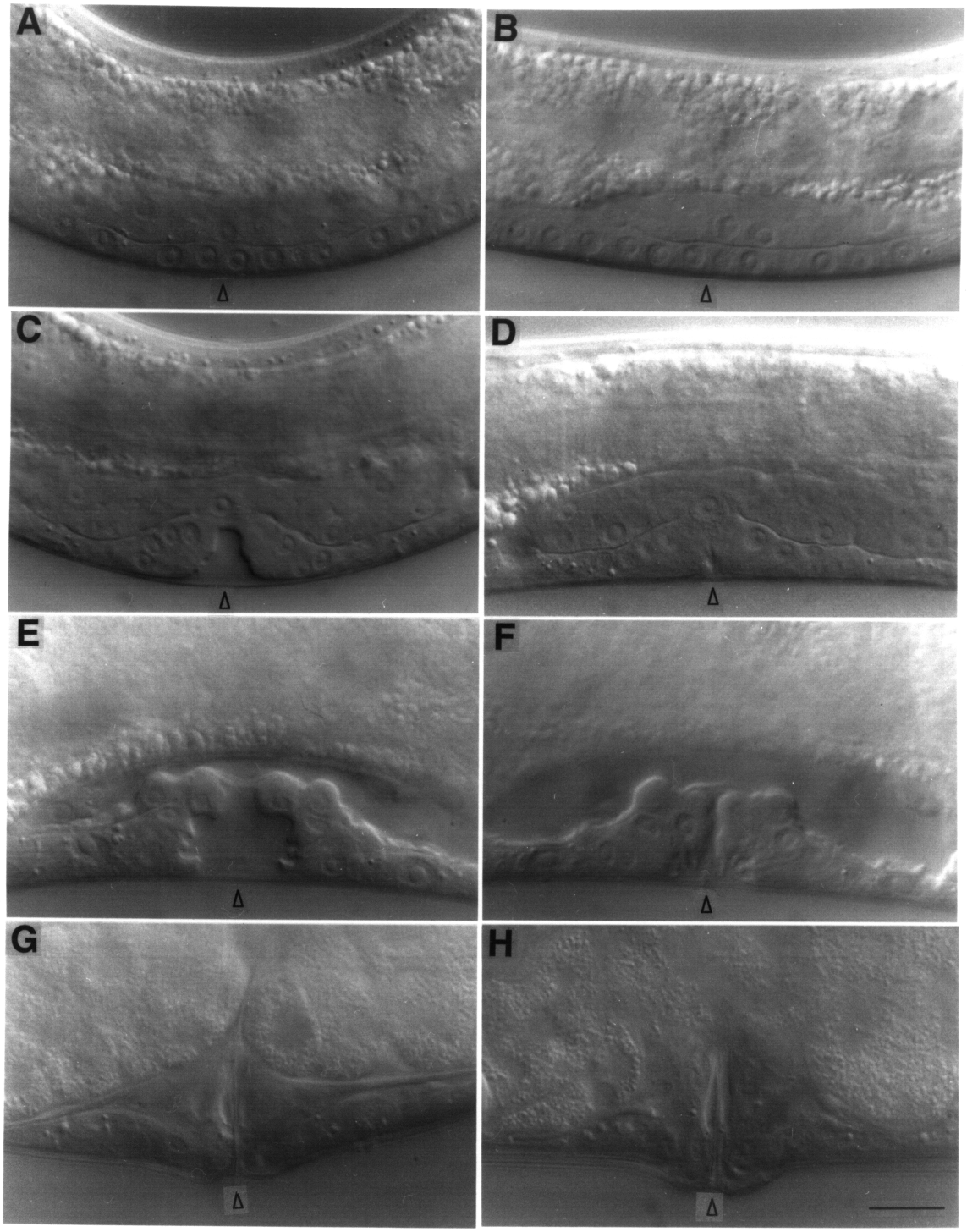
A
B
C
D
E
F
G
H

Figure 4. Both primary and secondary vulval lineage descendants display the Sqv phenotype. Nomarski micrographs of mid-L4 vulval invaginations derived entirely from primary cell descendants (A, B) or entirely from secondary cell descendants (C, D). (A) The *lin-12(n302n865) unc-50(e306)* vulval cells form a single large invagination, indicated by an arrowhead. (B) The *lin-12(n302n865) sqv-3(n2841)* vulval invagination is considerably reduced in size. The arrowhead points to the cluster of vulval cell nuclei. (C) The *dpy-19(e1259*ts,mat*) lin-12(n137*sd*) unc-69(e587*am*)* vulval cells form multiple small invaginations, each indicated by an arrowhead. (D) Again, the *dpy-19(e1259*ts,mat*) lin-12(n137*sd*) sqv-3(n2841)* invaginations are considerably reduced in size. Arrowheads indicate clusters of vulval cell nuclei.

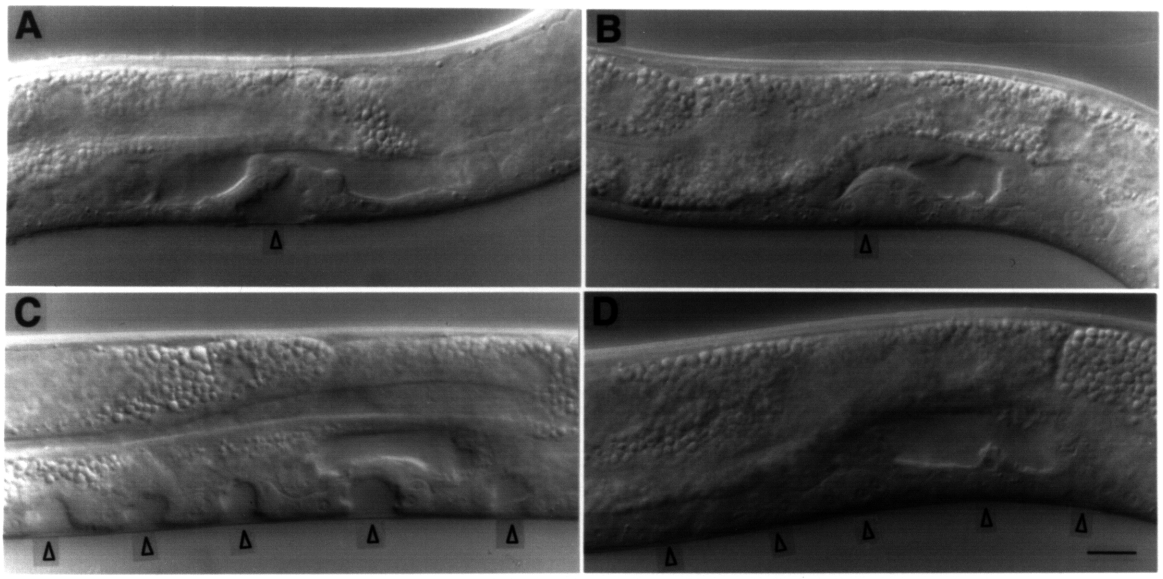
A
B
C
D

Figure 5. The vulval invagination space is more electron-dense, and the central vulval cells are more elongated in a *sqv* mutant than in the wild type. Electron micrographs of a wild-type (A) and a *sqv-3(n2842)* mutant (B) early L4 vulva in the plane at which the invagination space is largest. In each case the invagination space is the region of decreased electron density, and the cuticle is the ventralmost narrow grey band. The appropriate *sqv-3(n2842)* vulval cells have detached from the cuticle, but the resulting invagination space is reduced in size and more electron dense than that of the wild type. Tracings of vulval plasma and nuclear membranes and the cuticle from electron micrographs of N2 (C, E) and *sqv-3* (D, F). Cell identifications were made on the basis of the known arrangement of vulval nuclei as judged from Nomarski DIC microscopy and are indicated by the letter name of the L4 toroid they eventually form a part of (Greenwald, 1997). Tracings C and D are of the micrographs partly shown in A and B, and tracings E and F are of sections located roughly the same lateral distance from those traced in A and B. The central *sqv-3* vulval cells (in particular, those labeled F, E, and D) are abnormally elongated, extending into and reducing the size of the invagination space. The wild-type animal may be at a slightly earlier stage of development than the *sqv-3(n2842)* (see text for details). The bars at the lower right of B and F are 1μm.

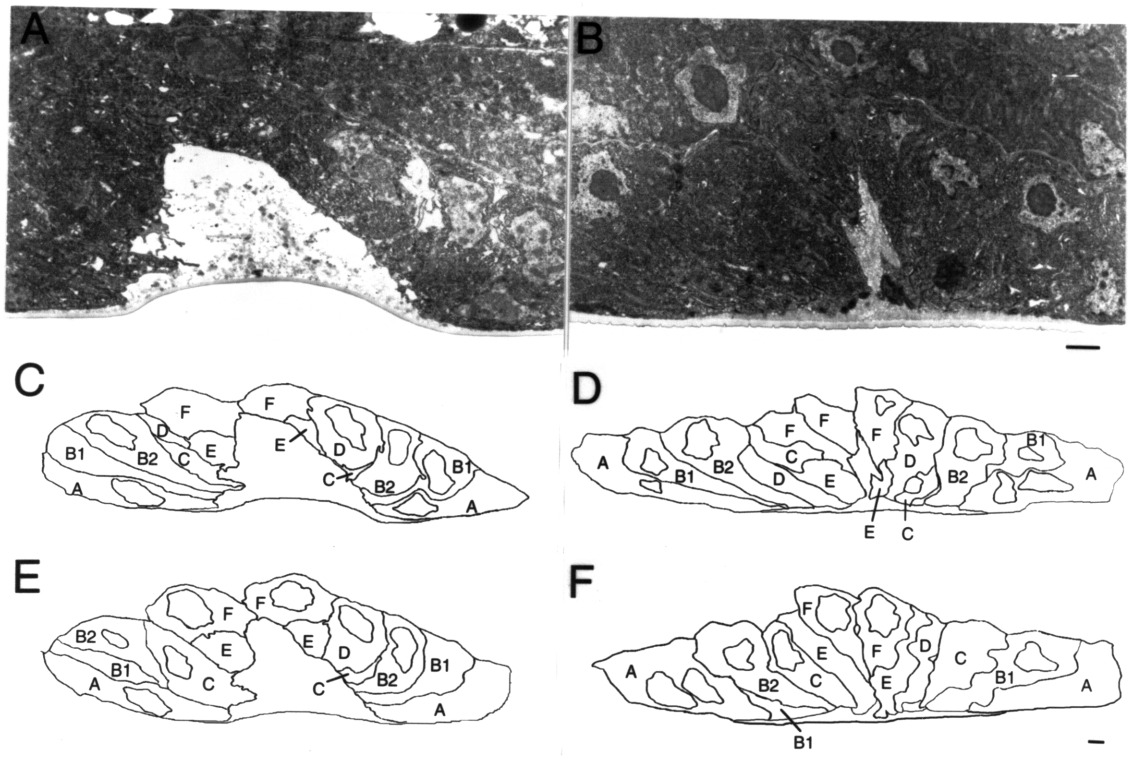
A
B
C
F
D
B1
B2
C
E
E
D
C
B2
B1
A
A
D
A
B1
B2
C
D
E
F
F
F
D
B2
B1
A
E
C
E
C
E
F
F
B2
A
B1
E
C
E
D
C
B2
B1
A
F
A
B2
C
E
F
D
C
B1
A
B1

Figure 6. *sqv* mutant vulval cells can form toroids. Confocal images of wild-type (A) and *sqv-3(n2841)* mutant (B) mid-L4 stage vulvae stained with MH27 antibodies and FITC-conjugated secondary antibodies. (A) The MH27 antibody stains the rings of contact between wild-type vulval toroids. (B) The MH27 antibody also stains the *sqv-3(n2841)* vulva in a pattern of stacked rings, indicating that, as in the wild type, the invaginating *sqv-3* vulval cells can form toroids, although we did not ascertain whether their number and connection to the uterus were precisely correct. The *sqv-3* animal shown is somewhat twisted back on itself, causing the bright gonadal staining to the left of the vulva to appear closer and therefore be present in panel B and also accounting for the two almost vertical bands of staining not present in panel A.

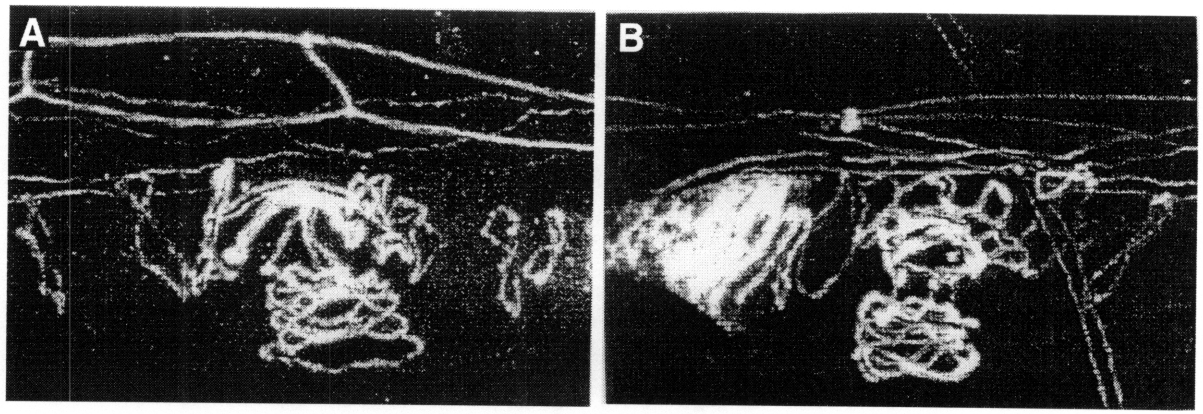
A
B

Table 1. Three-factor mapping of the new genes *sqv-1* to *sqv-7*.

Genotype of parent	Phenotype of recombinant	Proportion of recombinants segregating Sqv mutants
sqv-1/unc-24 dpy-20	Unc nonDpy	3/15
	Dpy nonUnc	6/6
sqv-1/dpy-20 unc-30	Dpy nonUnc	0/17
	Unc nonDpy	7/7
sqv-1/unc-5 dpy-20	Unc nonDpy	16/36
	Dpy nonUnc	25/40
sqv-2/dpy-10 unc-4	Dpy nonUnc	0/4
	Unc nonDpy	2/2
sqv-2/lin-31 clr-1	Lin nonClr	0/2
	Clr nonLin	2/2
sqv-3/dpy-17 unc-32	Dpy nonUnc	4/4
sqv-3/unc-69 dpy-18	Unc nonDpy	0/2
	Dpy nonUnc	8/8
sqv-3/dpy-19 unc-69	Dpy nonUnc	13/19
	Unc nonDpy	11/24
sqv-4/dpy-11 unc-42	Dpy nonUnc	4/4
	Unc nonDpy	0/5
sqv-4/unc-42 sma-1	Unc nonSma	14/22
	Sma nonUnc	5/8
sqv-5/dpy-5 unc-29	Dpy nonUnc	9/9
	Unc nonDpy	0/5
sqv-5/dpy-5 unc-75	Dpy nonUnc	6/8
	Unc nonDpy	2/4
sqv-7/dpy-10 unc-4	Dpy nonUnc	0/9
	Unc nonDpy	7/9
sqv-7/dpy-10 let-253 unc-4	Dpy nonLet	3/7
	Unc nonLet	14/14

Genotype of parent	Phenotype of recombinant	Proportion of recombinants segregating: *stP3* only	*stP192* only	*stP3* and *stP192*
sqv-6 unc-42/stP3 stP192	Sqv nonUnc	8/22	0/22	8/22

Each mutation isolated was tested for linkage to markers of known genetic map position (Williams et al., 1992). After this linkage was established, nearly all mutations were further mapped by standard three-factor methods (Brenner, 1974). Results for alleles of the same gene are here pooled. While *n2826* and the other three *sqv-2* alleles all showed strong linkage to *stP100* on the left arm of LG *II*, only one *sqv-2* allele, *n2826*, was used for three-factor mapping experiments.

Table 2. *sqv* mutant hermaphrodites are defective in laying eggs.

Genotype	Average number of eggs in uterus	Range
N2	18.7	10-25
sqv-1(n2849)	35.1	25-45
sqv-2(n3037)	29.1	12-63
sqv-3(n2841)	31.3	10-59
sqv-4(n2840)	25.0	14-47
sqv-5(n3039)	3.2	1-5
sqv-6(n2845)	32.1	17-71
sqv-7(n2844)	34.7	21-87
sqv-8(n2822)	44.0	26-63

Fifteen mid-L4 stage hermaphrodites of each genotype were aged for 41 hours and individually dissected to release eggs from the uterus. Mutant uteri of all genotypes often contained oocyte-like cells less than half the size of normal oocytes; these were not counted. *sqv-5* animals produced few oocytes. At least one allele of *sqv-1*, *n2819*, may also reduce the number of oocytes produced, since homozygotes are not significantly Egl in this assay but lay few if any eggs (the remaining *sqv-1* alleles were not tested in this assay).

Table 3. Most *sqv* mutations reduce hermaphrodite brood size.

Parental genotype		Hatched progeny per hermaphrodite	Stage of progeny 12-18 hours after removal from parent: one-cell	bean/ comma	two-/ three-fold	hatched larva: misshapen	hatched larva: normal
N2		243	0	0	0	0	46
sqv-1	*n2819*	0	34	0	0	0	0
	n2824	0	42	0	0	0	0
	n2828	0	38	0	0	0	0
	n2848	0	25	1	0	0	0
	n2849	0	30	2	0	0	0
	n2820	8	18	3	0	1	21
sqv-2	*n3037*	0.7	38	8	6	1	3
	n3038	0.8	30	14	1	0	1
	n2826	68	nd	nd	nd	nd	nd
	n2821	246	nd	nd	nd	nd	nd
sqv-3	*n2823*	0	40	0	0	0	0
	n2841	0	33	0	0	0	0
	n2842	0	45	0	2	0	0
sqv-4	*n2827*	0	31	0	0	0	0
	n2840	0	41	2	0	0	0
sqv-5	*n3039*	0	31	0	0	0	0
sqv-6	*n2845*	0	35	0	0	0	0
sqv-7	*n2844*	1	36	16	1	0	0
	n2839	101	nd	nd	nd	nd	nd
sqv-8	*n2822*	0	4	34	0	0	0
	n2850	0	6	38	1	0	0
	n2847	0	5	32	5	0	0
	n2851	0	5	30	2	0	0
	n2843	0.05	5	35	2	0	0
	mn63	0	1	12	18	2	0
	n2825	0.6	6	12	12	6	9

The total hatched progeny of five hermaphrodites from homozygous viable strains and 100 homozygous hermaphrodites selected from heterozygous strains were counted as described in Materials and Methods, and this number was divided by the number of original hermaphrodites. In a second experiment, embryos were dissected from homozygous adults, aged for approximately 12 to 18 hours, and the number at each stage of development estimated. These latter numbers were not determined (nd) for the three alleles that had substantially normal brood sizes.

Table 4. *sqv-8(n2822)* is a strong loss-of-function allele

Parental genotype	Number of progeny arrested at each stage		
	one-cell	bean/comma	two-/three-fold
sqv-8(n2822)	6	53	0
sqv-8(n2822)/mnDf29	4	49	0
sqv-8(mn63) unc-4(e120)	0	12	46
sqv-8(mn63) unc-4(e120)/sqv-8(n2822)	4	44	8
sqv-8(mn63) unc-4(e120)/mnDf29	5	37	5

Embryos were dissected from homozygotes 18 hours after the mid-L4 stage, aged for 12 hours, and the stage of developmental arrest estimated.

Chapter three

Three proteins involved in *C. elegans* vulval invagination are similar to components of a glycosylation pathway

To be submitted to *Cell*

Summary

We have molecularly analyzed three genes, *sqv-3*, *sqv-7*, and *sqv-8*, that are required for wild-type vulval invagination in *Caenorhabditis elegans*. The predicted SQV-3 protein is similar to members of a glycosyltransferase family consisting of vertebrate β(1,4)-galactosyltransferases, which add galactose (Gal) to N-acetylglucosamine (GlcNAc), and an invertebrate β(1,4)-N-acetylglucosaminyltransferase, which adds GlcNAc to GlcNAc. SQV-8 is similar to a β(1,3)-glucuronyltransferase, which adds glucuronic acid (GlcA) to Gal-β(1,4)-GlcNAc, and hence SQV-8 may use a SQV-3 product as a substrate. SQV-7 is similar to members of a family of nucleotide-sugar transporters. The *sqv* genes are therefore likely to encode components of a conserved glycosylation pathway that assembles a *C. elegans* carbohydrate moiety the absence of which perturbs vulval invagination.

Introduction

Most cell-surface and secreted proteins and some lipids are modified by the covalent addition of carbohydrate moieties, which are assembled in the endoplasmic reticulum (ER) and Golgi apparatus by the stepwise removal and addition of individual sugar molecules by glycosidases and glycosyltransferases (Kornfeld and Kornfeld, 1985; Kleene and Berger, 1993). Although entirely eliminating carbohydrate modification from a particular protein can affect its folding, stability, trafficking, or activity (Varki, 1993), mutant mammalian cell lines can survive without apparent decrease in viability even if the carbohydrate modifications on their proteins and lipids are considerably reduced in size and complexity (Stanley and Ioffe, 1995). By contrast, the first targeted gene disruptions of glycosyltransferases in mice indicate that multicellular organisms do require more elaborate sugar modifications to progress normally through development. For example, loss of the glycosyltransferase GlcNAc-T1, which is required early in the formation of N-linked carbohydrates, has no obvious effect on CHO cells (Stanley, 1984), but mice lacking GlcNAc-T1 die at mid-gestation (Ioffe and Stanley, 1994). These observations suggest that the variety and complexity of carbohydrate modifications may be required primarily for cell-cell and cell-matrix interactions. Indeed, *in vitro* experiments, including the use of inhibitors of glycosylation, competitive oligosaccarides, lectins, carbohydrate-specific antibodies, enzymatic modifiers of carbohydrates, and somatic cell mutants, as well as analyses of the expression patterns and biochemical properties of glycoconjugates, implicate the carbohydrate components of proteoglycans, glycoproteins, and glycolipids in cell-cell and cell-matrix adhesion, recognition, and signaling as well as in extracellular matrix structure and properties (Varki, 1993). However, the *in vivo* analysis of carbohydrate function in intact multicellular animals has been limited by the small number of mutants with defects in glycosylation. Recent genetic elimination of several glycosyltransferases from mice implicates carbohydrate modifications in normal mouse development (Ioffe and Stanley, 1994; Lu et al., 1997; Asano et al., 1997) and confirms the role of fucosylated carbohydrates as ligands for members of the selectin family (Maly et al., 1996).

We are using the nematode *Caenorhabditis elegans* to study epithelial invagination, a process that is fundamental to the development of multicellular organisms, in particular to the formation of tubular structures during gastrulation, neurulation, and organogenesis (Bard, 1990; Fristrom, 1988). The *C. elegans* vulva is an epithelial tube that connects the hermaphrodite uterus to the outer epithelium,

thereby allowing outward passage of eggs and inward passage of male sperm. The vulval tube is formed by the invagination of descendants of three epithelial cells that lie in a sheet with the outer epithelium (Sulston and Horvitz, 1977). The signaling pathways that specify the cell lineages of these descendants have been studied in detail and include components of the Ras and LIN-12/Notch pathways (reviewed by Sundaram and Han, 1996; Kornfeld, 1997). We have isolated mutations that perturb *C. elegans* vulval invagination without affecting vulval cell lineage (T. Herman, E. Hartwieg, and R. Horvitz, manuscript in preparation). These mutations define eight genes, *sqv-1* to *sqv-8*, and appear to cause identical vulval defects, a partial collapse of the invagination and elongation of the central invaginating cells, as well as defects in oocyte and embryonic development. In this paper we present evidence, the molecular analysis of *sqv-3*, *sqv-7*, and *sqv-8*, that these defects are likely to be caused by specific defects in glycosylation.

Results

Molecular identification of the *sqv-8* gene

sqv-8 maps genetically between the left breakpoints of the deficiencies *mnDf59* and *mnDf57* on Linkage Group (LG) *II* (Sigurdson et al., 1984). The positions of these breakpoints on the physical map had been previously defined: the left breakpoint of *mnDf59* is located on cosmid F35H8 (Morgan and Greenwald, 1993), and that of *mnDf57* is located in the gap between cosmids T09A10 and ZK1321 (C. Shamu and J. Hodgkin, personal communication). We assayed cosmids spanning the region between F35H8 and ZK1321 for their ability to rescue the *sqv-8* mutant phenotype and found that cosmid ZK1307 rescued both the vulval and fertility defects of *sqv-8(mn63)* hermaphrodites (Figure 1A). While *sqv-8(mn63) unc-4(e120)* hermaphrodites generate no progeny that hatch (T. Herman, E. Hartwieg, and R. Horvitz, manuscript in preparation), *sqv-8(mn63) unc-4(e120)* strains can be maintained if they contain a rescuing ZK1307 extrachromosomal array. We narrowed the region required for *sqv-8* rescue to a 4.6 kb Eag I-Spe I fragment, in which the *C. elegans* genome project predicted one complete coding sequence, ZK1307.5, and the first third of a second coding sequence, ZK1307.9. To test which of these predicted genes might correspond to *sqv-8*, we introduced into the Eag I-Spe I fragment an insert that results in a frameshift mutation predicted to eliminate the C-terminal 145 amino acids of the 356 amino acid ZK1307.5 protein. This construct did not have *sqv-8* rescue activity, suggesting that *sqv-8* activity requires an intact ZK1307.5 open reading frame. When the frameshifting insert was removed, *sqv-8* rescue activity was restored, confirming that the loss of this activity resulted from the insert (Figure 1A).

We used part of the Eag I-Spe I rescuing fragment to isolate eleven *sqv-8* cDNA clones from a library derived from animals of mixed developmental stages. Seven of these cDNAs had identical end-sequences, three others were slightly shorter at their 5' ends, and the eleventh was likely to be artifactual, since its end-sequences were not contained within the ZK1307 cosmid. We determined the sequence of one of the seven longest *sqv-8* cDNAs (Figure 1B). Its coding sequence is identical to ZK1307.5. We conclude that this 1.3 kb cDNA is likely to be full-length, since its 5' end contains seven nucleotides of the SL1 *trans*-spliced leader sequence (Krause and Hirsh, 1987), its 3' end contains a poly(A) tract, and a probe derived from the *sqv-8* cDNA hybridizes to a single band of approximately 1400 nt on a northern blot of total RNA (Figure 1C). The slight difference in size between the

cDNA and the hybridizing RNA band could be explained by additional polyadenylation on the RNA.

All seven *sqv-8* mutant alleles have DNA sequence changes within the open reading frame defined by the *sqv-8* cDNA (Figure 2). Three alleles, including the two strongest, *n2822* and *n2850*, as well as *mn63*, contain nonsense mutations predicted to eliminate, respectively, the final 276, 197, and 129 animo acids of the SQV-8 protein. *n2822* additionally contains a missense mutation, as do *n2825*, *n2843*, *n2847*, and *n2851*.

SQV-8 is similar to a β(1,3)-glucuronyltransferase that can catalyze the final sugar addition in the assembly of the HNK-1 epitope on glycoproteins

SQV-8 is similar in amino acid sequence to a mammalian glycosyltransferase, protein-specific β(1,3)-glucuronyltransferase from rat brain (GlcAT-P) (Terayama et al., 1997), and to several proteins of unknown function, one human, one from the human parasite *Schistosoma mansoni*, and five predicted from *C. elegans* genomic sequence (Figure 2). Glycosyltransferases catalyze the addition of sugars from nucleotide-sugar substrates to proteoglycans, glycoproteins and/or glycolipids (Kleene and Berger, 1993). GlcAT-P was purified on the basis of its ability to catalyze the addition of glucuronic acid (GlcA) from UDP-GlcA to galactose-β(1,4)-N-acetylglucosamine (Gal-β(1,4)-GlcNAc) disaccharides on glycoproteins, resulting in the trisaccharide GlcA-β(1,3)-Gal-β(1,4)-GlcNAc (Oka et al., 1992; Terayama et al., 1997). A sulfated form of this trisaccharide, SO4-3-GlcA-β(1,3)-Gal-β(1,4)-GlcNAc, is recognized by the monoclonal antibody HNK-1 (Voshol et al., 1996), which binds a variety of cell-surface proteins involved in cell-cell and cell-matrix adhesion in the vertebrate nervous system (Schachner and Martini, 1995).

An alignment among SQV-8 and similar proteins is shown in Figure 2. Of the 356 amino acids in SQV-8, 109 (30%) are identical to those of GlcAT-P. Using N-ethylmaleimide to block the cysteine at position 317 of GlcAT-P abolishes its enzymatic activity (Terayama et al., 1997), and this cysteine is conserved in SQV-8. Like GlcAT-P and most other glycosyltransferases, SQV-8 has a putative transmembrane domain at its N-terminus. From the Washington University-Merck EST Project (Gerhold and Caskey, 1996) we identified and determined the sequence of a partial human cDNA (data not shown), which, along with a schistosomal protein of unknown function (Davis et al., 1995), is also quite similar to SQV-8 and GlcAT-P and has an N-terminal transmembrane domain as well as a cysteine in the position equivalent to Cys317 of GlcAT-P.

Five other *C. elegans* proteins predicted by the genome project (Sulston et al., 1992) are also highly similar to SQV-8 and GlcAT-P. Four of the five open reading frames, T15D6.7, E03H4.12, C54C8.5, and T09E11.1, are located within a 120 kb region of the *C. elegans* genome and may therefore have originated from a single ancestral locus by relatively recent gene duplication; the fifth, K09B3.2, is located on a different chromosome. All five predicted proteins are more similar to one another than they are to SQV-8, GlcAT, and the human and schistosomal proteins and may therefore define a subfamily. For example, in the 34 amino acid region shown bracketed in Figure 2 (SQV-8 amino acid positions 156 to 189), SQV-8 is identical to GlcAT-P at 16 positions, of which 13 are not identical in either T15D6.7, E03H4.12, C54C8.5, or T09E11.1. In this same stretch, at least three of these latter four sequences are identical to one another at 23 positions, of which 19 are not identical in either SQV-8, GlcAT-P, or the human or schistosomal proteins. Analogous although less striking comparisons can be made for the region that includes the fifth predicted protein, K09B3.2. All five of the proposed subfamily members have an Arg residue instead of a Cys at the position equivalent to Cys317 of GlcAT-P. At least three and possibly four appear to lack N-terminal transmembrane domains; K09B3.2 is likely to be missing N-terminal sequence (the sequence of the genomic region 5' to K09B3.2 has not been completed), and so may also have a transmembrane region.

The similarity of SQV-8 to GlcAT-P suggests that the loss of SQV-8 might result in the loss of a carbohydrate moiety from one or more glycoconjugates and that the absence of this carbohydrate perturbs *C. elegans* vulval invagination. The molecular identity of SQV-3 supports this hypothesis.

Molecular identification of the *sqv-3* gene

sqv-3 maps to the genetic interval between *dpy-19* and *unc-69* on LG *III* (T. Herman, E. Hartwieg, and R. Horvitz, manuscript in preparation). We further mapped *sqv-3(n2842)* with respect to the *stP127* polymorphism in this region and found that two of eleven recombination events between *sqv-3(n2842)* and *unc-69(e587*am*)* occurred between *sqv-3(n2842)* and *stP127*, indicating that *sqv-3* was to the left of *stP127* and so on or to the left of the phage lambda clone RW#L127 (Williams et al., 1992). Because mutations in *sqv-3* fail to complement the deficiency *nDf40*, while mutations in *ced-7* complement *nDf40*, *sqv-3* was likely to be to the right of *ced-7*, which had been positioned on cosmid C29C23 (Y. Wu and R. Horvitz, unpublished results). We therefore assayed pools of cosmids spanning the region between C29C3 and RW#L127 for their ability to rescue the *sqv-3* mutant

phenotype. Cosmid C47F11 fully rescued the *sqv-3(n2842)* vulval defect and partially rescued the *sqv-3(n2842)* fertility defect (Figure 3A). The *sqv-3* rescuing activity was narrowed to a 2.4 kb Xba I-Sal I subclone, in which the *C. elegans* genome project predicted a single coding sequence, R10E11.4. Inserting an in-frame TAG stop codon predicted to eliminate the C-terminal 216 amino acids of the 289 amino acid R10E11.4 protein abolished the ability of the Xba I-Sal I fragment to rescue *sqv-3(n2842)*, suggesting that the *sqv-3* activity requires an intact R10E11.4 open reading frame (Figure 3A).

We used part of the Xba I-Sal I rescuing fragment to isolate seven *sqv-3* cDNA clones from a library derived from animals of mixed developmental stages. The end-sequences of three of these clones were identical to one another and matched sequence from the *sqv-3* genomic region, although the final 30 bp of 3' untranslated region from this cDNA is absent from the Xba I-Sal I rescuing fragment (Figure 3B). The four other clones contained sequence that was not from cosmid R10E11 and are likely to be artifactual. We determined the sequence of one of the three longest *sqv-3* cDNA clones (Figure 3B). Its coding sequence is identical to R10E11.4. This 1.2 kb *sqv-3* cDNA is likely to be full-length, since its 5' end contains nine nucleotides of the SL1 *trans*-spliced leader sequence, its 3' end contains a poly(A) tract, and a probe derived from the *sqv-3* cDNA hybridized to a single band of 1300 nt on a northern blot (Figures 3B and C).

Each of the three *sqv-3* mutant alleles contained a single nucleotide change within the open reading frame defined by the *sqv-3* cDNA. One, *n2842*, is predicted to result in an in-frame stop codon and the other two, *n2823* and *n2841*, in non-conservative changes in amino acid sequence (Figure 4).

SQV-3 is similar to mammalian β(1,4)-galactosyltransferases and pond snail β(1,4)-N-acetylglucosaminyltransferase

The SQV-3 protein is similar in amino acid sequence to a family of glycosyltransferases: the three human and other vertebrate β(1,4)-galactosyltransferases (the original human member of this family (GalT) is depicted in Figure 4) (Shaper et al., 1986; Masri et al., 1988; Almeida et al., 1997) and the pond snail *Lymnaea stagnalis* β(1,4)-N-acetylglucosaminyltransferase (GlcNAcT) (Bakker et al., 1994) (Figure 4). GalT catalyzes the addition of Gal from UDP-Gal onto GlcNAc, creating a Gal-β(1,4)-GlcNAc disaccharide, and GlcNAcT adds GlcNAc from UDP-GlcNAc onto GlcNAc, creating a GlcNAc-β(1,4)-GlcNAc disaccharide.

An alignment among SQV-3 and similar proteins is shown in Figure 4. Of the 289 amino acids in SQV-3, 57 (20%) are identical to those of the human GalT and 59 (20%) are identical to those of GlcNAcT. Like GalT and GlcNAcT, SQV-8 has a putative N-terminal transmembrane domain. Several residues have been implicated in the binding of GlcNAc and UDP-Gal by human GalT (Aoki et al., 1990) (Figure 4). All are conserved in SQV-3, and three of four residues are identical in GlcNAcT. This putative substrate-binding region is also similar to a region in a third glycosyltransferase, a human N-acetylgalactosaminyltransferase (GalNAcT), which has no other obvious sequence identities with GalT, GlcNAcT, or SQV-3 (data not shown). One of the *sqv-3* mutant alleles, *n2841*, results in a non-conservative amino acid change in this region.

The genome project predicts a second *C. elegans* protein, W02B12.11 (to which cDNA yk258c9 corresponds), which is also highly similar to GalT and GlcNAcT, slightly more so than is SQV-3. W02B12.11 has 78 identities with GalT and 81 with GlcNAcT, and, unlike that of SQV-3, the N-terminus of W02B12.11 is approximately as long as those of GalT and GlcNAcT.

There is some evidence that, unlike most glycosyltransferases, GalT may be located not only in the Golgi apparatus but also on the cell surface (Evans et al., 1995) and that cell surface GalT may have a longer N-terminus, resulting from an alternative upstream transcriptional start site (Shaper et al., 1988; Lopez et al., 1991). There is no evidence for analogously longer and shorter versions of SQV-3. We isolated only one class of cDNA, which is predicted to encode a SQV-3 protein with an even shorter N-terminus than that of the shorter GalT. This cDNA rescues the *sqv-3* mutant vulval defect when expressed under the control of the *C. elegans* heat-shock promoters (see Experimental Procedures), and there is no second ATG upstream of and in-frame with the likely ATG start site in the *sqv-3* genomic sequence (data not shown).

That SQV-3 is similar to GalT is of particular interest, since GalT catalyzes the formation of Gal-β(1,4)-GlcNAc, a substrate for the GlcAT-P that is similar to SQV-8. The molecular identities of SQV-8 and SQV-3 suggest that a carbohydrate related to GlcA-β(1,3)-Gal-β(1,4)-GlcNAc trisaccharide may be required for normal vulval invagination and that least some of the remaining *sqv* genes may encode other components required for the assembly of such a carbohydrate.

Molecular identification of the *sqv-7* gene

sqv-7 (T. Herman, E. Hartwieg, and R. Horvitz, manuscript in preparation) maps between *dpy-10* on cosmid ZK857 (Levy et al., 1993) and *let-253* on cosmids F31B8 and C24G10 on LG *II* (M. Labouesse, personal communication). The 17.3 kb Mlu I-Pst I subclone from cosmid C52E12, which maps to this interval, rescues both the vulval and fertility defects caused by *sqv-7(n2844)* (Figure 5A). This Mlu I-Pst I fragment is predicted by the *C. elegans* genome project to contain two coding sequences: C52E12.2, which corresponds to the *unc-104* gene (Otsuka et al., 1991), and C52E12.3 (Figure 5A). The *sqv-7* rescue activity seemed unlikely to correspond to C52E12.2 for the following reasons: *unc-104(e1265)* hermaphrodites have no Sqv vulval defect, *unc-104(rh142)/sqv-7(n2839)* animals are wild-type, and a construct that lacks the first half of C52E12.2, including its translational initiation codon, retains *sqv-7* rescue activity (Figure 5A). However, part of the *unc-104* genomic region, perhaps the large fourth intron, seems to be required for *sqv-7* rescue activity (Figure 5A); one possible explanation is that this region may be required for efficient expression of C52E12.3.

To test whether *sqv-7* corresponds to C52E12.3, we determined the molecular nature of the two existing *sqv-7* mutant alleles. Each contains a single nucleotide change within the predicted C52E12.3 open reading frame: *n2839* and *n2844* are missense alleles predicted to result in non-conservative changes in the C52E12.3 amino acid sequence (Figure 5B). We conclude that *sqv-7* corresponds to C52E12.3 or some variant of it that includes at least part of the exons affected by the two mutations described. That the predicted C52E12.3 protein shares considerable amino acid similarity with several previously identified proteins (Figure 5B; see below) increases the likelihood that this prediction is largely correct. In addition, the cDNA clone yk46f1 (5' read accession number D37556, 3' read accession number D34487) appears to correspond to part of C52E12.3 (data not shown), although it is incomplete (the first half of the open reading frame is missing) and contains an inversion when compared with C52E12 cosmid sequence. In the remainder of the paper we will refer to the protein product predicted from the C52E12.3 open reading frame as "SQV-7."

SQV-7 is similar to a putative nucleotide-sugar transporter

The SQV-7 protein is similar in amino acid sequence to a *Leishmania donovani* protein, LPG2, which is required for transport of GDP-mannose across membranes (Descoteaux et al., 1995; Ma et al., 1997) (Figure 5B). Because LPG2 is highly hydrophobic and somewhat similar to other proteins implicated in

transmembrane transport (Descoteaux et al., 1995), it has been suggested that LPG2 itself is a GDP-mannose transporter (Ma et al., 1997). Such transporters are required to bring nucleotide-sugars from the cytosol, where they are synthesized, into the ER and Golgi apparatus, where they are used as sugar-donor substrates by glycosyltransferases (Abeijon et al., 1997). Of the 329 amino acids in SQV-7, 67 (20%) are identical to those of LPG2 (Figure 5B), and the hydropathy plots (Kyte and Doolittle, 1982) of SQV-7 and LPG2 are highly similar (data not shown). From the Washington University-Merck EST Project we identified and determined the sequence of a partial human cDNA (data not shown), which encodes a protein that, along with a second human protein of unknown function, is also closely related in sequence to SQV-7.

Discussion

The *sqv* genes are likely to define components of a glycosylation pathway conserved from nematodes to humans

We have presented evidence that the *sqv* mutant defects in vulval invagination and early development are likely to result from defects in the assembly of a carbohydrate moiety. SQV-8 is similar to a vertebrate glucuronyltransferase, GlcAT-P, that catalyzes the addition of GlcA to Gal-β(1,4)-GlcNAc. Five other predicted *C. elegans* proteins also have sequence similarity to GlcAT-P but are more closely related in sequence to one another than they are to GlcAT-P and SQV-8 and lack the cysteine residue proposed to be required for GlcAT-P catalytic activity. They may be glucuronyltransferases with different acceptor specificities, as in the case of the human α-(1,3)-fucosyltransferase family (e.g., Weston et al., 1992; Holmes et al., 1995), which also includes members with and without a catalytic cysteine residue, one might be a homolog of the rat brain glucuronyltransferase, as yet characterized only biochemically, that appears to modify only glycolipid substrates (Oka et al., 1992), or, of course, they may have altogether different activities. None maps near any *sqv* gene so far identified. SQV-3 and a second predicted *C. elegans* protein, W02B12.11, which also does not map near any known *sqv* gene, are similar to β(1,4)-galactosyltransferases from vertebrates and GlcNAcT from a snail. Because SQV-8 is similar to a protein that uses Gal-β(1,4)-GlcNAc as a substrate, a simple model is that SQV-3 catalyzes the formation of this linkage (Figure 6), but clearly it is also possible that SQV-8 and/or SQV-3 have other glycosyltransferase activities or might even perform lectin-like rather than catalytic functions. SQV-7 is similar to a putative GDP-mannose transporter. Because human cells have no detectable GDP-mannose transport activity yet there are at least two human proteins similar to LPG2, it is likely that LPG2, SQV-7 and the two human proteins are members of a family of transporters that have a variety of nucleotide-sugar specificities (Ma et al., 1997). We therefore propose that SQV-7 may transport a nucleotide-sugar used as a substrate by SQV-3 or SQV-8. Because a human UDP-Gal transporter has been identified and has no sequence similarity to SQV-7 (Miura et al., 1996), one possibility is that SQV-7 is a UDP-GlcA transporter (Figure 6), although it is also possible that SQV-7 transports UDP-Gal or a different SQV-3 or SQV-8 substrate or that SQV-7 provides nucleotide-sugar to a third unidentified glycosyltransferase that can also affect vulval invagination. Other *sqv* genes might encode additional glycosyltransferases, additional proteins required for the biosynthesis or transport of nucleotide-sugar substrates of SQV-3, SQV-8, or other involved glycosyltransferases, or, possibly,

substrate for SQV-3 and SQV-8. The molecular and biochemical analysis of the SQV proteins may allow the systematic identification of many or all components of a conserved glycosylation pathway and may reveal new components not yet identified by purely biochemical means in other systems.

The *sqv* mutations are likely to disrupt only a small number of sugar linkages

Because relatively few (eight) *sqv* genes have been identified so far (T. Herman, E. Hartwieg, and R. Horvitz, manuscript in preparation), it is likely that the Sqv phenotype results from the disruption of only a small number of terminal glycosylation steps. That the glycosyltransferases similar to SQV-8 and SQV-3 are thought to act late in the glycosylation pathway is consistent with this idea, although, for example, SQV-8 and SQV-3 might instead synthesize the repeating disaccharide units of a glycosaminoglycan. These results support the general hypothesis that, although sufficient for the viability of mammalian cell lines (Stanley and Ioffe, 1995), minimal carbohydrate moieties are not sufficient for normal cell-cell and cell-matrix interactions in multicellular animals. *C. elegans* vulval invagination as well as oocyte and embryonic development apparently require more complex or specific oligosaccharides to proceed normally. That even the *sqv-3*-related ORF and the five *sqv-8*-related ORFs do not map near any *sqv* genes so far identified and hence are likely to have functions distinct from the *sqv* genes also suggests that the variety and complexity of carbohydrate modifications may reflect specificity of function *in vivo*. Clearly it will be of interest to identify the precise structure of the SQV-dependent carbohydrate as well as the nature of the glycoconjugate(s) it modifies: in particular, is this SQV-dependent carbohydrate acting indirectly to affect vulval invagination and other aspects of development, for example by affecting the stability or modulating the activity of the glycoconjugate(s) it modifies, or does it simply modify and thereby mask one or more carbohydrates or glycoconjugates that can otherwise perturb these processes, or, as in the case of glycosaminoglycans and the O-linked carbohydrates on mucins, does it exert its effect largely by virtue of its size and charge, or, as in the case of the selectin ligands, does it directly and specifically bind other molecules?

How might the absence of a carbohydrate moiety perturb vulval invagination?

Although the cellular basis for the Sqv vulval phenotype in particular is as yet unclear, several possible models are consistent with evidence that the carbohydrate moieties of glycoproteins and proteoglycans can affect cell-cell and cell-

matrix adhesion as well as the structure, rigidity, and hydration of the extracellular matrix (T. Herman, E. Hartwieg, and R. Horvitz, manuscript in preparation; reviewed by Varki, 1993). The future identification of the SQV-dependent carbohydrate, the glycoconjugate(s) modified, and the cellular and subcellular site(s) at which these act should clarify the nature of this involvement. While previous work has implicated glycoconjugates in some examples of epithelial invagination, all such evidence has come from *in vitro* manipulations of invaginating epithelia and from observing patterns of glycoconjugate expression (for example, Lane et al., 1993; Ingersoll and Ettensohn, 1994). The analysis of the *sqv* mutants provides *in vivo* evidence that glycosylation can affect epithelial morphogenesis as well as other aspects of development.

Experimental Procedures

Strains

Strains were cultured as described by Brenner (1974) and kept at 20°C. Most mutations and chromosomal rearrangements mentioned in this paper are described by Hodgkin et al. (1988) or Hodgkin (1997). Exceptions are *nDf40* (Hengartner et al., 1992), *qC1 dpy-19(e1259) glp-1(q339)* (Austin and Kimble, 1989; J. Austin and J. Kimble, personal communication), and *stP127* (Williams et al., 1992). The screen in which the *sqv-8*, *sqv-3*, and *sqv-7* mutations were obtained will be described elsewhere (T. Herman, E. Hartwieg, and R. Horvitz, manuscript in preparation). *sqv-8(mn63)* was isolated by Sigurdson et al. (1984) and was originally named *spe-2(mn63)*.

Complementation test between *sqv-7(n2839)* and *unc-104(rh142)*

Wild-type strain N2 males were mated to *sqv-7(n2839)* hermaphrodites and the male cross-progeny then mated to *dpy-10(e128) unc-104(rh142)/mnC1* hermaphrodites. The non-Dpy (cross) progeny were examined: none had Unc-104 or Sqv phenotypes. Twelve of these non-Dpy hermaphrodites were transferred one per plate; two generated both Sqv progeny and Dpy Unc-104 progeny, indicating that they were of genotype *dpy-10(e128) unc-104(rh142)/sqv-7(n2839)*.

Transformation rescue experiments

DNA transformation of *C. elegans* was accomplished as described by Mello et al. (1991). DNA was tested for *sqv-8* activity by injecting *sqv-8(mn63) unc-4(e120)/mnC1* hermaphrodites (at 1-10ng/ul). DNA was tested for *sqv-3* activity by injecting *sqv-3(n2842) unc-69(e587*am*)/qC1* hermaphrodites (at 1-10ng/ul). DNA was tested for *sqv-7* activity by injecting either *sqv-7(n2839)* or *sqv-7(n2844) unc-4(e120)/mnC1* hermaphrodites (at 10-50ng/ul). In all rescue experiments, the plasmid pRF4, which contains the dominant marker *rol-6(su1006)* (Kramer et al., 1990), was co-injected (at 80ng/ul) with the DNA to be tested, and independent lines of roller (Rol) animals were established. If Rol Unc animals, in the case of the *sqv-8(mn63) unc-4(e120)/mnC1*, *sqv-3(n2842) unc-69(e587*am*)/qC1*, and *sqv-7(n2844) unc-4(e120)/mnC1* strains, or Rol animals, in the case of the homozygous *sqv-7(n2839)* strain, were non-Sqv, then the injected DNA was considered to have rescuing activity. The two heat-shock *sqv-3* cDNA constructs (see below) were co-injected and together rescued the vulval defect of transgenic *sqv-3(n2842) unc-69(e587*am*)* animals (from *sqv-3(n2842) unc-69(e587*am*)/qC1* mothers) that had been

placed at 33°C for two hours at any time between the embyonic and late L3 stages. *sqv-3(n2842) unc-69(e587*am*)* animals transgenic for the heat-shock vectors pPD49.78 and pPD49.83 (see below) were Sqv even after heat shock.

General molecular methods

Standard molecular biology techiques were used (Sambrook et al., 1989). Database searches were performed with the BLAST program (Altschul et al., 1990) at the National Center for Biotechnology. The human cDNA clones, clone ID numbers 40880 and 132056, were from the Washington University-Merck EST Project (Gerhold and Caskey, 1996) and were provided to us by the I.M.A.G.E. consortium (Lennon et al., 1996). All genomic DNA fragments were subcloned into the pBluescript SK$^-$ vector (Stratagene, La Jolla).

To identify the DNA sequence changes in the mutant *sqv-8*, *sqv-3*, and *sqv-7* alleles, we PCR-amplified 0.5 to 1 kb regions of genomic DNA that spanned the *sqv-8*, *sqv-3*, and *sqv-7* regions from wild-type and mutant animals (Williams et al., 1992), and determined the sequences of the gel-purified PCR products. The sequences of all exons and intron-exon boundaries were determined for at least one strand, and any differences in DNA sequence between mutant and the wild type were confirmed by repeating the PCR amplification from single mutant worms and determining the sequence of the region for both strands.

***sqv-8* molecular biology**

A low-resolution restriction site map of the cosmid ZK1307 was determined by standard methods, and its Sac I-Eag I and two large EcoR V fragments subcloned. When the *C. elegans* genome project completed the sequence of cosmid ZK1307 the complete restriction map of this region and the Genefinder predictions of transcription units became available. The Eag I-Sac I subclone was predicted to contain two open reading frames, ZK1307.5 and ZK1307.9. The Eag I-Spe I subclone from this region was predicted to contain ZK1307.5 but eliminate the final two-thirds of ZK1307.9.

The Eag I-Spe I frameshift construct was made as follows: the oligonucleotides 5'-TATGGGCTAGCGCA-3' and 5'-TATGCGCTAGCCCA-3' were annealed to each other and inserted into the Nde I site of the Eag I-Spe I subclone; the presence of this insertion was confirmed by its introduction of a unique Nhe I site. This insertion results in an in-frame TGA codon, which is predicted to remove more than a third of the ZK1307.5 protein product. The insertion was precisely

removed by digesting the Eag I-Spe I frameshift construct with Nde I and reclosing; its absence was confirmed by the absence of any Nhe I site.

Eleven *sqv-8* cDNAs were isolated from a mixed-stage cDNA library (Okkema and Fire, 1994) by plaque hybridization (approximately 800,000 plaques were screened) to probe made from a 2.1 kb EcoR V-Kpn I fragment from the Eag I-Sac I subclone. The sequences of the ends of each positive cDNA clone were determined. The end-sequences of seven of these clones were identical to one another. Three others were shorter at their 5' ends: one by about 50 nt, one by about 170 nt and the third by about 310 nt. The insert of the final clone was much larger than the others (about 2.8kb), and its end-sequences were not contained within the ZK1307 cosmid. One of the seven identical cDNA clones was subcloned and the sequences of both strands determined. The 0.9kb Xba I-EcoR V fragment of the *sqv-8* cDNA was used to make probe for the northern blot.

***sqv-3* molecular biology**

A low-resolution restriction site map of the cosmid C47F11 was determined, and its Nhe I-Nar I, Apa I-Sac II and Sac II-Stu I fragments subcloned. When the *C. elegans* genome project completed the sequence of cosmid R10E11, which contains approximately the same genomic DNA as C47F11, the complete restriction map of this region and the Genefinder predictions of transcription units became available. The Xba I-Sal I subclone was predicted to contain a single transcription unit, R10E11.4.

The Xba I-Sal I frameshift construct was made as follows: the oligonucleotides 5'-TATGGGCTAGCGCA-3' and 5'-TATGCGCTAGCCCA-3' were annealed to each other and inserted into the Nde I site of the Xba I-Sal I subclone; the presence of this insertion was confirmed by its introduction of a unique Nhe I site. This insertion results in an in-frame TAG codon which is predicted to remove approximately the final three-quarters of the R10E11.4 protein product. The insertion was precisely removed by digesting the Xba I-Sal I frameshift construct with Nde I and reclosing; its absence was confirmed by the absence of any Nhe I site.

sqv-3 cDNAs were isolated from a mixed-stage cDNA library (Barstead and Waterston, 1989) by plaque hybridization (approximately 500,000 plaques were screened) to probe made from a 1.6kb Xba I-EcoR I fragment from the Xba I-Sal I subclone. The sequences of the ends of each positive cDNA clone were determined. The end-sequences of three of these clones were identical to one another. A fourth clone was approximately 44 bp shorter at the 5' end than the first three, and its 3'

end contained sequence that was not contained within cosmid R10E11, suggesting that a second fragment may have been misligated onto the 3' end. The remaining three clones contained no end-sequence that was from cosmid R10E11; one contained a poly(A) tract at each end. One of the three identical cDNA clones was subcloned using the flanking EcoR I linkers, and the sequences of both its strands were determined. The EcoR I-Xba I fragment of the *sqv-3* cDNA was used to make probe for the northern blot.

To express the *sqv-3* cDNA under the control of the heat-shock promoters, the EcoR I cDNA insert was blunted and ligated into the blunted Nhe I (5') and EcoR V (3') sites of the vectors pPD49.78 and pPD49.83 (Stringham et al., 1992; Mello and Fire, 1995).

sqv-7 molecular biology

A low-resolution restriction site map of the cosmid C52E12 was determined and its Sal I-Sal I fragment reclosed and Mlu I-Pst I fragment Eag I-Pst I fragments subcloned. The *C. elegans* genome sequencing project then made available the sequence and predicted transcription units of cosmid C52E12. The larger Sph I-Sph I fragment from the Mlu I-Pst I construct was reclosed, thereby removing the first half of the *unc-104* transcription unit, C52E12.2, and retaining the complete predicted C52E12.3 transcription unit.

Acknowledgments

We thank Beth James for help with DNA sequencing, and the *Caenorhabditis* Genetics Center for providing strains containing the *unc-104(rh142)* and *sqv-8(mn63)* mutations. This work was supported by United States Public Health Service research grant GM24663. H.R.H. is an Investigator of the Howard Hughes Medical Institute.

References

Abeijon, C., Mandon, E.C., and Hirschberg, C.B. (1997). Transporters of nucleotide sugars, nucleotide sulfate and ATP in the Golgi apparatus. Trends in Biochem. Sci. *22,* 203-207.

Almeida, R., Amado, M., David, L., Levery, S.B., Holmes, E.H., Merkx, G., van Kessel, A.G., Rygaard, E., Hassan, H., Bennett, E., and Clausen, H. (1997). A family of human β4-galactosyltransferases. Cloning and expression of two novel UDP-galactose:β-N-acetylglucosamine β1,4-galactosyltransferases, β4-Gal-T2 and β4-Gal-T3. J. Biol. Chem. *272,* 31979-31991.

Altschul, S.F., Gish, W., Miller, W., Myers, E.W., and Lipmann, D.J. (1990). J. Mol. Biol. *215,* 403-410.

Aoki, D., Appert, H.E., Johnson, D., Wong, S.S., and Fukuda, M.N. (1990). Analysis of the substrate binding sites of human galactosyltransferase by protein engineering. EMBO J. *9,* 3171-3178.

Asano, M., Furukawa, K., Kido, M., Matsumoto, S., Umesaki, Y., Kochibe, N., and Iwakura, Y. (1997). Growth retardation and early death of β-1,4-galactosytransferase knockout mice with augmented proliferation and abnormal differentiation of epithelial cells. EMBO J. *16,* 1850-1857.

Austin, J., and Kimble, J. (1989). Transcript analysis of *glp-1* and *lin-12,* homologous genes required for cell interactions during development of *C. elegans*. Cell *58,* 565-571.

Bakker H., Agterberg, M., Van Tetering, A., Koeleman, C.A., Van den Eijnden, D.H., and Van Die, I. (1994). A *Lymnaea stagnalis* gene, with sequence similarity to that of mammalian beta 1,4-galactosyltransferases, encodes a novel UDP-GlcNAc:GlcNAc beta-R beta 1,4-N-acetylglucosaminyltransferase. J. Biol. Chem. *269,* 30326-30333.

Bard, J. (1990). Morphogenesis: the cellular and molecular basis of developmental anatomy. Cambridge, England: Cambridge University Press.

Barstead, R.J., and Waterston, R.H. (1989). The basal component of the nematode dense-body is vinculin. J. Biol. Chem. *264,* 10177-10185.

Brenner, S. (1974). The genetics of *Caenorhabditis elegans*. Genetics *77,* 71-94.

Davis, R.E., Hardwick, C., Tavernier, P., Hodgson, S., and Singh, H. (1995). RNA trans-splicing in flatworms. Analysis of trans-spliced mRNAs and genes in the human parasite, *Schistosoma mansoni*. J. Biol. Chem. *270,* 21813-21819.

Descoteaux, A., Luo, Y., Turco, S.J., and Beverly, S.M. (1995). A specialized pathway affecting virulence glycoconjugates of *Leishmania*. Science *269,* 1869-1872.

Evans S.C., Youakim, A., and Shur, B.D. (1995). Biological consequences of targeting beta 1,4-galactosyltransferase to two different subcellular compartments. Bioessays *17*, 261-268.

Fristrom, D. (1988). The cellular basis of epithelial morphogenesis. A review. Tissue Cell *20*, 645-690.

Gerhold, D. and Caskey, C.T. (1996). It's the genes! EST access to human genome content. Bioessays *18*, 973-981.

Hengartner, M.O., Ellis, R.E., and Horvitz, H.R. (1992). *Caenorhabditis elegans* gene *ced-9* protects cells from programmed cell death. Nature *356*, 494-499.

Hodgkin, J. (1997). Appendix 1: Genetics. In *C. elegans* II, D.L. Riddle, T. Blumenthal, B.J. Meyer, and J.R. Priess, eds. (Cold Spring Harbor, New York: Cold Spring Harbor Laboratory Press), pp. 881-1047.

Hodgkin, J., Edgley, M., Riddle, D.L., and Albertson, D.G. (1988). Appendix 4: Genetics. In The Nematode *Caenorhabditis elegans*, W.B. Wood and the Community of *C. elegans* Researchers, eds. (Cold Spring Harbor, New York: Cold Spring Harbor Laboratory Press), pp. 491-586.

Holmes, E.H., Xu, Z., Sherwood, A.L., and Macher, B.A. (1995). Structure-function analysis fo human alpha 1-3fucosyltransferases. A GDP-fucose-protected N-ethylmaleimide-sensitive site in FucT-III and FucT-V corresponds to Ser178 in FucT-IV. J. Biol. Chem. *270*, 8145-8151.

Ingersoll, E.P. and Ettensohn, C.A. (1994). An N-linked carbohydrate-containing extracellular matrix determinant plays a key role in sea urchin gastrulation. Dev. Biol. *163*, 351-366.

Ioffe, E. and Stanley, P. (1994). Mice lacking N-acetylglucosaminyltransferase I activity die at mid-gestation, revealing an essential role for complex or hybrid N-linked carbohydrates. Proc. Natl. Acad. Sci. USA *91*, 728-732.

Kleene, R. and Berger, E.G. (1993). The molecular and cell biology of glycosyltransferases. Biochim. Biophys. Acta *1154*, 283-325.

Kornfeld, K. (1997). Vulval development in *Caenorhabditis elegans*. Trends Genet. *13*, 55-61.

Kornfeld, R. and Kornfeld, S. (1985). Assembly of asparagine-linked oligosaccharides. Annu. Rev. Biochem. 54, 631-664.

Kramer, J.M., French, R.P., Park, E.C., and Johnson, J.J. (1990). The *Caenorhabditis elegans rol-6* gene, which interacts with the *sqt-1* collagen gene to determine organismal morphology, encodes a collagen. Mol. Cell. Biol. *10*, 2081-2089.

Krause, M. and Hirsh, D. (1987). A trans-spliced leader sequence on actin mRNA in *C. elegans*. Cell *49,* 753-761.

Kyte, J. and Doolittle, R.F. (1982). A simple method for displaying the hydropathic character of a protein. J. Mol. Biol. *157,* 105-132.

Lane, M.C., Koehl, M.A.R., Wilt, F., and Keller, R. (1993). A role for regulated secretion of apical extracellular matrix during epithelial invagination in the sea urchin. Development *117,* 1049-1060.

Lennon, G.G., Auffray, D., Polymeropoulos, M., and Soares, M.B. (1996). The I.M.A.G.E. Consortium: an integrated molecular analysis of genomes and their expression. Genomics *33,* 151-152.

Levy, A.D., Yang, J., and Kramer, J.M. (1993). Molecular and genetic analyses of the *Caenorhabditis elegans dpy-2* and *dpy-10* collagen genes: a variety of molecular alterations affect organismal morphology. Mol. Biol. Cell *4,* 803-817.

Lopez, L.C., Youakim, A., Evans, S.C., and Shur, B.D. (1991). Evidence for a molecular distinction between Golgi and cell surface forms of beta 1,4-galactosyltransferase. J. Biol. Chem. *266,* 15984-15991.

Lu, Q., Hasty, P., and Shur, B.D. (1997). Targeted mutation in β1,4-galactosyltransferase leads to pituitary insufficiency and neonatal lethality. Dev. Biol. *181,* 257-267.

Ma, D., Russell, D.G., Beverly, S.M., and Turco, S.J. (1997). Golgi GDP-mannose uptake requires *Leishmania* LPG2. A membber of a eukaryotic family of putative nucleotide-sugar transporters. J. Biol. Chem. *272,* 3799-3805.

Maly, P., Thall, A., Petryniak, B., Rogers, C.E., Smith, P.L., Marks, R.M., Kelly, R.J., Gersten, K.M., Cheng, G., Saunders, T.L., Camper, S.A., Camphausen, R.T., Sullivan, F.X., Isogai, Y., Hindsgaul, O., von Andrian, U.H., Lowe, J.B. (1996). The alpha(1,3)fucosyltransferase Fuc-TVII controls leukocyte trafficking through an essential role in L-, E-, and P-selectin ligand biosynthesis. Cell *86,* 643-653.

Masri, K.A., Appert, H.E., and Fukuda, M.N. Identification of the full-length coding sequence for human galactosyltransferase (beta-N-acetylglucosaminide: beta 1,4-galactosyltransferase). (1988). Biochem. Biophys. Res. Commun. *157,* 657-663.

Mello, C. and Fire, A. (1995). DNA Transformation. Methods Cell. Biol. *48,* 451-482

Mello, C.C., Kramer, J.M., Stinchcomb, D., and Ambros, V. (1991). Efficient gene transfer in *C. elegans*: extrachromosomal aminenance and integration of transforming sequences. EMBO J. *10,* 3959-3970.

Miura, N., Ishida, N., Hoshino, M., Yamauchi, M., Hara, T., Ayusawa, D., and Kawakita, M. (1996). Human UDP-galactose translocator: molecular cloning of a

complementary DNA that complements the genetic defect of a mutant cell line deficient in UDP-galactose translocator. J. Biochem. (Tokyo) *120,* 236-241.

Morgan, W.R. and Greenwald, I. (1993). Two novel transmembrane protein tyrosine kinases expressed during *Caenorhabditis elegans* hypodermal development. Mol. Cell. Biol. *13,* 7133-7143.

Oka, S., Terayama, K., Kawashima, C., and Kawasaki, T. (1992). A novel glucuronyltransferase in nervous system presumably associated with the biosynthesis of HNK-1 carbohydrate epitope on glycoproteins. J. Biol. Chem. *267,* 22711-22714.

Okkema, P.G., and Fire, A. (1994). The *Caenorhabditis elegans* NK-2 class homeoprotein CEH-22 is involved in combinatorial activation of gene expression in pharyngeal muscle. Development *120,* 2175-2186.

Otsuka, A.J., Jeyaprakash, A., García-Añoveros, J., Tang, L.Z., Fisk, G., Hartshorne, T., Franco, R., and Born, T. (1991). The *C. elegans unc-104* gene encodes a putative kinesin heavy chain-like protein. Neuron *6,* 113-122.

Sambrook, J., Fritsch, E.F., andManiatis, T. (1989). Molecular Cloning: A Laboratory Manual (Cold Spring Harbor, New York: Cold Spring Harbor laboratory Press).

Schachner M. and Martini, R. (1995). Glycans and the modulation of neural-recognition molecule function. Trends Neurosci. *18,* 183-191.

Shaper N.L., Hollis, G.F., Douglas, J.G., Kirsch, I.R., Shaper, J.H. (1988). Characterization of the full length cDNA for murine beta-1,4-galactosyltransferase. Novel features at the 5'-end redict two translational start sites at two in-frame AUGs. J. Biol. Chem. *263,* 10420-10428.

Shaper N.L., Shaper, J.H., Meuth, J.L., Fox, J.L., Chang, H., Kirsch, I.R., and Hollis, G.F. (1986). Bovine galactosyltransferase: identification of a clone by direct immunological screening of a cDNA expression library. Proc. Natl. Acad. Sci. USA *83,* 1573-1577.

Sigurdson, D.C., Spanier, G.J., and Herman, R.K. (1984). *Caenorhabditis elegans* deficiency mapping. Genetics *108,* 331-345.

Stanley, P. (1984). Glycosylation mutants of animal cells. Annu. Rev. Genet. *18,* 525-552.

Stanley, P. and Ioffe, E. (1995). Glycosyltransferase mutants: key to new insights in glycobiology. FASEB J. *9,* 1436-1444.

Stringham, E.G., Dixon, D.K., Jones, D., and Candido, E.P.M. (1992). Temporal and spatial expression patterns of the small heat-shock (HSP16) genes in transgenic *Caenorhabditis elegans*. Mol. Biol. Cell *3,* 221-233.

Sulston, J.E. and Horvitz, H.R. (1977). Post-embryonic cell lineages of the nematode, *Caenorhabditis elegans*. Dev. Biol. *56,* 110-156.

Sulston, J., Du, Z., Thomas, K., Wilson, R., Hillier, L., Staden, R., Halloran, N., Green, P., Thierry-Mieg, J., Qiu, L., et al. (1992). The *C. elegans* genome sequencing project: a beginning. Nature *356,* 37-41.

Sundaram, M. and Han, M. (1996). Control and integration of cell signaling pathways during *C. elegans* vulval development. Bioessays *18,* 473-480.

Terayama, K., Oka, S., Seiki, T., Miki, Y., Nakamura, A., Kozutsumi, Y., Takio, K., and Kawasaki, T. (1997). Cloning and functional expression of a novel glucuronyltransferase involved in the biosynthesis of the carbohydrate epitope HNK-1. Proc. Natl. Acad. Sci. USA*94,* 6093-6098.

Varki, A. (1993). Biological roles of oligosaccharides: all of the theories are correct. Glycobiology *3,* 97-130.

Voshol, H., van Zuylen, C.W.E.M., Orberger, G., Vliegenthart, J.F.G., and Schachner, M. (1996). Structure of the HNK-1 carbohydrate epitope on bovine peripheral myelin glycoprotein P0. J. Biol. Chem. *271,* 22957-22960.

Weston, B.W., Nair, R.P., Larsen, R.D., and Lowe, J.B. Isolation o f a novel human alpha (1,3)-fucosyltransferase gene and molecular comparison to the human Lewis blood group alpha (1,3/1,4)-fucosyltransferase gene. Syntenic, homologous, nonallelic genes encoding enzymes with distinct acceptor substrate specificities. (1992). J. Biol. Chem. *267,* 4152-4160.

Williams, B.D., Schrank, B., Huynh, C., Shownkeen, R., and Waterston, R.H. (1992). A genetic mapping system in *Caenorhabditis elegans* based on polymorphic sequence-tagged sites. Genetics *131,* 609-624.

Figure 1. Identification of the *sqv-8* Gene by Transformation Rescue, *sqv-8* cDNA Sequence, and Northern Blot Analysis.
(A) Cosmid ZK1307 and plasmid clones assayed for *sqv-8* rescue activity. A '+' indicates that three or more independently transformed lines contained rescued *sqv-8* animals, and a '-' indicates that five or more independently transformed lines contained no rescued *sqv-8* animals. Underlined restriction sites are unique in the subset of the cosmid that is depicted. The open arrowhead indicates the site at which a frameshifting insert was introduced, and the vertical line in the bottom clone indicates the site from which this insert was precisely removed.
(B) Sequence of the *sqv-8* cDNA. Residues not contained within the *sqv-8* genomic region are underlined. The first such region matches the sequence of the SL1 trans-splice, and the second is a poly(A) tract. The predicted translational start codon is boxed, as is the predicted translational termination codon.
(C) Northern blot analysis of *sqv-8*. Radiolabeled *sqv-8* cDNA was used to probe a blot containing total RNA from a worm population of mixed stages. The black arrowhead indicates the single *sqv-8* transcript.

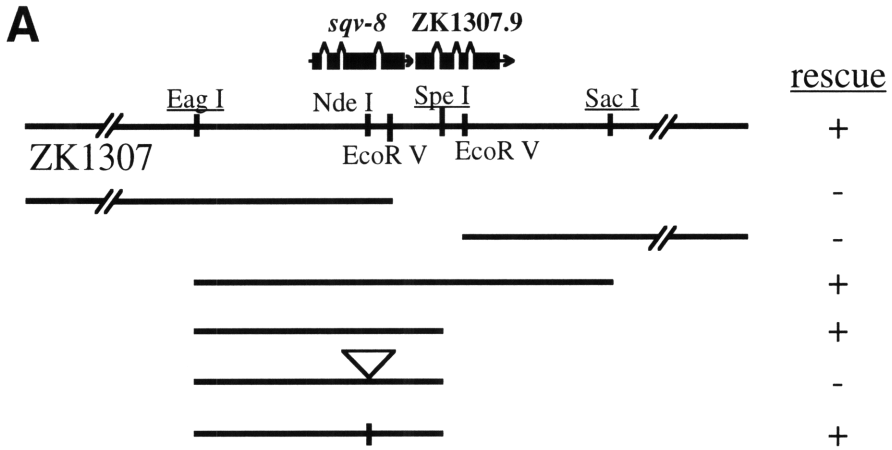

B

```
   1 GTTTGAGGGATAAATAAACCAAATGAAACTGTTCGACCTGTCGCCGCACC
  51 GACATAATGTTTCCATCTAGATTACTAGAAAAATGGTGGCTCCGAGCATT
 101 TATTGCACTTGTTATTTTCTTCGTTTGGCAACTATTTTATGCAATTAATC
 151 GGGTACAAAGTTTGGAAGAAGAACGGGCCACTTTGCAAGCTACCATAGAA
 201 GTTTTGACACGAAAAAGCGACGGGTTAAGAACGCAGATATTCGAAAAAGA
 251 ACGAAATTTGGTTCGATTAAATGGGAAAGTTGAGGAGATTGATACACAAA
 301 TACGCGATCATCTTTCCCTCCTGCCACGTGTTAATCGTTCAACGCCTTTC
 351 ATTTATTTTATAACTCCAACACATTTCCGCGCTGCTCAGCGAGCCGATCT
 401 CACTCGTCTATCCTACACGCTTTCCCATGTTCCCAACCTCCATTGGATCG
 451 TTGTAGAAGATTCCGATGAACTCACACCATCCATCGCCGGAATTCTGAAA
 501 AGATCAAAAATTCCAAATACACATCTAAATGCTCGAACTCCGTCTGATCA
 551 AAAAATGAGATACGATGACCCCAATTGGACGTTGCCACGTGGCGTTGAGC
 601 AACGAAATCGAGCACTTTTATGGATTCAAAATCAATTGAGTGGTGTGAAA
 651 GAGGGCGTTGTGTACTTTGGAGATGATGATAACACATATGATCTGAAAAT
 701 TTTCGGAGAAATGCGGAAAGTGAAAAATGCAGGAGTTTGGCCAGTTGGAA
 751 TAGTTGGTGGAATGTTTGTAGAAACGCCAATTTTAGAGAAAAATGGATCG
 801 ATTTCCCATTTCAACGCTGTCTGGAAACCGGAGCGTCCATTTCCGATCGA
 851 TATGGCTGCATTTGCAGTCAATATTTCTCTGGTTCTCTCCAACGCGAACG
 901 CTCTTTTCTCATTCGACGTGCCTCGTGGATATCAAGAATCTACTTTTCTT
 951 GAAAATCTTGGAATTCATCGTTATAATATGGAACCACTTGCGGAAATGTG
1001 CACGAAAGTGTATGTGTGGCATACGAGAACTGAAAAACCGAAATTGTCGA
1051 AAGAATCGATTGATCGATTGACTAAAAAGACAGGATTCAACTCGTTAGAA
1101 GCACATGCGCTTGGTGTGGATAATTAAGAAAAGTTCTAATTTTGTTATTT
1151 TTGTTGAAGTACCCATTTTAGTTTGATATAATTCATTTTCCACAGATTTT
1201 ACCCAATGTACAAAAACCTACGAGTACCCTTTTATTGCATTTTGACTAAC
1251 TTTCATAAATATTTTTCTTTAAAAAAAAAAAAAAAAAA
```

C

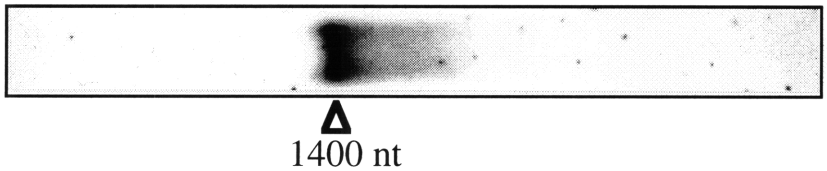

Figure 2. SQV-8 is Similar to a Glucuronyltransferase.
Alignment of the SQV-8 and rat protein-specific glucuronyltransferase (GlcAT-P) protein sequences as well as protein sequences predicted from a human cDNA (40880), a schistosomal cDNA, and five *C. elegans* open reading frames (T15D6.7, E03H4.12, C54C8.5, T09E11.1, and K09B3.2) predicted by the genome project. Identities between SQV-8 and any other protein are boxed in black. Three or more identical residues that are not shared with SQV-8 are boxed in grey (in some cases two different sets of three identities are in grey within a single column). The underlined amino acids were predicted by the algorithm of Kyte-Doolittle (1982) (using spans of seven) to have positive hydrophobicity and may therefore be contained within transmembrane domains. The predicted change in amino acid sequence caused by each mutant *sqv-8* allele is indicated directly above the amino acid affected, and the DNA sequence of mutant stop codons is noted in parentheses. Cys317 of GlcAT is indicated by a black arrowhead. The region of the alignment from SQV-8 amino acid positions 156 to 189 is bracketed underneath (see text). The human cDNA is likely to be incomplete at its 5' end, as indicated by three dots at the N-terminus of the human protein. The K09B3.2 prediction is also likely to be missing N-terminal amino acids, since the sequence of the corresponding genomic region has not been completed.

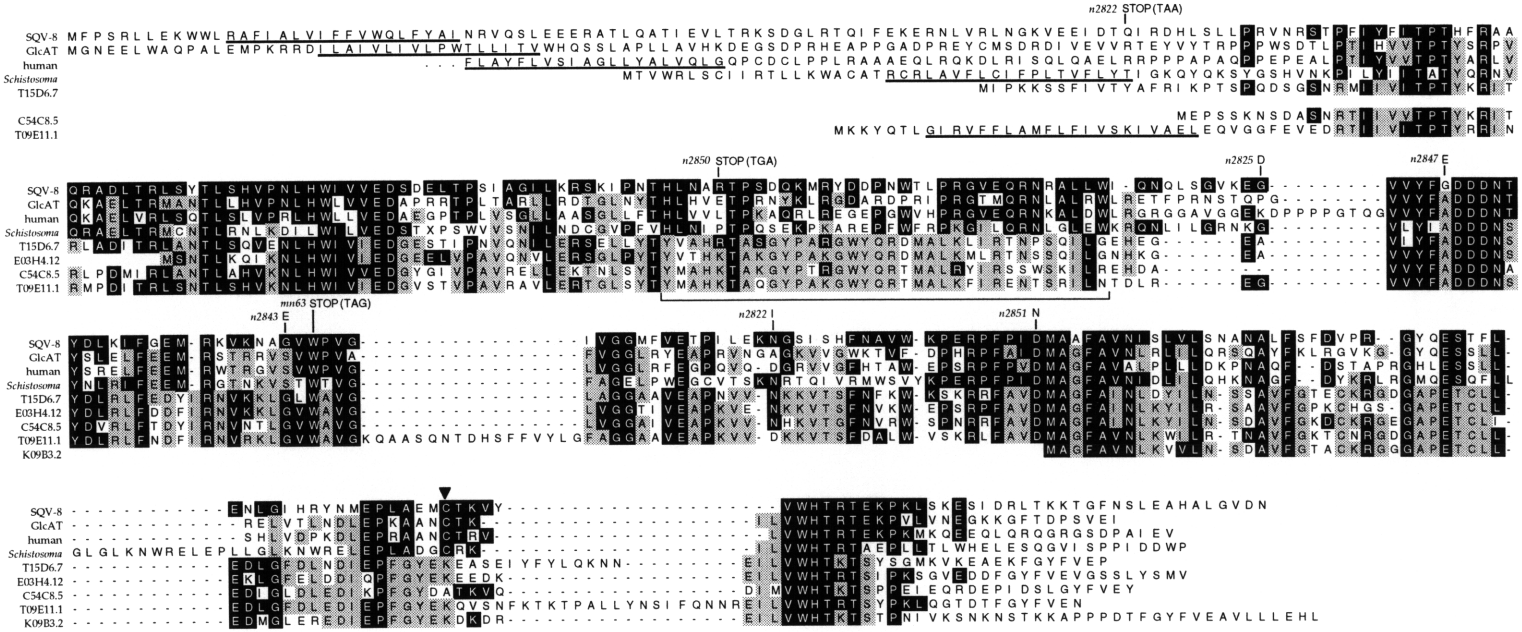
n2822 STOP(TAA)
SQV-8
GlcAT
human
Schistosoma
T15D6.7
C54C8.5
T09E11.1
n2850 STOP(TGA)
n2825 D
n2847 E
E03H4.12
K09B3.2
mn63 STOP(TAG)
n2843 E
n2822 I
n2851 N

Figure 3. Identification of the *sqv-3* Gene by Transformation Rescue, *sqv-3* cDNA Sequence, and Northern Blot Analysis.
(A) Cosmid C47F11 and plasmid clones assayed for *sqv-3* rescue activity. Symbols are used as in Figure 1A.
(B) Sequence of the *sqv-3* cDNA. Symbols are used as in Figure 1B. The open arrowhead indicates the end of the Xba I site of the Sal I-Xba I genomic fragment that rescues *sqv-3*.
(C) Northern blot analysis of *sqv-3*. Radiolabeled *sqv-3* cDNA was used to probe a blot containing total RNA from a worm population of mixed stages. The black arrowhead indicates the single *sqv-3* transcript.

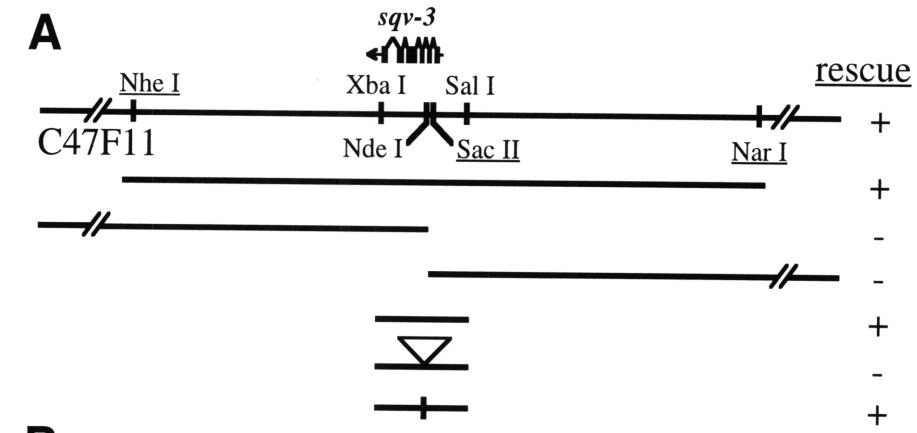

B

```
   1 AAGTTTGAGAAGAAGCCTCTTCTCTTTAGCACAAGCTGTACCAGATGAAA
  51 TGAAGCTCAAAACGCGGTTAATCCTTTCGGGAACCATTTTAATCTCGTTA
 101 GCTGCATGTTATTTCTTAGTTCTTTTGGTTCTCGATTTAGAGATAACGAG
 151 GGATCTTATGACTGATTATGTAGATCCGCGGCCATTACAAACCAGCTATC
 201 ATAAACTGTGCGTTATCGTTCCGTATCGAGATCGGCTTGAAGAACTTCGA
 251 GAATTTTCTCCCCATATGTCAAAATTTCTACATAATCAAAACGTCTCTCA
 301 TCACATTTTAATCATCAATCAAACGGATCCTCTTCGATTTAATAGAGCTT
 351 CTCTAATAAATGTTGGCTGGAACGAAGCAGATCGTCTTGGATGTGACTAC
 401 ATGGTGATGAACGATGTAGATCTGTTGCCTGTCAATCCAGAAGTTCCGTA
 451 CGATTTTCCGGGAATCGGTGTGATTCGGCACATAACCTCTCCCCAGTATC
 501 ATCCGAAATATCACTATGAAAAGTTTATCGGAGGAATATTGATGCTGACA
 551 CTGAAAGATTACAAAAAACTAAATGGAATGTCGAATAAGTATTGGGGATG
 601 GGGACTTGAAGACGATGAGTTTTATCTCAGAATTATCGACAGCAAGCTCA
 651 ATCTAACTCGAGTTTCTGGTCTATCAACAGATAGTTCAAACACTTTTCGG
 701 CATATTCATGGACCAAAAAGAAAAAGAGATTATACTCCAAAGAAAAATGA
 751 TAAGAATCAATGGGAGATTAAACGGAAAAGAGATCATGTATCCGGTCTCC
 801 ACGACGTCCGCTACCTCATCGATAGTCGCCAACTCCTCGACTTTTCTGGA
 851 ACTTCAGTTACCATTATCAATGTCGCCTTACACTGCGATCTGAATTGGAC
 901 ACCTTATTGCAAATCATAGTCCATAATATTATATCATTTATTTATTGTTA
 951 TCCTCATTCCAGTTTTGCAATTTTCATTTTTTCCAGTCTTTCCCCCCAGT
1001 TATTCAGTGCCTTTTCTTACTTTTTTGTACGCGGGTCTCCCCCTCATTCG
1051 GGTTCTCATTTGTGATTTTTCAAAAAGATTTAATCGGTTTAATTTAATTT
1101 TCCAAGTGCCTTTCAAATTCTAGAATAATTTATCCATAAAATATACAAAT
1151 GATAAAAAAAAAAA
```

C

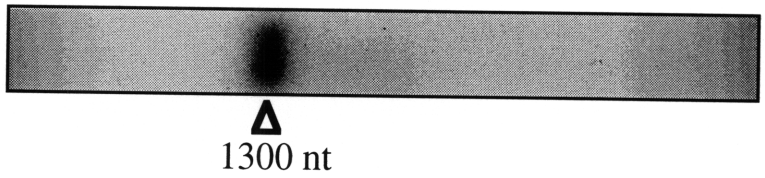

Figure 4. SQV-3 is Similar to Members of a Glycosyltransferase Family. Alignment of the SQV-3, human β(1,4)-galactosyltransferase (GalT), pond snail β(1,4)-N-acetylglucosaminyltransferase (GlcNAcT), and partial human N-acetylgalactosaminyltransferase (GalNAcT) protein sequences and a *C. elegans* protein sequence, W02B12.11, predicted by the genome project. Identities, transmembrane domains, and predicted changes in mutant alleles are indicated as in Figure 2. Open arrowheads indicate GalT Tyr and Trp residues implicated in binding GlcNAc and/or UDP-Gal, the black arrowhead indicates a GalT Trp residue required for catalytic activity, and the grey arrowhead indicates a GalT Tyr residue that can be replaced by Phe without affecting catalytic activity (Aoki et al., 1990). The long version of GalT is shown, and the initiator methionine of the short version is circled.

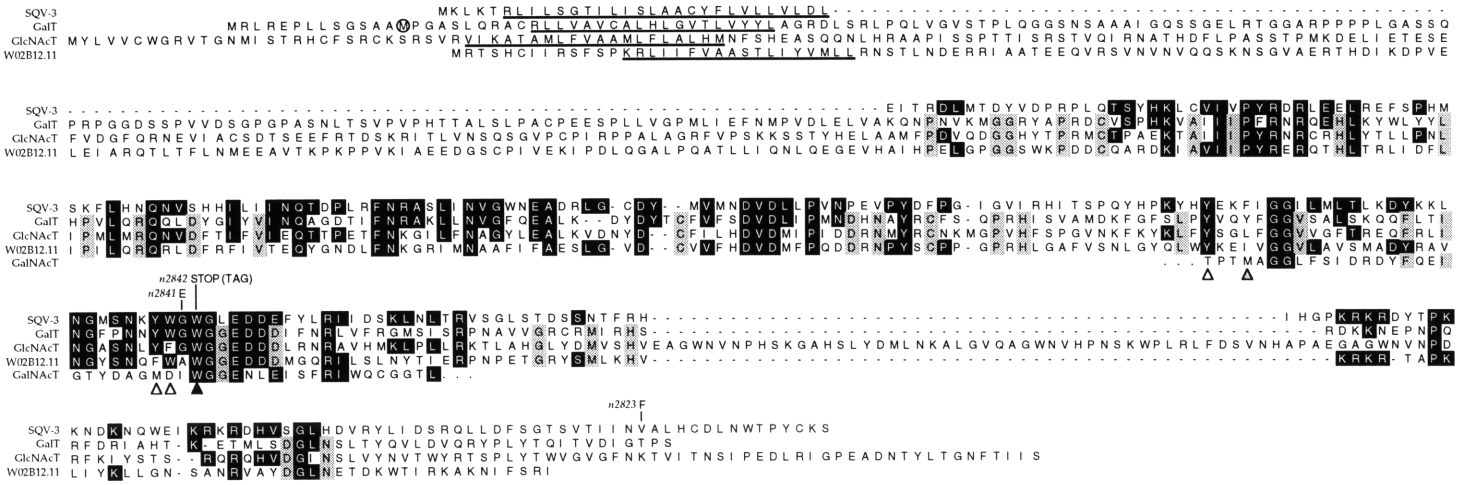
SQV-3
GalT
GlcNAcT
W02B12.11
GalNAcT
n2842 STOP (TAG)
n2841 E
n2823 F

Figure 5. Identification of the *sqv-7* Gene by Transformation Rescue. SQV-7 is Similar to LPG2, a Protein Required for GDP-mannose Transport.
(A) Cosmid C52E12 and plasmid clones assayed for *sqv-7* rescue activity. A '+' indicates that two or more independently transformed lines contained rescued *sqv-7* animals. Otherwise symbols are used as in Figure 1A.
(B) Alignment of the SQV-7 and *Leishmania* LPG2 protein sequences and protein sequences predicted from two human cDNAs. human 1 is predicted from cDNA accession number D87449, and human 2 from clone 132056. The human 2 cDNA is likely to be incomplete at its 5' end, and this is indicated by three dots at the human 2 N-terminus. Identities and predicted changes in mutant alleles are indicated as in Figure 2.

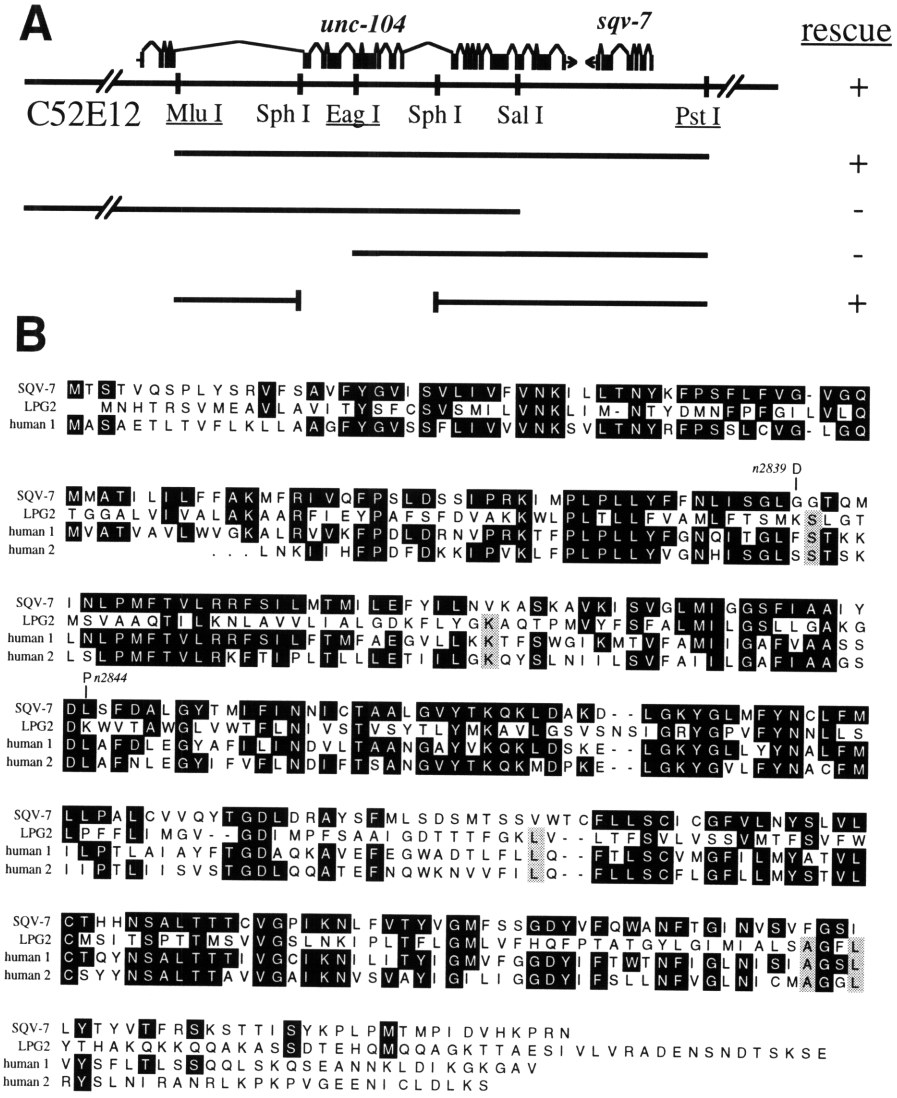
A
unc-104
sqv-7
rescue
C52E12
Mlu I
Sph I
Eag I
Sph I
Sal I
Pst I
+
+
-
-
+
B
SQV-7
LPG2
human 1
human 2
n2839 D
P n2844

Figure 6. A Model for *sqv* Gene Function.
SQV-3, SQV-7, and SQV-8 may catalyze the formation of an oligosaccharide on one or more glycoproteins. The black squiggle represents a transmembrane glycoprotein and the straight line an oligosaccharide of unspecified structure. The biochemical activities proposed for SQV-3, SQV-7, and SQV-8 are based on those defined for the proteins related to them in amino acid sequence (see text). Because a human UDP-Gal transporter has been identified and is unrelated in sequence to SQV-7, SQV-7 is depicted as a UDP-GlcA transporter. The terminal oligosaccharide is depicted as an unsulfated version of the HNK-1 epitope but may instead be less closely related to this epitope, may be further modified by the addition of sugars and/or sulfate groups, or may occur as a repeating rather than terminal unit (see text).

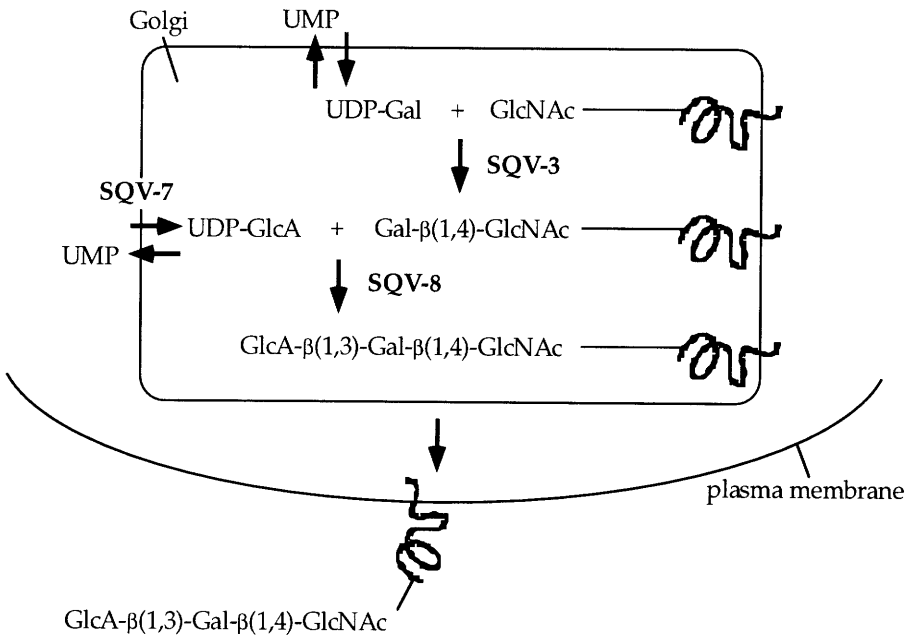
Golgi
UMP
UDP-Gal + GlcNAc
SQV-3
SQV-7
UDP-GlcA + Gal-β(1,4)-GlcNAc
UMP
SQV-8
GlcA-β(1,3)-Gal-β(1,4)-GlcNAc
plasma membrane
GlcA-β(1,3)-Gal-β(1,4)-GlcNAc

Cold Spring Harbor Symp. Quant. Biol. **62**, in press.

Appendix one

Mutations that Perturb Vulval Invagination in *C. elegans*

Tory Herman and H. Robert Horvitz

Correction after submission: the description of vulval development in the text and Figure 1 is incorrect in its description of the order in which vulval cell fusions occur and also contains misattributions. The section from "The middle cell, P6.p, gives rise to..." to "... (reviewed by Greenwald 1997)" is incorrect in its description of the order of vulval cell fusion (for the primary cell descendants) and misattributes the error to Greenwald (1997), and the phrases "...each of the 14 vulval cells..." and "These cells fuse pairwise..." are also incorrect and misattribute the error to personal communication from John White. For an accurate description see chapter one of this thesis.

During development, animals undergo dramatic changes in patterning as a result of the movement and shaping of epithelial cell layers (Bard 1990). Sheets of epithelial cells fold, branch, spread, and detach from or fuse with one another to generate the three-dimensional topology of an embryo. One example of such a morphogenetic process is epithelial invagination, which generates tubular structures from flat epithelia. To invaginate, a flat sheet of epithelial cells bends and moves inward, its apical surface facing the concave side of the depression. During sea urchin and *Drosophila* gastrulation, an epithelium bends inward about a point to form the digestive tract. The result is a tube that is perpendicular to the original sheet (Sweeton et al. 1991; reviewed by Davidson et al. 1995). By contrast, vertebrate neurulation, which forms the spinal cord and brain, is initiated by the invagination of a sheet that bends along a line and results in a tube that is parallel to the original sheet (reviewed by Schoenwolf and Smith 1990).

Many models have been proposed for the mechanistic basis of epithelial invagination (for reviews see Ettensohn 1985; Fristrom 1988; Davidson et al. 1995). In general, these models postulate a mechanical force that decreases the area of the apical surface of the epithelial sheet relative to the area of its basal surface, causing an inward bend. The models differ in which cellular process initially provides this mechanical force.

A simple cytoskeleton-based model is that invagination results from individual changes in cell shape. Apically-localized actin filaments contract and thereby decrease the apical surface area of each epithelial cell in the sheet, resulting in inward bending. This type of mechanism has been proposed for *Drosophila* gastrulation (Sweeton et al. 1991; Costa et al. 1994) and for neurulation (Clausi and Brodland 1993). A more complex cytoskeleton-based model involves cell crawling: cells in the invaginating region pull themselves toward the center of the region by extending their apices along the extracellular matrix (Burke et al. 1991). If the volume and basal surface areas of each cell remain constant, this apical extension decreases the apical surface area, again resulting in bending of the sheet. This type of mechanism has been proposed for sea urchin gastrulation (Burke et al. 1991).

Changes in cell-cell adhesion also could initiate epithelial invagination (Gustafson and Wolpert 1963). If the adhesion between adjacent cells increases, it would be energetically favorable for the contact between them to increase in extent, causing the cells to increase in height and become thin and columnar. However, if the basal side of each cell remains strongly adherent to a basal lamina, forcing the basal surface area to remain constant, the increase in cell height would decrease only

the apical surface area, and the epithelial sheet would bend inward. There are also more complex models of invagination based on local differences in cell-cell adhesivity within a sheet (Nardi 1981; Mittenthal and Mazo 1983). Although adhesion-based models explain the columnarization of epithelial cells that is nearly always observed during invagination (Fristrom 1988), they seem to be less popular than cytoskeleton-based models.

A third type of model, which has been proposed for sea urchin gastrulation, is based on changes in the composition of the extracellular matrix (Lane et al. 1993). According to this model, the apical surface of the epithelial sheet in the region where invagination is to occur secretes a proteoglycan, which forms a hygroscopic layer of matrix between the epithelium and the original extracellular matrix. The inner matrix layer swells as it becomes hydrated, increasing in surface area, while the outer layer remains the same. This difference in surface areas results in the bending inward of the outer matrix layer and a concomitant bending inward of the underlying epithelial sheet.

Although each of these models proposes that a single cellular process provides the mechanical force required for epithelial invagination, each requires the coordinated regulation of other cellular processes. For instance, if the cells in a sheet adhere too greatly to the apical extracellular matrix, they will not be able to constrict their apical surfaces appropriately. Similarly, if the cells in a sheet have too rigid a cytoskeleton, an increase in cell-cell adhesion will not cause an increase in cell height. Thus, disruption of a cellular process that is not the primary initiator of epithelial invagination may affect the invagination process. Furthermore, these models are not mutually exclusive: the mechanical force required for epithelial invagination might be provided simultaneously by several cellular processes, with partially or fully redundant abilities to initiate invagination. Finally, different instances of epithelial invagination may have different mechanistic bases.

To identify molecules involved in epithelial invagination, we have been analyzing an example of this process in the nematode *Caenorhabditis elegans*. During the larval development of the *C. elegans* hermaphrodite, a specialized group of outer epithelial cells invaginates to form the vulva, a tube that connects the outer epithelium to the uterine epithelium and allows outward passage of eggs and inward passage of male sperm. Many basic problems of developmental biology have been studied by analyzing the development of the *C. elegans* vulva, including the generation of cell diversity and the determination of cell type, intercellular signaling and signal transduction, and the control of developmental timing (Ferguson et al.

1987; Labouesse et al. 1994; Clark et al. 1993; Euling and Ambros 1996; reviewed by Horvitz and Sternberg 1991; Kornfeld 1997). We have begun a genetic analysis of vulval invagination.

The vulva is formed by the descendants of three epithelial cells

C. elegans larvae and adults are enclosed by a single layer of epithelial cells interconnected by desmosomes. The apical surface of this epithelium faces outward and secretes the cuticle, a multi-layered extracellular structure consisting in large part of collagens. The basal surface contacts a basal lamina (White 1988).

The vulva is formed by the descendants of three epithelial cells, P5.p, P6.p, and P7.p (Fig. 1). During the third larval (L3) stage, these vulval precursor cells lie in an outer epithelial sheet, and their basal sides abut a basement membrane that lies between them and the developing gonad. A specialized cell in the developing gonad, the anchor cell, overlies P6.p. During L3 stage, the anchor cell signals the vulval precursor cells to divide. The middle cell, P6.p, gives rise to a symmetric lineage termed "primary" and generates four binucleate descendants (two E cells and two F cells). P5.p and P7.p, the two cells flanking P6.p, give rise to asymmetric mirror-image lineages termed "secondary;" each generates two binucleate (A and C) and three mononucleate (B1, B2 and D) descendants (reviewed by Greenwald 1997).

Just before and during the final round of vulval cell division, the epithelium thickens slightly in the region at which invagination will occur. As this final division is completed, the central vulval cells, consisting of all of the primary descendants and some of the secondary descendants, detach from the rigid cuticle, and the epithelial layer buckles inward, resulting in a fluid-filled invagination space between the vulva and the cuticle. During the fourth larval stage (L4), each of the 14 vulval cells becomes U-shaped, extending lateral arms toward its mirror-image equivalent (J. White, personal communication). These cells fuse pairwise, resulting in seven toroidal cells stacked one on top of another and connected by desmosomes (Podbilewicz and White 1994; Newman and Sternberg 1996). The vulval cell at the top of the stack forms an attachment with the uterine epithelium, while the vulval cell at the bottom remains attached to the outer epithelium (Newman et al. 1996). The inner holes of these vulval toroids define the tube through which eggs and sperm pass in the adult.

During the second half of the L4 stage, the inner and outer diameters of the vulval toroids decrease. At the molt between the L4 and adult stages, the vulva

everts, causing the outer toroids to become considerably stretched (White 1988; J. White, personal communication).

The anchor cell is required for wild-type vulval invagination

Several cells are in direct contact with the vulval cells during vulval morphogenesis and are thus candidates for affecting vulval invagination. The function of some of these cells in invagination has been tested by eliminating or displacing them and observing the consequences on vulval development.

The anchor cell is required not only to signal the vulval precursor cells to divide, but also to organize the invagination of the P6.p descendants. This conclusion is based upon experiments in which a laser microbeam was used to ablate the anchor cell just after it had signaled P5.p, P6.p, and P7.p to divide (Kimble 1981) and from observations of *dig-1* mutant hermaphrodites, in which the entire gonad, including the anchor cell, detaches from the basement membrane adjoining the vulval cells and becomes mislocalized (Thomas et al. 1990). In both cases, the vulval precursors often undergo a completely wild-type pattern of cell divisions, but, in the absence of direct contact with the anchor cell, their descendants invaginate abnormally: the primary descendants do not remain symmetrically arranged and fail to form toroids, and no inner invagination space is formed between them. The secondary descendants appear to invaginate correctly. Within the gonad, the anchor cell is not only necessary but also sufficient to organize the primary cells: the rest of the gonad can be ablated without affecting the initial stages of vulval invagination (Kimble 1981), although the absence of the uterine uv1 cells prevents the attachment of the developing vulva to the uterus (Newman et al. 1996).

Although the vulval muscles form specific attachments to the vulval toroids and the outer epithelium during the L4 stage, these muscles are not required for vulval invagination. *sem-4* mutant hermaphrodites, which entirely lack vulval muscles (Basson and Horvitz 1996), appear to have wild-type invaginations and can receive sperm through their adult vulvae (Desai et al. 1988; T. Herman, E. Hartwieg, and H. Horvitz, in prep.).

Throughout their development the vulval cells are surrounded by hyp7, the main body epithelium. The function of hyp7 in vulval invagination cannot easily be tested, since ablation of hyp7 is lethal to the animal (Sulston et al. 1983).

Mutations in eight genes affect vulval invagination

To identify genes involved in vulval invagination, we sought mutations that affected the invagination of the vulva but did not alter vulval cell lineages. Although one might expect that a hermaphrodite abnormal in vulval invagination would be unable to lay eggs as an adult, previous screens for fertile mutants with defects in laying eggs (Trent et al. 1983) had not identified any that met our criteria. We therefore performed a genetic screen for mutants with abnormal vulval invaginations in a way that allowed the recovery of mutations that additionally caused sterility or maternal-effect lethality (T. Herman, E. Hartwieg, and H. Horvitz, in prep.). Single F1 progeny of hermaphrodites mutagenized with ethyl methanesulfonate (EMS) were placed on Petri plates, and their L4 progeny were examined first with a dissecting microscope for abnormal vulval invaginations and then with Nomarski differential interference contrast microscopy to determine whether their vulval cell lineages were normal. Mutations that caused sterility were recovered in heterozygous siblings from the same F2 brood. In a screen of 12,000 mutagenized haploid genomes, we identified 25 mutations that define eight genes required for wild-type vulval invagination. We named these genes *sqv-1* to *sqv-8*, for squashed vulva. None of the *sqv* mutations affects the number or lineage of the vulval cells. Nearly all cause sterility.

All 25 mutations isolated result in the same abnormal vulval phenotype (Fig. 2). In the *sqv* mutants from the time the final round of vulval cell divisions begins there is a reduction in the size of the space that separates the anterior and posterior halves of the vulva (T. Herman, E. Hartwieg, and H. Horvitz, in prep.). Both primary and secondary descendants are affected: *lin-12(lf) sqv-3* double mutants, in which the vulval precursor cells generate primary but no secondary lineages (Greenwald et al. 1983), have decreased invaginations when compared with *lin-12(lf)* single mutants. Similarly, *lin-12(gf) sqv-3* double mutants, in which the vulval precursor cells generate secondary but no primary lineages (Greenwald et al. 1983), have decreased invaginations when compared with *lin-12(gf)* single mutants (T. Herman, E. Hartwieg, and H. Horvitz, in prep.). This reduction in the invagination space, and later in the vulval tube, remains evident throughout the L4 stage until adulthood, when both the mutant and wild-type vulval tubes are closed and therefore indistinguishable.

Despite being abnormal in invagination, *sqv* mutant vulval cells are wild-type in lineage, movement toward the anchor cell, and detachment from the cuticle, and mutant vulval nuclei migrate to and occupy wild-type positions throughout the L4 and adult stages.

The decreased invagination space in *sqv-3* mutants is a consequence of elongated vulval cells

To examine the ultrastructural basis of the Sqv vulval defect, we analyzed electron micrographs of serial sections of wild-type and *sqv-3* mutant vulvae at the early L4 stage (T. Herman, E. Hartwieg, and H. Horvitz, in prep.). We detected two main differences. First, at least some *sqv-3* mutant vulval cells appear to be more elongated than their wild-type equivalents. The central vulval cells, in particular, appear to extend too far into the region that is normally occupied by the invagination space.

Second, the material within the vulval invagination space is more electron-dense and more uniform in *sqv-3* animals than that in the wild type. This electron-dense material may be qualitatively identical to that in the wild type but may look different because it is compressed into a smaller volume. Alternatively, the difference in appearance may reflect a difference in the composition of the material in the mutant invagination space. The electron microscopic studies confirm that the *sqv-3* mutant vulval cell bodies are arranged in grossly wild-type positions relative to one another and that the appropriate cells have detached from the cuticle.

***sqv* vulval cells form a partially functional tube**

Despite the abnormal appearance of the *sqv* vulval invagination, *sqv* mutant vulval cells form a vulval tube. The antibody MH27, which recognizes desmosomal connections between epithelial cells (Waterston 1988), stains the wild-type mid-L4 vulva in a pattern of rings, the points of contact between the vulval toroids. A *sqv* mutant vulva stained with MH27 has the same pattern of rings as a wild-type vulva, suggesting that the vulval toroids have formed correctly (T. Herman, E. Hartwieg, and H. Horvitz, in prep.).

Furthermore, *sqv* mutant adults are able to lay eggs, indicating the presence of a functional vulval tube; nonetheless, these animals retain an abnormally large number of eggs in their uterus (T. Herman, E. Hartwieg, and H. Horvitz, in prep.). This defect in egg-laying is likely to be a consequence of the vulval abnormality, since the other components of the egg-laying system, the vulval muscles and the HSN neurons (Trent et al. 1983), are present in *sqv* mutant animals, although their adult differentiation and function has not been tested (T. Herman, E. Hartwieg, and H. Horvitz, in prep.).

Several models could explain the Sqv vulval phenotype

The *sqv* mutations result in an abnormal elongation of the central vulval cells but do not prevent the bending inward of the vulval epithelium or the subsequent formation of the stack of toroidal vulval cells. One simple explanation for the Sqv phenotype can be derived from the adhesion-based model of invagination discussed above (Gustafson and Wolpert 1963). During normal vulval invagination, the adhesiveness between adjacent vulval cells may increase, resulting in an increased contact between them and their visible increase in cell height (Fig. 3). The Sqv phenotype could result from a greater than normal increase in the adhesiveness between adjacent vulval cells. Such a greater adhesiveness could abnormally increase the extent of contact between the vulval cells, resulting in an elongation of *sqv* mutant vulval cells compared with wild-type vulval cells. The sheet of *sqv* mutant vulval cells would still bend inward, since this greater elongation would still decrease the apical surface area of the sheet without affecting its basal surface area.

Alternatively, the *sqv* mutations may affect a cellular process not normally involved in vulval invagination. For instance, the *sqv* mutations might cause an abnormal accumulation of adhesive material in the extracellular matrix adjoining the vulval cells, causing them to adhere to it abnormally as they invaginate and thus to become abnormally elongated. Or the *sqv* mutations might cause a decrease in the hydrostatic pressure within the invagination space relative to the internal hydrostatic pressure of the worm, resulting in a collapse of the vulval invagination space; such a collapse can result from a punctured cuticle (P. Sternberg, personal communication).

We have begun to clone and molecularly analyze the *sqv* genes. The molecular identities of the SQV-3, SQV-7, and SQV-8 proteins suggest that they may be required for the synthesis of a carbohydrate moiety.

SQV-3 is similar to a family of glycosyltransferases

The SQV-3 protein has sequence similarity to a protein family that includes two proteins with glycosyltransferase activity: mammalian β(1,4)-galactosyltransferase (GalT) and *Lymnaea stagnalis* β(1,4)-N-acetylglucosaminyltransferase (T. Herman and H. Horvitz, in prep.). Other members of this family include a predicted *C. elegans* protein and several human proteins, all with unknown biochemical activity. SQV-3 has not been demonstrated

to have glycosyltransferase activity, but the amino acid residues of GalT that are implicated in substrate binding (Aoki et al. 1990) are conserved in SQV-3.

Most glycosyltransferases are transmembrane proteins located in the endoplasmic reticulum (ER) or Golgi membrane, where they catalyze the sequential addition of sugars to glycoproteins and/or glycolipids (Kleene and Berger, 1993). Each glycosyltransferase removes a donor sugar from a nucleotide-sugar molecule and adds it to an acceptor sugar or sugars on a glycoconjugate. GalT catalyzes the addition of galactose (Gal) from UDP-Gal to N-acetylglucosamine (GlcNAc) residues.

SQV-8 is similar to a glucuronyltransferase involved in the synthesis of the HNK-1 epitope on glycoproteins

The SQV-8 protein has sequence similarity to a second glycosyltransferase, glucuronyltransferase (GlcAT-P), which transfers glucuronic acid (GlcA) to Gal on proteins but not lipids (T. Herman and H. Horvitz, in prep.; Terayama et al. 1997). In vertebrates, this reaction is the final glycosyltransferase reaction in the assembly of the carbohydrate epitope recognized by the HNK-1 monoclonal antibody. The HNK-1 epitope was originally identified on human natural killer cells (Abo and Balch 1981) and has subsequently been found on a large number of neural adhesion molecules in the vertebrate nervous system (for review see Schachner and Martini 1995). The carbohydrate structure of glycolipids and a glycoprotein recognized by the HNK-1 antibody share the terminal trisaccharide SO4-3-GlcA-β1,3-Gal-β(1,4)-GlcNAc, which is therefore likely to be the HNK-1 epitope itself. SQV-3 and SQV-8, if they have the biochemical activities predicted from their sequence similarities, would therefore be the two glycosyltransferases required for the formation of this structure: SQV-3 would add Gal to GlcNAc, and SQV-8 would add GlcA to Gal (Fig. 4). The HNK-1 antibody cross-reacts with invertebrates (Dennis et al. 1988; Bajt et al. 1990), including *C. elegans* (K. Nomura, personal communication as cited in Terayama et al. 1997).

SQV-7 is similar to a protein required for transport of a nucleotide-sugar

The nucleotide-sugar substrates used by glycosyltransferases are synthesized in the cytoplasm and transported into the ER and Golgi compartments by specific antiports (Abeijon et al. 1997). In exchange, these antiports export the nucleotide-monophospate products of the glycosyltransferase reactions.

The SQV-7 protein has sequence similarity to a family of proteins implicated in transport across membranes and is most closely related to the *Leishmania*

donovani protein LPG2, which is required for assembly of a specific galactose-mannose repeat on glycoconjugates (Ma et al. 1997; T. Herman and H. Horvitz, in prep.). Microsomal vesicles derived from an *lpg2*$^-$ deletion mutant are defective in the uptake of the nucleotide-sugar donor GDP-mannose. Because LPG2 is predicted to contain multiple transmembrane domains and has sequence similarity to members of a large family of potential transporters, LPG2 is proposed to be the antiport for GDP-mannose. There are so far two human proteins that are very similar in sequence to SQV-7/LPG2, suggesting that higher eukaryotes may have multiple such transporters. Since only yeast and protozoa are known to transport GDP-mannose into the Golgi (Abeijon et al. 1997), it seems likely that some of these family members, including SQV-7, have diverged to transport other nucleotide-sugars.

We hypothesize that the SQV-7 antiport may directly provide either the SQV-3 or SQV-8 glycosyltransferase with its nucleotide-sugar donor (Fig. 4). A human UDP-Gal antiport has been cloned and is not similar to SQV-7/LPG2 (Miura et al. 1996). We therefore propose that SQV-7 acts as a GlcA antiport. It is, however, possible that SQV-7 provides SQV-3 with its substrate, either UDP-Gal or another nucleotide-sugar. It is also possible that one or more additional glycosyltransferases are involved in vulval invagination and that SQV-7 instead provides one of these enzymes with its nucleotide-sugar substrate.

Sugar modifications in multicellular organisms may be required primarily for cell-cell interactions

In general, defects in glycosylation have little or no affect on the viability of cell lines; even mammalian cell lines that lack nearly all glycosylation are able to grow normally (Krieger et al. 1989; Stanley and Ioffe 1995). By contrast, targeted gene disruptions of glycosyltransferases in mice suggest that multicellular organisms require complex sugar modifications to progress normally through development. For example, mice lacking N-acetylglucosaminyltransferase I, which is required early in the formation of N-linked carbohydrates, die at mid-gestation (Ioffe and Stanley 1994). As might be expected, disruption of glycosyltransferases that act later in the glycosylation pathway and hence affect a smaller number of glycoconjugates cause less severe and more specific developmental defects. For example, mice lacking fucosyltransferase VII, which is required for the final step in the formation of the selectin ligands sLex and 6'-sulfo sLex, are viable but are specifically defective in selectin-mediated adhesion between endothelial cells and leukocytes (Maly et al.

1996). There are no vertebrate mutants that lack GlcAT-P glycosyltransferase, and so the function of the HNK-1 epitope has not been tested genetically.

Experiments in which the glycosylation sites on particular proteins have been eliminated suggest that sugar modifications can be required for the folding, stability, trafficking, and/or activity of secreted and cell-surface proteins, and can mediate cell-cell recognition, cell-cell adhesion, and axonal guidance (for review see Varki 1993). Several sugar modifications have been implicated in directly modulating cell-cell adhesion. One example is that of the regulation of cell-cell adhesion by polysialic acid moieties on the neural adhesion molecule N-CAM. Polysialylation decreases N-CAM homophilic binding and can also decrease cell-cell adhesion mediated by other molecules, perhaps by physically increasing the intercellular space and thereby preventing their interaction (for review see Rutishauser 1996).

Abnormal glycosylation of adhesion molecules could cause the Sqv phenotype

Each of the models presented above to explain the Sqv vulval defect could be consistent with the loss of a carbohydrate modification. The first model was based on the degree of adhesiveness between *sqv* mutant vulval cells being abnormally high. SQV-3-, SQV-8-, and SQV-7-dependent glycosylation of one or more substrates might prevent excessive cell-cell adhesion in a way analogous to the way that polysialic acid decreases the cell-cell adhesion mediated by N-CAM.

The two other models mentioned above would also be consistent with abnormalities caused by alterations in glycoconjugates. One model postulated an abnormally adhesive extracellular matrix and the other an abnormally leaky cuticle; both the extracellular matrix and the cuticle contain glycoproteins and carbohydrates, and the absence of SQV-3-, SQV-8-, or SQV-7- dependent glycosylation might affect the properties of one or both of these structures.

The *sqv* genes are required for early development

In addition to the vulval defect discussed above, *sqv* mutations also cause hermaphrodites to be self-sterile (T. Herman, E. Hartwieg, and H. Horvitz, in prep.). This sterility is likely to be caused by a defect in *sqv* mutant oocytes, since *sqv* mutant hermaphrodites have grossly normal gonads with both oocytes and sperm, and sperm from *sqv* mutant hermaphrodites can produce viable cross-progeny in artificial insemination experiments.

The most severe terminal phenotype of progeny from *sqv-1* to *sqv-7* hermaphrodites is arrest before the first cell division (T. Herman, E. Hartwieg, and

H. Horvitz, in prep.). The arrested one-cell eggs maintain their shape when laid, suggesting that they have eggshells and hence have been fertilized by sperm (Kemphues and Strome 1997), but unlike eggs with normal eggshells, the arrested eggs are permeable to hypochlorite. Glycosylation may therefore be involved in oocyte or early embryonic development. Since the arrest caused by strong mutations in *sqv-1* to *sqv-7* occurs well before the first events of epithelial morphogenesis, we have not ascertained whether *sqv-1* to *sqv-7* are required for these later events as well.

sqv-8 may affect epithelial development more specifically than do _sqv-1_ to 7

Progeny of *sqv-8* hermaphrodites arrest development much later than the one-cell stage, at which the progeny of *sqv-1* to *sqv-7* hermaphrodites are blocked (T. Herman, E. Hartwieg, and H. Horvitz, in prep.). The self-progeny of hermaphrodites homozygous for strong alleles of *sqv-8* arrest about halfway through embryogenesis just as the outer epithelium would normally enclose the embryo. After this enclosure the outer epithelial cells normally constrict in a roughly cylindrical pattern, squeezing the ovoid embryo into the elongated shape of a worm (Priess and Hirsh 1986). Progeny of *sqv-8* mutant hermaphrodites are often defective in epithelial enclosure and fail to elongate. Maternal *sqv-8* product, and hence SQV-8-modified glycoproteins, may therefore be involved in these epithelial morphogenetic events in addition to vulval morphogenesis.

Genetic and molecular evidence suggests that this failure in embryonic epithelial enclosure is the null phenotype of *sqv-8*. For example, one of the strong *sqv-8* alleles is a nonsense mutation predicted to eliminate the C-terminal 78% of the protein (T. Herman and H. Horvitz, in prep.). *sqv-8* therefore appears to have later and presumably more specific effects on development than does *sqv-3*. This conclusion is consistent with our predicted molecular pathway, in which the SQV-8 glucuronyltransferase acts after the SQV-3 galactosyltransferase and modifies only a subset of proteins modified by SQV-3. The SQV-7 antiport may supply SQV-3 with its substrate or may be required to supply substrate to SQV-8 and to one or more additional glycosyltransferases which are less developmentally specific than SQV-8.

Additional genes are probably involved in vulval invagination

All of the mutations isolated in our screen cause the same abnormal vulval phenotype, a reduced invagination space. Interestingly, none blocked invagination *per se*. It is possible that mutations in other genes involved in vulval invagination

cause an earlier zygotic lethality, have only a maternal effect on the vulva, also cause vulval lineage defects, or are functionally redundant so that they disrupt only one of multiple processes with overlapping functions in invagination. Such genes would not have been identified in our screen, and we plan to seek them in other ways.

The *sqv* mutations may genetically define conserved components of a glycosylation pathway

SQV-3, SQV-7 and SQV-8 are similar to components in a pathway for the synthesis of a carbohydrate moiety in vertebrates, the HNK-1 epitope, which has been implicated in adhesive interactions. It seems likely that SQV-3, SQV-7 and SQV-8 are required in *C. elegans* for the synthesis of a carbohydrate moiety and that the remaining *sqv* genes will prove to define additional conserved components required for assembly of this carbohydrate. One possible explanation for the Sqv vulval phenotype is that the *sqv* genes are normally involved in mediating cell-cell adhesion during vulval invagination. If so, a similar regulation of adhesion by glycoconjugates might therefore be involved in epithelial invagination in other species. Whether or not the *sqv* genes are normally involved in vulval invagination, these genes seem likely to define components of a glycosylation pathway conserved among organisms as diverse as nematodes and mammals.

Acknowledgments

We thank Mark Alkema, Mark Metzstein, Rajesh Ranganathan, Gillian Stanfield, and Jeffrey Thomas for critically reading this manuscript. This work was supported by United States Public Health Service research grant GM24663. H.R.H. is an Investigator of the Howard Hughes Medical Institute.

References

Abeijon C., Mandon E.C., and Hirschberg C.B. 1997. Transporters of nucleotide sugars, nucleotide sulfate and ATP in the Golgi apparatus. *Trends in Biochem. Sci.* **22:** 203-207.

Abo T. and Balch C.M. 1981. A differentiation antigen of human NK and K cells identified by a monoclonal antibody (HNK-1). *J. Immunol.* **127:** 1024-1029.

Aoki D., Appert H.E., Johnson D., Wong S.S., and Fukuda M.N. 1990. Analysis of the substrate binding sites of human galactosyltransferase by protein engineering. *EMBO J.* **9:** 3171-3178.

Bajt M.L., Schmitz B., Schachner M., and Zipser B. 1990. Carbohydrate epitopes involved in neural cell recognition are conserved between vertebrates and leech. *J. Neurosci. Res.* **27:** 276-285.

Bard J. 1990. *Morphogenesis: the cellular and molecular basis of developmental anatomy.* Cambridge University Press, Cambridge, England.

Basson M. and Horvitz H.R. 1996. The *Caenorhabditis elegans* gene *sem-4* controls neuronal and mesodermal cell development and encodes a zinc finger protein. *Genes Dev.* **10:** 1953-1965.

Burke R.D., Myers R.L., Sexton T.L., and Jackson C. 1991. Cell movements during the initial phase of gastrulation in the sea urchin embryo. *Dev. Biol.* **146:** 542-557.

Clark S.G., Chisholm A.D., and Horvitz H.R. 1993. Control of cell fates in the central body region of *C. elegans* by the homeobox gene *lin-39*. *Cell* **74:** 43-55.

Clausi D.A. and Brodland G.W. 1993. Mechanical evaluation of theories of neurulation using computer simulations. *Development* **118:** 1013-1023.

Costa M., Wilson E.T., and Wieschaus E. 1994. A putative cell signal encoded by the *folded gastrulation* gene coordinates cell shape changes during *Drosophila* gastrulation. *Cell* **76:** 1075-1089.

Davidson L.A., Koehl M.A., Keller R., and Oster G.F. 1995. How do sea urchins invaginate? Using biomechanics to distinguish between mechanisms of primary invagination. *Development* **121:** 2005-2018.

Dennis R.D., Antonicek H., Wiegandt H., and Schachner M. 1988. Detection of the L2/HNK-1 epitope on glycoproteins and acidic glycolipids of the insect *Calliphora vicina*. *J. Neurochem.* **51:** 1490-1496.

Desai C., Garriga G., McIntire S.L., and Horvitz H.R. 1988. A genetic pathway for the development of the *Caenorhabditis elegans* HSN motor neurons. *Nature* **336:** 638-646.

Ettensohn C.A. 1985. Mechanisms of epithelial invagination. *Q. Rev. Biol.* **60:** 289-307.

Euling S. and Ambros V. 1996. Heterochronic genes control cell cycle progress and developmental competence of *C. elegans* vulva precursor cells. *Cell* **84:** 667-676.

Ferguson E.L., Sternberg P.W., and Horvitz H.R. 1987. A genetic pathway for the specification of the vulval cell lineages of *Caenorhabditis elegans. Nature* **326:** 259-267.

Fristrom D. 1988. The cellular basis of epithelial morphogenesis. A review. *Tissue Cell* **20:** 645-690.

Greenwald I. 1997. In *C. elegans II* (ed. Riddle D.L., Blumenthal T., Meyer B.J., and Priess J.R.), pp.519-541. Cold Spring Harbor Laboratory Press, Cold Spring Harbor, New York.

Greenwald I.S., Sternberg P.W., and Horvitz H.R. 1983. The *lin-12* locus specifies cell fates in *C. elegans. Cell* **34:** 435-444.

Gustafson T. and Wolpert L. 1963. The cellular basis of morphogenesis and sea urchin development. *Int. Rev. Cytol.* **15:** 139-214

Horvitz H.R. and Sternberg P. W. 1991. Multiple intercellular signaling systems control the development of the *Caenorhabditis elegans* vulva. *Nature* **351:** 535-541.

Ioffe E. and Stanley P. 1994. Mice lacking N-acetylglucosaminyltransferase I activity die at mid-gestation, revealing an essential role for complex or hybrid N-linked carbohydrates. *Proc. Natl. Acad. Sci.* **91:** 728-732.

Kemphues K.J. and Strome S. 1997. In *C. elegans II* (ed. Riddle D.L., Blumenthal T., Meyer B.J., and Priess J.R.), pp. 335-359. Cold Spring Harbor Laboratory Press, Cold Spring Harbor, New York.

Kimble J. 1981. Alterations in cell lineage following laser ablation of cells in the somatic gonad of *Caenorhabditis elegans. Dev. Biol.* **87:** 286-300.

Kleene R. and Berger E.G. 1993. The molecular and cell biology of glycosyltransferases. *Biochim. Biophys. Acta* **1154:** 283-325.

Kornfeld K. 1997. Vulval development in *Caenorhabditis elegans. Trends Genet.* **13:** 55-61.

Krieger M., Reddy P., Kozarsky K., Kingsley D., Hobbie L., and Penman M. 1989. Analysis of the synthesis, intracellular sorting, and function of glycoproteins using a mammalian cell mutant with reversible glycosylation defects. *Methods Cell Biol.* **32:** 57-84.

Labouesse M., Sookhareea S., and Horvitz H.R. 1994. The *Caenorhabditis elegans* gene *lin-26* is required to specify the fates of hypodermal cells and encodes a presumptive zinc-finger transcription factor. *Development* **120:** 2359-2368.

Lane M.C., Koehl M.A., Wilt F., and Keller R. 1993. A role for regulated secretion of extracellular matrix during epithelial invagination in the sea urchin. *Development* **117:** 1049-1060.

Ma D., Russell, D.G., Beverley S.M., and Turco, S.J. 1997. Golgi GDP-mannose uptake requires *Leishmania LPG2*. A member of a eukaryotic family of putative nucleotide-sugar transporters. *J. Biol. Chem.* **272:** 3799-3805.

Maly P., Thall A., Petryniak B., Rogers C.E., Smith P.L., Marks R.M., Kelly R.J., Gersten K.M., Cheng G., Saunders T.L., Camper S.A., Camphausen R.T., Sullivan F.X., Isogai Y., Hindsgaul O., von Andrian U.H., Lowe J.B. 1996. The alpha(1,3)fucosyltransferase Fuc-TVII controls leukocyte trafficking through an essential role in L-, E-, and P-selectin ligand biosynthesis. *Cell* **86:** 643-653.

Mittenthal J.E. and Mazo R.M. 1983. A model for cell shape generation by strain and cell-cell adhesion in the epithelium of an arthropod leg segment. *J. Theor. Biol.* **100:** 443-483.

Miura, N., Ishida N., Hoshino M., Yamauchi M., Hara T., Ayusawa D., and Kawakita M. 1996. Human UDP-galactose translocator: molecular cloning of a complementary DNA that complements the genetic defect of a mutant cell line deficient in UDP-galactose translocator. *J. Biochem. (Tokyo)* **120:** 236-241.

Nardi J.B. 1981. Induction of invagination in insect epithelium: paradigm for embryonic invagination. *Science* **214:** 564-566.

Newman A.P. and Sternberg P.W. 1996. Coordinated morphogenesis of epithelia during development of the *Caenorhabditis elegans* uterine-vulval connection. *Proc. Natl. Acad. Sci.* **93:** 9329-9333.

Newman A.P., White J.G., and Sternberg P.W. 1996. Morphogenesis of the *C. elegans* hermaphrodite uterus. *Development* **122:** 3617-3626.

Podbilewicz B. and White J.G. 1994. Cell fusions in the developing epithelia of *C. elegans*. *Dev. Biol.* **161:** 408-424.

Priess J.R. and Hirsh D.I. 1986. *Caenorhabditis elegans* morphogenesis: the role of the cytoskeleton in elongation of the embryo. *Dev. Biol.* **117:** 156-173.

Rutishauser U. 1996. Polysialic acid and the regulation of cell interactions. *Curr. Opin. Cell Biol.* **8:** 679-684.

Schachner M. and Martini R. 1995. Glycans and the modulation of neural-recognition molecule function. *Trends Neurosci.* **18:** 183-191.

Schoenwolf G. and Smith J.L. 1990. Mechanisms of neurulation: traditional viewpoint and recent advances. *Development* **109:** 243-270.

Stanley P. and Ioffe E. 1995. Glycosyltransferase mutants: key to new insights in glycobiology. *FASEB J.* **9:** 1436-1444.

Sulston J.E., Schierenberg E., White J.G., and Thomson J.N. 1983. The embryonic cell lineage of the nematode *Caenorhabditis elegans*. *Dev. Biol.* **100:** 64-119.

Sweeton D., Parks S., Costa M., and Wieschaus E. 1991. Gastrulation in *Drosophila*: the formation of the ventral furrow and posterior midgut invaginations. *Development* **112:** 775-789.

Terayama K., Oka S., Seiki T., Miki Y., Nakamura A., Kozutsumi Y., Takio K., and Kawasaki T. 1997. Cloning and functional expression of a novel glucuronyltransferase involved in the biosynthesis of the carbohydrate epitope HNK-1. *Proc. Natl. Acad. Sci.* **94:** 6093-6098.

Thomas J.H., Stern M.J., and Horvitz H.R. 1990. Cell interactions coordinate the development of the *C. elegans* egg-laying system. *Cell* **62:** 1041-1052.

Trent C., Tsung N., and Horvitz H.R. 1983. Egg-laying defective mutants of the nematode *C. elegans*. *Genetics* **104:** 619-647.

Varki A. 1993. Biological roles of oligosaccharides: all of the theories are correct. *Glycobiology* **3:** 97-130.

Waterston, R.H. 1988. In *The Nematode Caenorhabditis elegans* (ed. Wood W.B. and the community of *C. elegans* researchers), pp. 281-335. Cold Spring Harbor Laboratory Press, Cold Spring Harbor, New York.

White J. 1988. In *The Nematode Caenorhabditis elegans* (ed. Wood W.B. and the community of *C. elegans* researchers), pp. 81-122. Cold Spring Harbor Laboratory Press, Cold Spring Harbor, New York.

Figure 1. Schematic of *C. elegans* vulval development. The descendants of three epithelial cells, P5.p, P6.p, and P7.p, invaginate and fuse pairwise to form a stack of toroids. The inner hole of the toroids forms a passage between the gonad and the outside. Cell nuclei are indicated by small ovals but are not indicated in the stacks of toroids. The cuticle and cell bodies are indicated in each diagram. Toroids B1 and B2 are fused in the adult. See text for details.

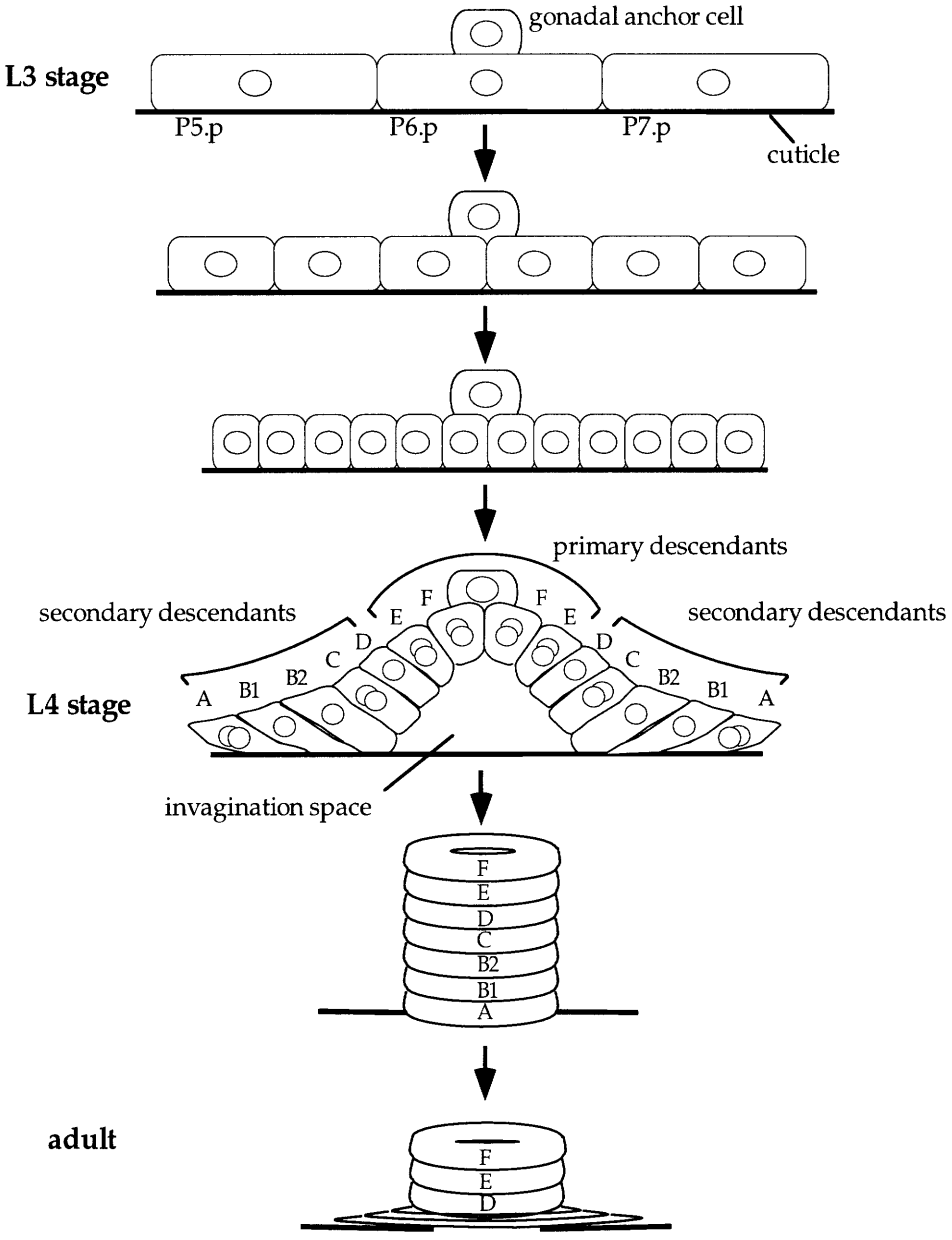
L3 stage
gonadal anchor cell
P5.p
P6.p
P7.p
cuticle
primary descendants
secondary descendants
secondary descendants
L4 stage
A
B1
B2
C
D
E
F
invagination space
adult

Figure 2. Schematic of wild-type and *sqv* mutant vulvae at the early L4 stage, as they appear in their central focal plane when viewed with Nomarski optics. Cell nuclei, the basal lamina, and the separation between the vulval cells and the cuticle are visible. A *sqv* mutant has a considerably reduced vulval invagination space compared with the wild type.

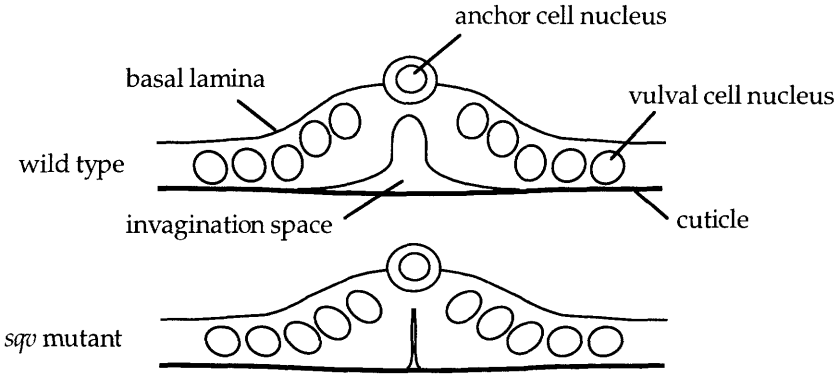
anchor cell nucleus
basal lamina
vulval cell nucleus
wild type
invagination space
cuticle
sqv mutant

Figure 3. One model of the Sqv phenotype. The extent of contact between vulval cells is determined by the balance between their adhesiveness and their rigidity. During normal vulval invagination, an increase in adhesiveness occurs and drives an increase in the extent of contact between vulval cells. Because the vulval cell surface area in contact with the basal lamina is maintained, the resulting increase in cell height causes apical narrowing and invagination. The Sqv phenotype results from an abnormally great increase in adhesiveness. In this figure, the thickness of the cell membranes indicates their degree of adhesiveness.

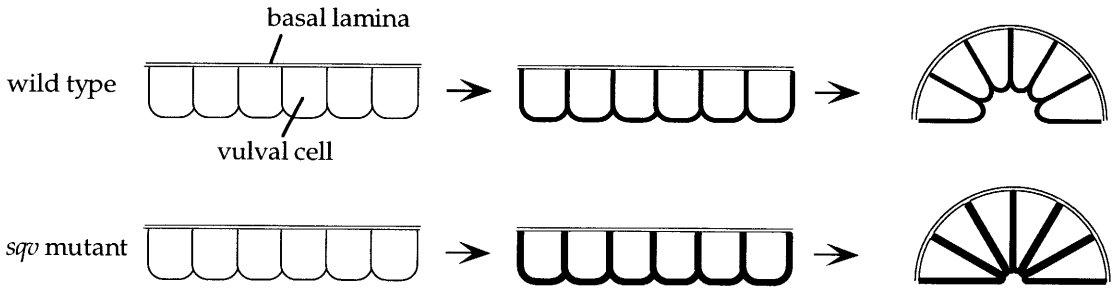
basal lamina
wild type
vulval cell
sqv mutant

Figure 4. Model: SQV-3, SQV-7 and SQV-8 catalyze the formation of an oligosaccharide
present on one or more cell-surface glycoproteins. Part or all of this oligosaccharide is depicted as an unsulfated version of the HNK-1 epitope, but the biochemical activities of SQV-3, SQV-7 and SQV-8 have not been defined, and the addition of other sugars and/or sulfate groups to the putative GlcA-β(1,3)-Gal-β(1,4)-GlcNAc oligosaccharide has not been investigated. See text for details.

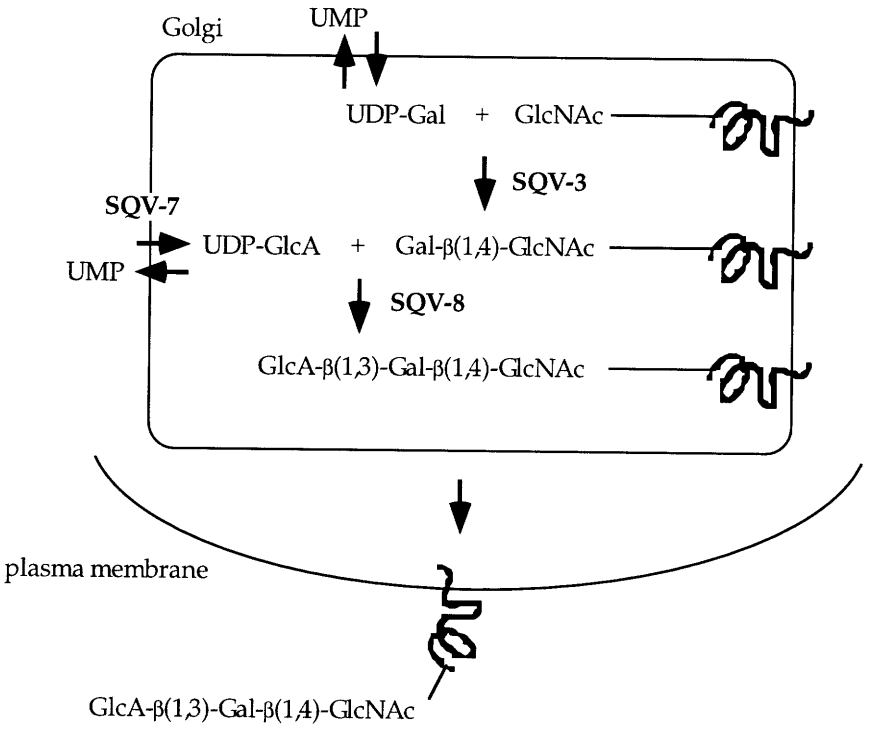
Golgi
UMP
UDP-Gal + GlcNAc
SQV-3
SQV-7
UDP-GlcA + Gal-β(1,4)-GlcNAc
UMP
SQV-8
GlcA-β(1,3)-Gal-β(1,4)-GlcNAc
plasma membrane
GlcA-β(1,3)-Gal-β(1,4)-GlcNAc

Appendix two

Oligonucleotides and DNA clones used and available

Oligonucleotides used and available

Gene	Oligo	Nucleotide sequence
sqv-3	galt-1	CAC AAA TGA GAA CCC GAA TGA G
"	galt-2	AAC TGG AAT GAG GAT AAC AAT A
"	galt-3	CGC GAT CTC AGC TAC AGT AAG T
"	galt-4	TAA AGT TCT AGT CTC CGT GAC T
"	galt-5	CAT CAC CAT GTA GTC ACA TCC A
"	galt-6	ATA CGG AAC GAT AAC GCA CAG T
"	galt-7	TTA CAA ATC TCC CGC CAG AT
"	galt-8	CCA GTA TCA TCC GAA ATA TCA C
"	galt-9	GGG AAT TCG ATT TAG AGA TAA CGA GGG AT
"	galt-10	ATT CAG ATG GGT CTT GCC
sqv-7	pi4-1TH	AAT TGA AAT ATT GCT AC
"	pi4-2TH	TAC TAC AAC CTG CGT TG
"	pi4-3TH	GAT CTT GGA AAG TAT GG
"	pi4-4TH	ACA TAG TAC CAC GGT AG
"	pi4-5TH	AAA GTA AAC AAA AGG AG
"	pi4-6TH	TGA TGA CGA TGA TCT TG
"	pi4-7TH	ATT CGG AAC ATT TTG GC
"	pi4-8TH	ATT TCT GTT CGT TGG AG
"	pi4-9TH	ATT TAC GGT CAG TTA CG
"	pi4-10TH	TAC GGT CAG TTA CGC CCG
"	pi4-11TH	GTT GAA ACA TTC GAC ATG AAG
"	pi4-12TH	CAA GGG TGT TCT TAT TTT CCC
sqv-8	spe-2-1	CCA CAT ACG TCA AAT CCG GC
"	spe-2-2	GGA ATT CAG AAG AAC GGG CCA CTT TGC
"	spe-2-3	TTA ATC GTT CAA CGC CTT TC
"	spe-2-4	AAT TGA GTG GTG TGA AAG AG
"	spe-2-5	ATC GAT ATG GCT GCA TTT GC
"	spe-2-6	GTC CTT TAC GCT CTC CCA TC
"	spe-2-7	TTC CAA CTG GCC AAA CTC
"	spe-2-8	ACG AGG CAC GTC GAA TG
"	spe-2-9	GTG GCC CGT TCT TCT TC
"	spe-2-10	CCA ATG GAG GTT GGG AAC
"	spe-2-11	GCA ATA AAT GCT CGG AGC
sqv-3 and *sqv-8*	R10E11.4 INS C	TAT GGG CTA GCG CA
"	R10E11.4 INS W	TAT GCG CTA GCC CA

(These latter two oligos were annealed and inserted into the Nde I sites of the genomic DNA clones that rescue *sqv-3* and *sqv-8*, resulting in in-frame stop codons either within the insert itself (*sqv-3*) or shortly thereafter (*sqv-8*).)

DNA clones used and, with one exception (noted below), available from the Horvitz lab collection

Clone	Brief description
pTH1	7.1kb Eag I-Kpn I genomic fragment from cosmid C47F11 inserted into pBluescript SK minus (Stratagene) at Eag I/Kpn I sites. Rescues vulval but not fertility defect of *sqv-3(n2842)* (same result as for entire C47F11 cosmid). Spans *sqv-3* cDNA sequence (see clone pTH3) and contains two other predicted ORFs (one complete, one incomplete). The end sequences of the insert are given below (see cosmid R10E11 in GenBank for the remainder).

CGGCCGTTTCGAGAAAAAGTTCTCAATTACAAGCAAACTTTGAAGAAATC.....
GCACACCTCGTCGCATTAAACTAAATTTTGTCGTGTCGGGGCCGGGTACC

pTH2	2.4kb Xba I-Sal I fragment derived from pTH1 inserted into pBluescript SK minus at Xba I/Sal I I sites. Rescues *sqv-3(n2842)*. Contains entire open reading frame of *sqv-3* cDNA (see clone pTH3), but, unlike pTH1, lops off 3' untranslated region (see Chapter 3). Rescue looks the same as for pTH1.
pTH3	1.2kb canonical *sqv-3* cDNA isolated by hybridization to the Xba I-EcoR I fragment of pTH2 (see Chapter 3). Isolated and popped out from Barstead lambda ZAP library (cDNA insert is flanked by EcoR I sites). Contains part of SL1 spliced-leader sequence at 5' end so presumably full-length. The end sequences of the insert (including Barstead library flanking sequences) are given below (see Chapter 3 for the remainder).

GAATTCCGAAGTTTGAGAAGAAGCCTCTTCTCTTTAGCACAAGCTGTACC.....G
AATAATTTATCCATAAAATATACAAATGATAAAAAAAAAAACGGAATTC

cDNA-PCR	This construct was used to make pTH4b, pTH5, and pTH6b but was not itself preserved, since the useful part of it (the EcoR I fragment) is available from the latter three clones. Oligos galt-5 and galt-9 (see above) were used in a PCR reaction with pTH3 as a template. The PCR product was cut with EcoR I and BamH I and used to replace the (5')EcoR I-BamH I fragment of pTH3. This region of the resulting construct was sequenced to confirm that no errors had been introduced by Vent polymerase during PCR. The result is a*sqv-3* cDNA that starts and contains an EcoR I site immediately after the last codon for the putative SQV-3 transmembrane domain.
pTH4a	The Eae I-Cla I (the Cla I blunted) fragment of pTH3 inserted into pET21d (Novagen) at Not I/Xho I (Xho I blunted) sites. Note that the 6 His tag is in-frame at the 3' end. Expresses highly in BL21 cells. Insoluble. Possible to purify using Ni-NTA-agarose resin. Injected insoluble gel-purified band (not Ni-purified) into rabbits 94-56 and 94-57 to make antibodies (and cross-reacts with the latter on a western blot).

pTH4b The EcoR I fragment of "cDNA-PCR" inserted into pET21a at the EcoR I site. Note that the 6 His tag is not in frame--the stop codons of the cDNA occur before it does. Expresses highly in BL21 cells (induced for three hours). Insoluble. Cross-reacts with antibodies generated against protein from pTH4a (western blot). The end sequences of the insert is given below (the remainder is the same as that of pTH3, as is, in fact, the 3' end).

GAATTCGATTTAGAGATAACGAGGGATCTTATGACTGATTATGTAGATCC.....
GAATAATTTATCCATAAAATATACAAATGATAAAAAAAAAAACGGAATTC

pTH5 The EcoR I fragment of "cDNA-PCR" inserted into pGEX-1lT (Pharmacia) at the EcoR I site (replacing the amino terminus of SQV-3, up to and including the putative transmembrane domain, with the glutathione-S-transferase protein). Expresses highly in TG1 cells. Soluble. Possible to purify using gluthathione-sepharose resin. Expressed protein cross-reacts with antibodies generated against protein from pTH4a (western blot).

pTH6a The blunted Eae I fragment of pTH3 inserted into pIN-III-ompA-1 (*EMBO J.* **3:** 2437-2442) at the blunted EcoR I site. Expression too weak to see on Coomassie-stained gel. Expressed protein cross-reacts with antibodies generated against protein from pTH4a (western blot).

pTH6b The EcoR I fragment of "cDNA-PCR" inserted into pIN-III-ompA-2 at the EcoR I site. Expression too weak to see on Coomassie-stained gel. Expressed protein cross-reacts with antibodies generated against protein from pTH4a (western blot).

pTH7 4.6kb Eag I-Spe I fragment from ZK1307 inserted into pBluescript SK minus at Eag I/Spe I sites. Spans *sqv-8* cDNA sequence (see pTH8) and contains some of a second predicted ORF (see Chapter 3). Rescues both vulval and fertility defects of *spe-2(mn63)*. The end sequences of the insert are given below (see cosmid ZK1307 in GenBank for the remainder).

CGGCCGTCTTAATCTTCGAGACATCATACGGAAAAGCGAACTTACTTAAC.....
AAAAATCTTCAAAAAAAATCATAACTTCAGAATTTCGACTACGAACTAGT

pTH8 Canonical *sqv-8* cDNA isolated from Okkema mixed-stage library by hybridization to Kpn I-EcoR V of pTH7. 1.7kb BsiW I-BsiW I fragment from lambda gt11 inserted into pSL1190 (Pharmacia) at the BsiW I site. Contains *sqv-8* cDNA with some lambda DNA on either side. Contains part of SL1 spliced-leader sequence at 5' end so presumably full-length. The end sequences of the insert (including lambda gt11 and Okkema library flanking sequences) are given below (see Chapter 3 for the remainder).

CGTACGCCATGGCCGGAGTGGCTCACAGTCGGTGGTCCGGCAGTACAATGGAT
TTCCTTACGCGAAATACGGGCAGACATGGCCTGCCCGGTTATTATTATTTTTGA
CACCAGACCAACTGGTAATGGTAGCGACCGGCGCTCAGCTGGAATTCGAGGAT
CCGGGTACCATGGGTTTGAGGGATAAATAAACCAAATGAA.....CCTTTTATTG

CATTTTGACTAACTTTCATAAATATTTTTCTTTAAAAAAAAAAAAAAAAAA
CCGCCGATACTGACGGGCTCCAGGAGTCGTCGCCACCAATCCCCATATGGAAA
CCGTCGATATTCAGCCATGTGCCTTCTTCCGCGTGCAGCAGATGGCGATGGCTG
GTTTCCATCAGTTGCTGTTGACTGTAGCGGCTGATGTTGAACTGGAAGTCGCCG
CGCCACTGGTGTGGGCCATAATTCAATTCGCGCGTCCCGCAGCGCAGACCGTTT
TCGCTCGGGAAGACGTACG

pTH9 Almost the Xba I-EcoR V (blunted) fragment of pTH8. inserted into pET21b at blunted BamH I/Xho I sites. Sequence at 3' junction okay but 5' junction sequence is TCGGGATCTAGATT instead of TCGGGATCCTAGATT. So cut this incorrect clone with Xba I and Sty I and inserted into pET21b at Nhe I/Sty I sites (all sticky). Note that the 6 His tag is in frame at the 3' end. Expresses well in BL21 cells (induced for 3 hours). Insoluble. Possible to purify using Ni-NTA-agarose resin. Injected insoluble gel-purified band (not Ni-purified) into rabbits 95-72 and 95-73 to make antibodies.

pTH10 The Xba I-Spe I (blunted) fragment of pTH8 inserted into pGEX-4T-3 at the blunted EcoR I site. Expresses very weakly in TG1 cells. Soluble. Cross-reacts with antibodies generated against protein from pTH9 (western blot).

pTH11 Contains the 17kb Mlu I-Pst I fragment from C52E12. This had a complicated construction, and unfortunately there is incomplete documentation on whether the Mlu I site is blunted or preserved or whether the construct is in part of the pBluescript SK minus vector or part of the pJB8 cosmid vector. My guess is that the Mlu I (blunted)-Pst I (sticky) fragment from C52E12 is in the Sac II (blunted)/Pst I sites of pBluescript SK minus. Rescues both the vulval and fertility defects of *sqv-7(n2844)* and the vulval defect of *sqv-7(n2839)* (which is fertile). Contains some *unc-104* coding sequences (see Chapter 3). The end sequences of the insert (unblunted Mlu I to unblunted Pst I) are given below (see cosmid C52E12 in GenBank for the remainder).

ACGCGTGTACGCGGCCTATCCCTCGCCTGTATTTCGCTTGTTAGCGGCCC.....TCA
TTGTCTTCTGCTCTTTTGGTAACTTGTCAACTTCTTTTTTCCTGCAG

pTH12 pTH11 was cut with Sph I and the largest fragment religated. Rescues vulval and fertility defects of *sqv-7(n2844)* and vulval defect of *sqv-7(n2839)*. Contains some *unc-104* coding sequences but a smaller amount than pTH11 contains (see Chapter 3).

pTH13 The Hind III-Not I (blunted) fragment of dbest clone ID 40880 inserted into pBluescript SK minus at the EcoR V site. Clone 40880 was from the Soares human infant brain cDNA library 1NIB which was constructed by priming with AACTGGAAGAATTCGCGGCCGCAGGATTTTT..., adding Hind III adaptors, digesting with Hind III and Not I, and cloning into "Lafmid BA vector" (quote from the dbest description). Its 5' sequence corresponds to GenBank #R56166 and 3' sequence to GenBank

#R56054. The clone was identified by the Washington University-Merck EST Project and provided to us by the I.M.A.G.E. consortium and is predicted to encode a protein similar to SQV-8 (see Chapter 3). The complete insert sequence (blunted Hind III to blunted Not I) is given below.

AGCTTGGCACGAGGGTGTTTCTCGCCTACTTCCTGGTGTCGATCGCCGGCCTCCT
CTACGCGCTGGTACAGCTCGGCCAGCCATGTGACTGCCTTCCTCCCCTGCGGGC
AGCAGCCGAGCAGCTACGGCAGAAGGATCTGAGGATTTCCCAGCTGCAAGCG
GAACTCCGACGGCCACCCCCTGCCCCTGCCCAGCCCCCTGAACCCGAGGCCCTGC
CTACTATCTATGTTGTTACCCCCACCTATGCCAGGCTGGTACAGAAGGCAGAG
CTGGTACGACTGTCCCAGACACTGAGCCTGGTGCCCCGGCTGCATTGGCTGCTG
GTGGAGGATGCTGAGGGTCCCACCCCGCTGGTCTCAGGGCTGCTGGCTGCCTCT
GGCCTCCTCTTCACACACCTGGTGGTCCTCACGCCCAAAGCCCAGCGGCTTCGG
GAGGGCGAGCCTGGCTGGGTTCATCCCCGTGGTGTCGAGCAGCGGAACAAGGC
CCTGGACTGGCTCCGGGGCAGAGGGGGTGCTGTGGGTGGGGAGAAGGACCCAC
CACCACCAGGGACCCAAGGAGTCGTCTACTTTGCTGACGATGACAACACCTAC
AGCCGGGAGCTGTTTGAGGAGATGCGCTGGACCCGTGGTGTCTCAGTGTGGCCT
GTGGGGCTGGTGGGCGGCCTGCGATTCGAGGGCCCTCAGGTACAGGACGGCCG
GGTAGTGGGCTTCCACACAGCATGGGAGCCCAGCAGGCCCTTCCCTGTGGATA
TGGCTGGATTTGCCGTGGCCCTGCCCTTGCTGTTAGATAAGCCCAATGCCCAAT
TTGATTCCACCGCTCCCCGGGGCCACCTGGAGAGCAGTCTTCTGAGCCACCTTG
TGGATCCCAAGGACCTGGAGCCACGGGCTGCCAACTGCACTCGGGTACTGGTG
TGGCATACTCGGACAGAGAAGCCCAAGATGAAGCAGGAGGAGCAGCTGCAGC
GGCAGGGCCGGGGCTCAGACCCAGCAATTGAGGTGTGATGGCGGCCCCACCCC
AACTACCACCTCTTTTCAGGCACAGACCTTGTGGGACTGGGCCCCAGGCCTGCC
CAGGATGTGGTTTTCCAAGTCCTGACCCTTGGAGCCAGAAGTGGCCCCTCTGCC
CCTCCAGGCCCAGGGCATGGTCCTGCTGCTTCACCCCTCCCCTAGCCTGCCGTGT
GGCACTGCCCACAGGCTGGGGACAAGCAGCCCTTGTGTTGAGTCAGGTTGGCC
CTGTCTAGGGTGGAACAGAAGGACAGATGGACCCAGGAGGGAGGGCAGCTGA
GTAACTGGGTAACTTATTGGGGCTGGGCATGCACTGGGGGGCTGGAGGAGCTG
GGCTGGACCCTTCCCACCTGAGCATGCTGACCCCCTTCCTACCTCCAGAATAAA
GAATCTCAACCTGGAAAAAAAAAAAAAAAAAAAAAAAAATTCCTGCGGCC

pTH14a The dbest clone ID 132056 from the Soares human placenta library Nb2HP which was constructed by priming with AACTGGAAGAATTCGCGGCCGCAGGATTTTT..., adding EcoR I adaptors, digesting with EcoR I and Not I, and cloning into the "modified pT7T3 (Pharmacia) vector" (quote from the dbest description). Its 5' sequence corresponds to GenBank #R24922 and 3' sequence to GenBank #R32471. The clone was identified by the Washington University-Merck EST Project and provided to us by the I.M.A.G.E. consortium and is predicted to encode a protein similar to SQV-7 (see Chapter 3). The complete insert sequence (EcoR I to Not I) is given below.

GAATTCGGCACGAGGCTAAACAAAATCATTCACTTCCCTGATTTTGATAAGA
AAATTCCTGTAAAGCTGTTTCCTCTGCCTCTCCTCTACGTTGGAAACCACATAA
GTGGATTATCAAGCACAAGTAAATTAAGCCTACCGATGTTCACCGTGCTCAGG
AAATTCACCATTCCACTTACCTTACTTCTGGAAACCATCATACTTGGGAAGCA
GTATTCACTCAACATCATCCTCAGTGTCTTTGCCATTATTCTCGGGGCTTTCAT

AGCAGCTGGGTCTGACCTTGCTTTTAACTTAGAAGGCTATATTTTTGTATTCCT
GAATGATATCTTCACATCAGCAAATGGAGTTTATACCAAACAGAAAATGGA
CCCAAAGGAGCTAGGGAAATACGGAGTACTTTTCTACAATGCCTGCTTCATGA
TTATCCCAACTCTTATTATTAGTGTCTCCACTGGAGACCTCCAACAGGCTACTG
AATTCAACCAATGGAAGAATGTTGTGTTTATCCTACAGTTTCTTCTTTCCTGTT
TTTTGGGGTTTCTGCTGATGTACTCCACGGTTCTGTGCAGCTATTACAATTCAG
CCCTGACGACAGCAGTGGTTGGAGCCATCAAGAATGTATCCGTTGCCTACATT
GGGATATTAATCGGTGGAGACTACATTTTCTCTTTGTTAAACTTTGTAGGGTT
AAATATTTGCATGGCAGGGGGCTTGAGATATTCCTTTTTAACACTGAGCAGCC
AGTTAAAACCTAAACCTGTGGGTGAAGAAAACATCTGTTTGGATTTGAAGAG
CTAAAGAGTCTGCAGCAGGATTGGAGACTGACTTGTGACTGCGGGCTGGGGGG
GCATTCCCAGTAGGAATGTGAAGCCAGAGGTTTCGGATTCGTGACATCCACCC
CCTGGGCAAGTGAGAGCATCTGCAAAATGCAAAGAGAACTACCTCATATGCA
GGATGAGCCAATGGCAGTCTCAAGAAATGTACTCGGGCGACACCTTACCTGTG
GAAAGCAAATCTTTTCAAAATAAGCCACTGGGACTCGGTAGGTGGAGCCCCA
GCTGCTCTTCTAGGGACCTATGGGGCCTTCGTGGCATCTCTGTGCTGTGTGCTGG
GGAGGAGGTTGATGTAATGGTGACTCTTTTCTGATCAGCACCTTGGCCGTGAT
TCCCAAGGTCCCAGCCAAAGCAAAGGGCCAGTTGTTTCAGTTTAAACAGACA
TGTCTTTAGTCTAATAAAATTAGTTAACTGCCAGTAAAGTTATTTGTTAGCTT
TGATGAAAGCTATGTTGGTATCTTTCCCTAATCATCAAAGTAAATAAAAAAT
CATTTCTATGTAAAAAAAAAAAAAAAAATTCCTGCGGCCGC

pTH14b pTH14a was cut with EcoR I and Not I and the resulting smaller fragment (EcoR I-EcoR I) inserted into the EcoR I site of pBluescript SK minus.

pTH14c pTH14a was cut with EcoR I and Not I and the resulting larger fragment (EcoR I-Not I) inserted into the EcoR I/ Not I sites of Bluescript SK minus.

pTH15a The EcoR I (blunted) fragment of pTH3 inserted into the Nhe I/EcoR V (blunted) sites of the heat-shock vector pPD49.78 (see Chapter 3). The vulval defect of *sqv-3* mutants carrying pTH15a and pTH15b is rescued if heat shock is administered before vulval development. Poor rescue of *sqv-3* infertility.

pTH15b The EcoR I (blunted) fragment of pTH3 inserted into the Nhe I/EcoR V (blunted) sites of the heat-shock vector pPD49.83 (see Chapter 3). The vulval defect of *sqv-3* mutants carrying pTH15a and pTH15b is rescued if heat shock is administered before vulval development. Poor rescue of *sqv-3* infertility.

Appendix three

Additional results

Unusual vulval phenotypes observed in a *sqv-8(mn63) unc-4(e120); dpy-17(e164) ncl-1(e1865) unc-36(e251); Ex[sqv-8; dpy-17; ncl-1; unc-36; pHS::GFP]* strain

The strain *sqv-8(mn63) unc-4(e120); dpy-17(e164) ncl-1(e1865) unc-36(e251) ; Ex[sqv-8; dpy-17; ncl-1; unc-36; pHS::GFP]* was originally constructed for the purpose of genetic mosaic analysis of *sqv-8* (see below for description of this strain's construction). Theoretically the extrachromosomal array ("*Ex[...]*") should rescue the *sqv-8*, *dpy-17*, *ncl-1* and *unc-36* defects, and since *ncl-1* cell-autonomously causes cells to have larger nucleoli, cells should be scorable for the presence or absence of the rescuing array. However, the array in this strain appeared to incompletely rescue the *ncl-1* phenotype, preventing its use in mosaic analysis. In particular, the Ncl phenotypes of cells scored in the pharynx (MI, M2, and m1 from the AB.a lineage, and M4, I4, I6, and M5 from the P1 lineage) and tail (DVA and DVB from the AB.p lineage, and DVC from the P1 lineage) suggested that the extrachromosomal array was either frequently lost at multiple points in an animal's cell lineage or could be present in a cell and yet fail to rescue its Ncl phenotype. The latter is likely to be at least part of the explanation since certain cells, the HSNs and excretory cell in particular, were nearly always Ncl. In addition, other *sqv-8(mn63) unc-4(e120)/mnC1; dpy-17(e164) ncl-1(e1865) unc-36(e251); Ex[sqv-8; dpy-17; ncl-1; unc-36; pHS::GFP]* strains containing independently-isolated arrays showed very poor or no rescue of the Ncl phenotype.

However, in the course of this analysis, we noticed that a small number (<5%) of L4 hermaphrodites from this strain had abnormal vulval phenotypes not previously observed in *sqv-8* (or any other *sqv*) homozygous mutants; examples are shown in Figure 1. The most striking of these phenotypes, and the least frequent (observed in five animals), is that shown in Figure 1A and B: the anterior vulva appears wild-type while the posterior is collapsed in a way that resembles the Sqv phenotype. As in the Sqv phenotype, the vulval nuclei appear to be arranged in grossly wild-type positions relative to one another, although the shape of the invagination space is abnormal. The latter is true also of the vulvas shown in Figure 1C and D.

To test whether these vulval phenotypes depended on *sqv-8* and *sqv-8* alone, we used a dissecting microscope to examine a *dpy-17(e164) ncl-1(e1865) unc-36(e251)* and a *sqv-8(mn63) unc-4(e120); Ex[sqv-8; rol-6(*dm*)]* strain for animals with the asymmetric vulval phenotype shown in Figure 1A and B (we did not look for the phenotypes shown in Figure 1C and D) (see below for construction of the latter strain). No such animals were found, although this phenotype was originally

noticed and is readily apparent at the dissecting microcope level. We occasionally did observe asymmetric vulvae in the *sqv-8(mn63) unc-4(e120); Ex[sqv-8; rol-6(*dm*)]* strain, but upon inspection by Nomarski DIC microscopy these all turned out to have fewer than the normal number of secondary cell descendants (data not shown); animals with such a lineage defect were also occasionally observed in the *sqv-8(mn63) unc-4(e120); dpy-17(e164) ncl-1(e1865) unc-36(e251) ; Ex[sqv-8; dpy-17; ncl-1; unc-36; pHS::GFP]* and the *dpy-17(e164) ncl-1(e1865) unc-36(e251)* strains.

While it is also possible that the single *sqv-8(mn63) unc-4(e120); dpy-17(e164) ncl-1(e1865) unc-36(e251); Ex[sqv-8; dpy-17; ncl-1; unc-36; pHS::GFP]* strain tested or the single *sqv-8(mn63) unc-4(e120); Ex[sqv-8; rol-6*dm*]* strain tested had some peculiarity and that other independently-derived strains of these genotypes might behave differently, these results suggest that the abnormal vulval phenotype in Figure 1A and B is caused by loss of *sqv-8* activity in conjunction with loss of *dpy-17*, *ncl-1*, and/or *unc-36* activity (and/or of the *HS::GFP* constructs, though this seems unlikely). We have not examined Unc-4 animals from the original *sqv-8(mn63) unc-4(e120)/mnC1; dpy-17(e164) ncl-1(e1865) unc-36(e251)* for this phenotype and so cannot say whether it requires animals to be mosaic (for instance, one might propose that the phenotype is caused cell-autonomously by loss of the array from the posterior vulval cells, although one might then expect to see vulvas in which only the anterior had collapsed as a result of loss of the array from the anterior cells).

It is interesting to speculate that one of these other genes might sensitize the vulval cells, causing them to express the Sqv phenotype in circumstances under which they would not normally do so (e.g. in the example of mosaicism just described or in the case of relatively and perhaps variably poor *sqv-8* rescue by the array). *ncl-1* affects nucleolus size and is not known to cause any other phenotype (Hedgecock and Herman, 1995). *unc-36* encodes a protein with similarity to a calcium channel subunit (L. Lobel and H.R. Horvitz) and affects several *C. elegans* behaviors but *unc-36* mutations do not appear to have gross developmental defects. By contrast, *dpy-17* affects body shape (animals are dumpy) and has been proposed to encode a protein with similarity to cuticular collagens (based on *dpy-17* rescue by cosmid F54D8, A. Smardon and E. Maine, pers. comm.), although this is by no means certain. There is some evidence that *dpy-17* may also affect cell-matrix interactions within the body of the animal: the *dpy-17(e124)* mutation may enhance the cell migration and process outgrowth defects caused by a weak mutation in a gene (*pat-3*) encoding a β1 integrin (M. Buechner and E. Hedgecock, pers. comm.;

Gettner et al., 1995). It is possible, therefore, that loss of *dpy-17* affects extracellular matrix in such a way as to sensitize the vulval cells to the effects of losing *sqv-8*.

(Strain construction. The strain *sqv-8(mn63) unc-4(e120)/mnC1; dpy-17(e164) ncl-1(e1865) unc-36(e251)* was co-transformed with the *dpy-17*-rescuing cosmid F54D8, the *ncl-1*-rescuing cosmid C33C3, the *unc-36*-rescuing cosmid C50C3, the *sqv-8*-rescuing Eag I-Spe I genomic fragment (plasmid pTH7), and two constructs (which will be referred to as "*pHS::GFP*") containing DNA encoding the green fluorescent protein (GFP) under the control of the two heat-shock promoters (Y. Wu, pers. comm.). Wild-type transformants were picked to individual plates from which was identified a single line that transmitted rescue of all four markers. Unc-4 animals from this line were used to establish the strain *sqv-8(mn63) unc-4(e120); dpy-17(e164) ncl-1(e1865) unc-36(e251) ; Ex[sqv-8; dpy-17; ncl-1; unc-36; pHS::GFP]*. The strain *sqv-8(mn63) unc-4(e120)/mnC1* was co-transformed with the *sqv-8*-rescuing genomic fragment Eag I-Spe I (plasmid pTH7) and the *rol-6(*dm*)*-containing plasmid pRF4. Rol transformants were used to establish independent transformed lines that also transmitted rescue of *sqv-8*, and Rol Unc-4 animals were picked from one such line to establish a *sqv-8(mn63) unc-4(e120); Ex[sqv-8; rol-6(*dm*)]* strain.)

sqv-3 mutant males have abnormal tails

Adult Unc males from the strain *sqv-3(n2842) unc-69(e587*am*)/qC1* have a tail defect, which was also observed in Unc males from the strains *sqv-3(n2841) unc-69(e687*am*)/qC1*, and *sqv-3(n2842) unc-50(e306)/qC1* but not in the strain *unc-69(e587*am*); him-5(e1467*ts*)*, suggesting that it results from a loss of *sqv-3* (Figure 2). The rays of the *sqv-3* tails are often shorter and stubbier than those of wild-type or *unc-69* male tails. It is possible that *sqv-3* rays may sometimes be misplaced, missing, or abnormally fused with neighboring rays, but this was not carefully ascertained since *sqv-3* tails are difficult to visualize in Nomarski microscopy (they are less easily spread and flattened than the longer wild-type or *unc-69* mutant rays).

Adult Unc males from the strains *sqv-5(n3039) unc-75(e950)/hT2 bli-4(e937); +/hT2 h661*, *sqv-7(n2844) unc-4(e120)/mnC1*, and *sqv-8(mn63) unc-4(e120)/mnC1*, and non-Unc males from the strains *sqv-1(n2819)/nT1 n754; +/nT1*, *sqv-2(n2826), +/nT1 n754; sqv-4(n2840)/nT1*, and *+/nT1 n754; sqv-6(n2845)/nT1 n754* were also examined for a tail defect. None had as striking a defect as that of *sqv-3*, although some, *sqv-1(n2819)* males in particular, occasionally had rays positioned abnormally anteriorly (data not shown).

Tracings of electron micrographs of serially-sectioned N2 and *sqv-3(n2842)* vulvas

As described in Chapter 2, we made electron micrographs of a serially sectioned wild-type vulva and a serially sectioned *sqv-3(n2842)* vulva (from strain MT7556 *sqv-3(n2842)/eT1*) of the early L4 stage. Longitudinal sections were made through the vulva laterally (from left to right or from right to left), and the plasma and nuclear membranes of the vulval cells were traced from electron micrographs of representative sections. In Figure 3 are the results of scanning xeroxed reductions of these tracings into the computer; a subset of these were more fully completed and presented in Chapter 2. The identities of the vulval cells given in Figure 3 are based on the relative positions of the nuclei as known from Nomarski DIC microscopy; each cell is labeled with the letter name of the toroid it ultimately forms a part of (Greenwald, 1997). In particular, the four inner primary descendants (derived from two transverse cell divisions) are labeled "F", and the four outer primary descendants (two on either side, each derived from a transverse division) are "E", and in each of the two secondary lineages, the single vulval cell that did not undergo a final division is labeled "D", the two cells derived from a transverse division are labeled "C", the two mononucleate cells derived from a longitudinal division are labeled "B2" and "B1", and the binucleate cell derived from a longitudinal division is labeled "A". The anchor cell is labeled "AC".

Not all plasma membranes were fully traced: some were difficult to resolve in the micrograph, very small regions enclosed by membrane were often not fully traced, and the anchor cell was arbitrarily not included in some tracings. Most micrographs were taken at the same magnification (6500X) but several were at 6000X, and tracings of these are labeled as such (in Figure 5F of Chapter two, the 6000X tracing was increased in scale by 6500/6000 = 108%). The tracings of the *sqv-3(n2842)* vulva encompass nearly the entire vulva (every vulval cell is present in at least one tracing), but the tracings of the N2 vulva stop just after the mid-point of the body has been passed. Finally, as mentioned in Chapter two, the *sqv-3(n2842)* vulva may be at a somewhat later stage in development than that of the N2 vulva.

Production and analysis of polyclonal antisera to SQV-3 and SQV-8

Insoluble SQV-3 (from amino acids 45 to 258 out of the total 289) was expressed in *E. coli* by means of construct pTH4a (see Appendix 2). Inclusion bodies were prepared and run on a preparative SDS-PAGE gel, and the partial SQV-3 protein was visualized by means of $CuCl_2$, cut out, and electrophoresed from the gel

by standard methods. The resulting eluate was dialyzed, lyophilized, and resuspended in 1XPBS. After giving a sample of preimmune serum, rabbits 94-56 and 94-57 were initially injected with 1mg each of protein prepared in this way and were later boosted with 500ug each (no more often than every 4-6 weeks). Beginning after the second boost, bleeds were taken 10-14 days after a boost.

Insoluble SQV-8 (from amino acids 5 to 292 out of the total 356) was expressed in *E. coli* by means of construct pTH9 (see Appendix 2) and was prepared in the same way as SQV-3. Rabbits 95-72 and 95-73 were initially injected with 500ug each of the partial SQV-8 protein and were later boosted with 250ug each.

In each case, the antisera were affinity-purified (using the appropriate purified GST fusion immobilized on nitrocellulose) for use on western blots of total worm protein and for use on whole, fixed worms. Although crude (at 1:2000) and purified antisera of both types recognized bacterially-expressed protein on western blots (see brief descriptions of DNA clones pTH4a, pTH4b, pTH5, pTH6a, pTH6b, pTH9, and pTH10 in Appendix 2), no reliable staining was observed of whole N2 worms fixed by the method of Finney and Ruvkun (1990). However, some staining was observed in strains presumed to be overexpressing the protein of interest. Two independent arrays containing the *sqv-3*-rescuing plasmid pTH2 were each integrated in an N2 background, yielding two strains that might overexpress SQV-3 (MT8788 *nIs77* and MT8805 *nIs79*), and, similarly, two independent arrays containing the *sqv-8*-rescuing plasmid pTH7 were each integrated, yielding two strains that might overexpress SQV-8 (MT8789 *nIs78* and MT8804 *nIs80*). When purified anti-SQV-3 antisera were tested on whole MT8788 and MT8805 worms fixed by the Finney and Ruvkun (1990), we observed punctate staining in intestinal cells at adult and all larval stages and staining of the head mesodermal cell and/or excretory canal. In a single animal punctate staining was observed in two L4 vulval cells (P5.ppal and P7.pppl?). Purified anti-SQV-8 antisera stained several unidentified cells in the head and tail and occasionally stained the sperm of MT8789 and MT8804 hermaphrodites fixed by the Finney and Ruvkun method.

References

Finney, M. and Ruvkun, G.B. (1990). The *unc-86* gene product couples cell lineage and cell identity in *C. elegans*. *Cell* **63,** 895-905.

Gettner, S.N., Kenyon, C., and Reichardt, L.F. (1995). Characterization of beta-pat-3 heterodimers, a family of essential integrin receptors in *C. elegans*. *J. Cell Biol.* **129,** 1127-1141.

Greenwald, I. (1997). In *C. elegans II* (ed. D.L. Riddle, T. Blumenthal, B.J. Meyer, and J.R. Priess), pp.519-541. Cold Spring Harbor Laboratory Press, Cold Spring Harbor, New York.

Hedgecock, E.M. and Herman, R.K. (1995). The *ncl-1* gene and genetic mosaics of *Caenorhabditis elegans*. *Genetics* **141,** 989-1006.

Figure 1. Unusual vulval phenotypes that may depend in part on *sqv-8*. Nomarski micrographs of mid- to late L4 vulvas in animals from a *sqv-8(mn63) unc-4(e120); dpy-17(e164) ncl-1(e1865) unc-36(e251); Ex[sqv-8; dpy-17; ncl-1; unc-36; pHS::GFP]* strain. See text for details.

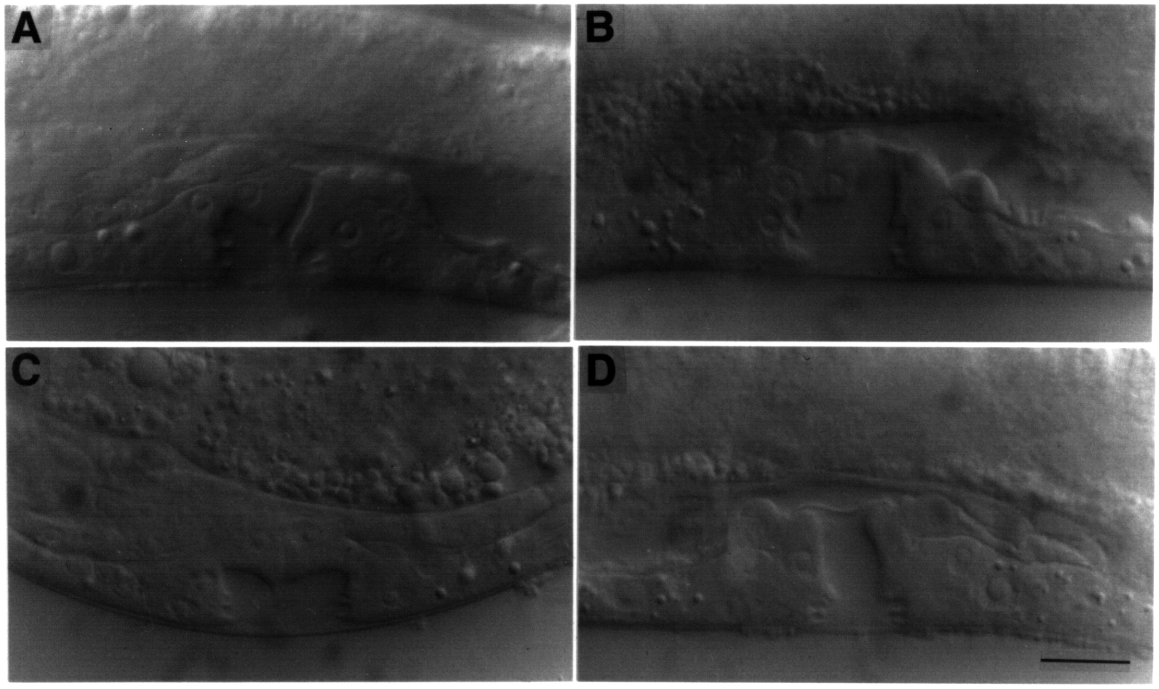
A
B
C
D

Figure 2. Adult *sqv-3* mutant males have abnormal tails. Nomarski micrographs of *unc-69(e587*am*); him-5(e1467*ts*)* (A, C) and *sqv-3(n2842) unc-69(e587*am*)* male tails (B, D). The tails of *sqv-3 unc-69* males appear crumpled and have stubbier rays than the tails of *unc-69* males. See text for details.

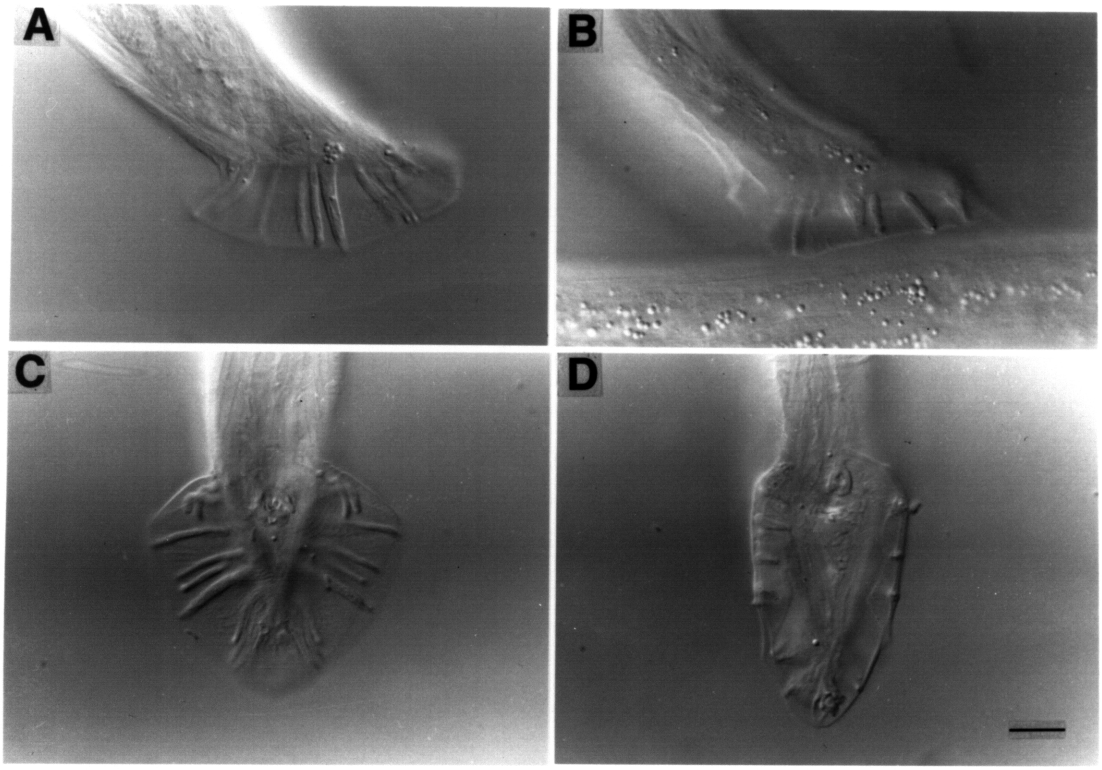
A
B
C
D

Figure 3. Tracings of the plasma and nuclear membranes of the vulval cells in an N2 (A to B) and a *sqv-3(n2842)* (C to E) animal of the early L4 stage. See text for details.

A

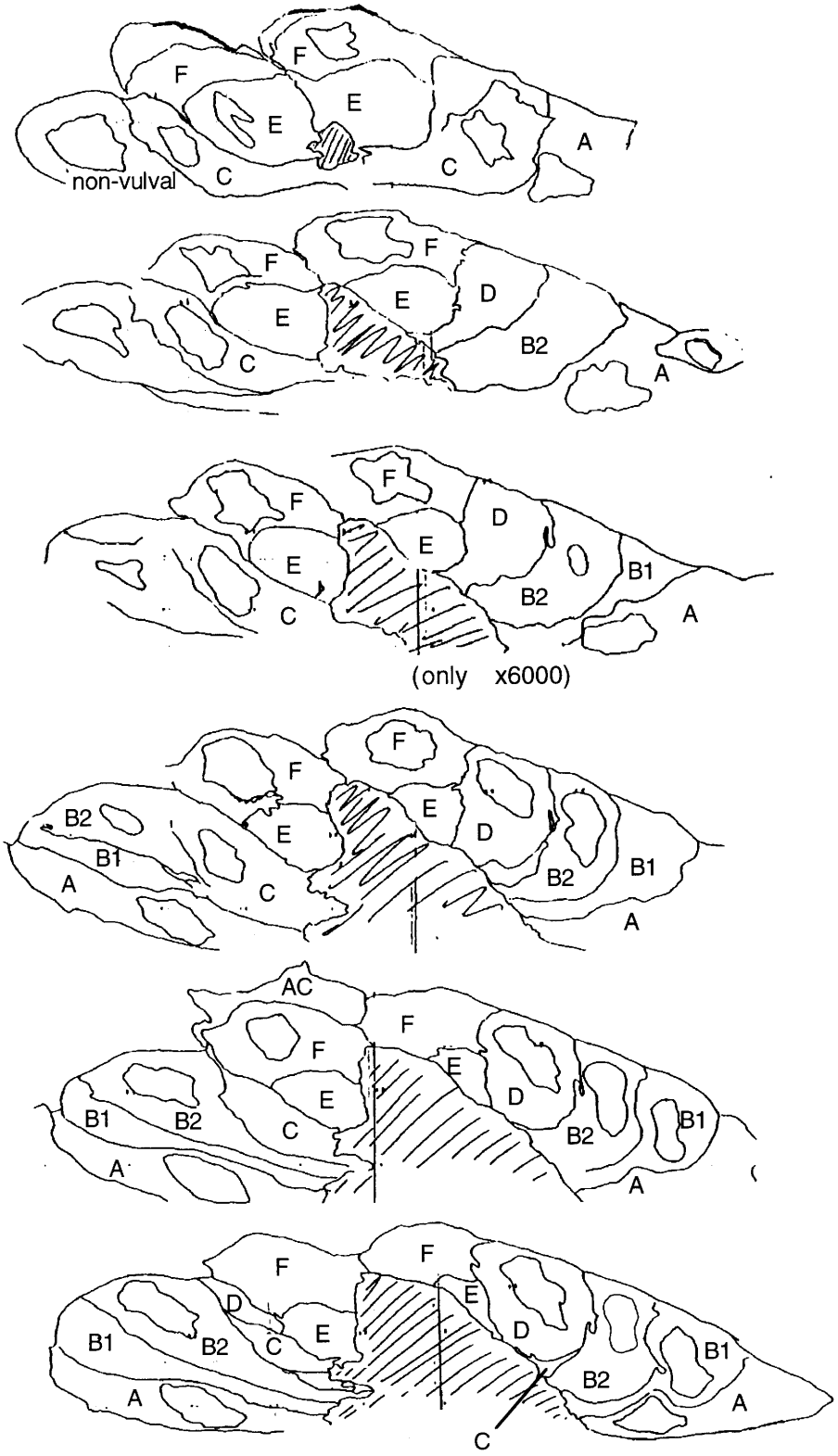
F
F
E
E
A
non-vulval
C
C
F
F
E
E
D
B2
C
A
F
F
D
E
E
B1
B2
C
A
(only x6000)
F
F
B2
E
E
D
B1
B2
B1
A
C
A
AC
F
F
E
E
D
B1
B2
C
B2
B1
A
A
F
F
D
E
E
D
B1
B1
B2
C
B2
A
A
C

B

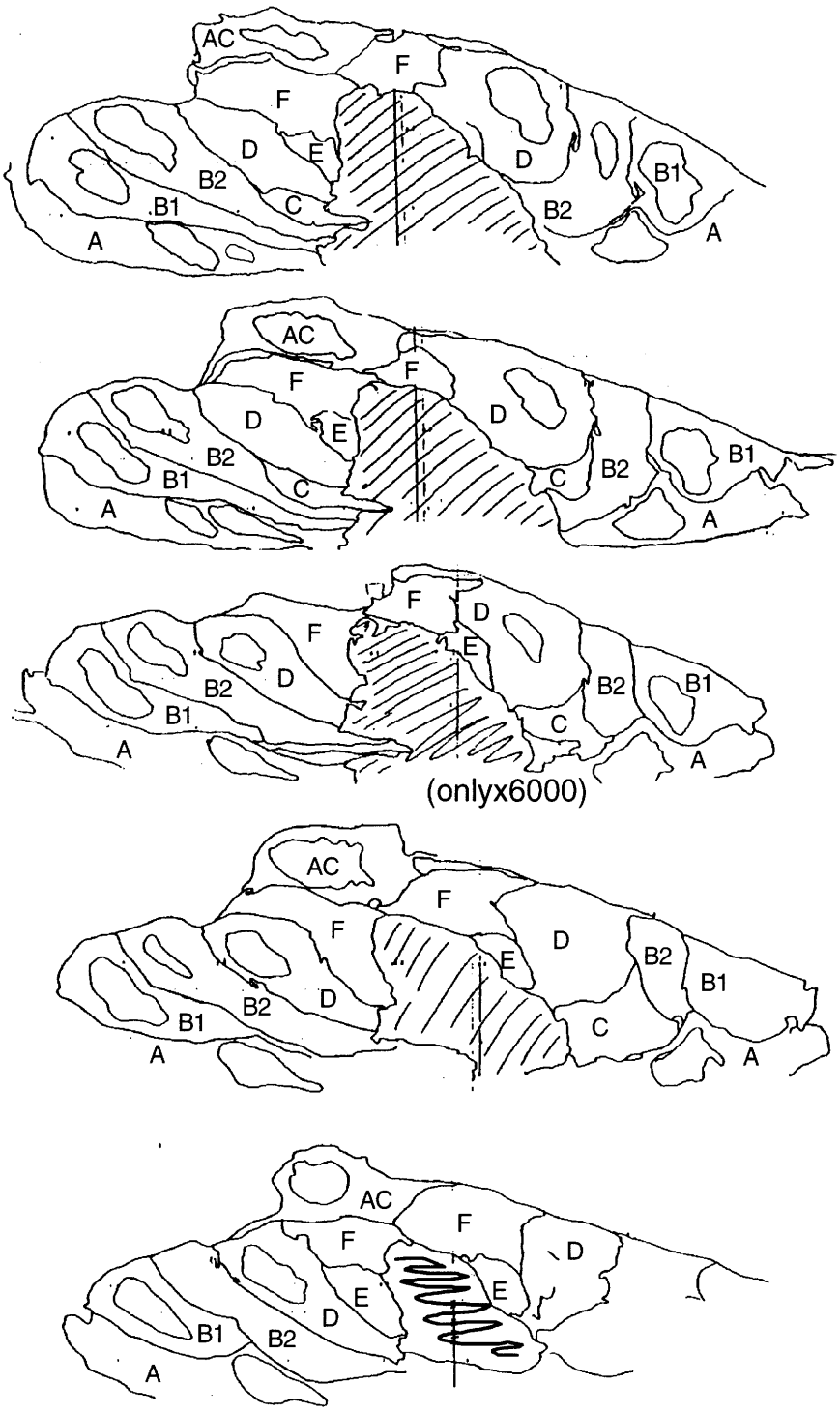
AC
F
F
D
E
B2
B1
C
A
D
B1
B2
A
AC
F
F
D
E
B2
B1
C
A
D
C
B2
B1
A
F
F
D
E
B2
D
B1
C
B2
B1
A
A
(onlyx6000)
AC
F
F
D
E
B2
B1
D
B2
B1
C
A
A
AC
F
F
D
E
E
D
B1
B2
A

C

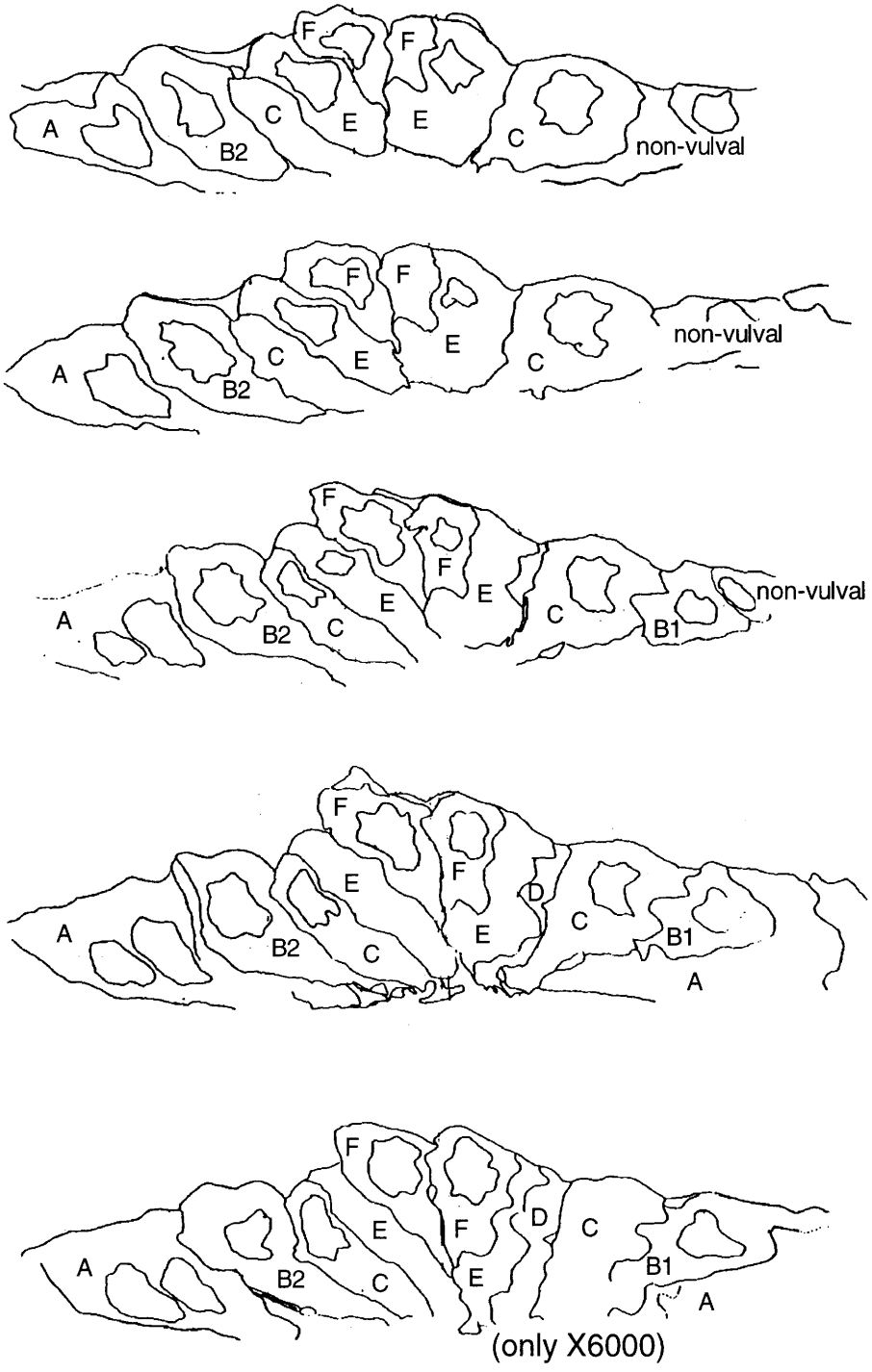
F
F
A
C
E
E
C
non-vulval
B2
F
F
A
C
E
E
C
non-vulval
B2
F
F
E
E
C
non-vulval
A
B2
C
B1
F
E
F
D
C
B1
A
B2
C
E
A
F
E
F
D
C
B1
A
B2
C
E
(only X6000)

D

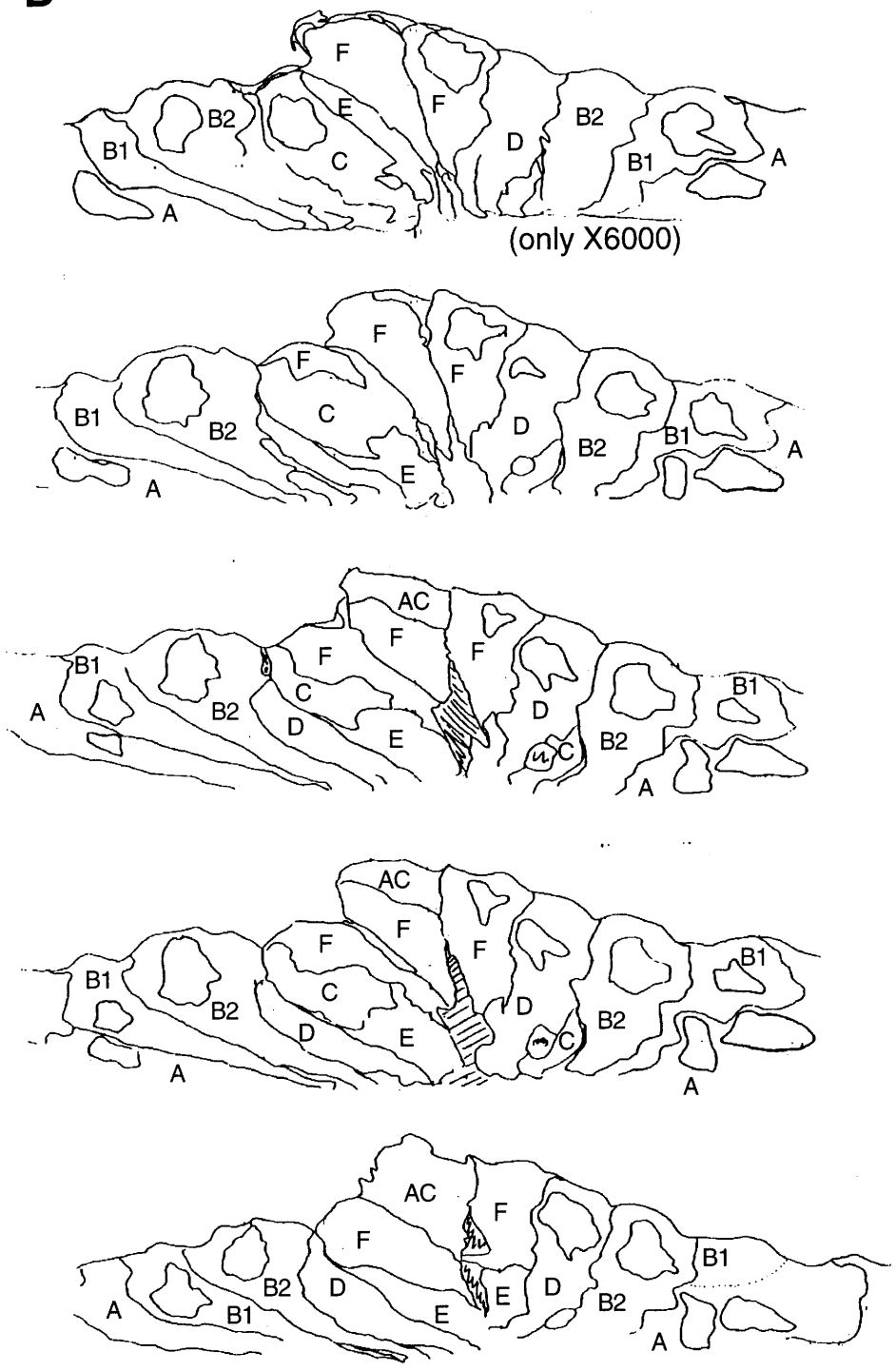
F
E
F
B2
B2
B1
C
D
B1
A
A
(only X6000)
F
F
F
B1
B2
C
D
B2
B1
A
A
E
AC
F
F
F
B1
B1
A
B2
C
D
D
E
C
B2
A
AC
F
F
F
B1
B1
C
B2
D
D
E
C
B2
A
A
AC
F
F
B1
B2
D
D
E
E
D
B2
A
A
B1

E

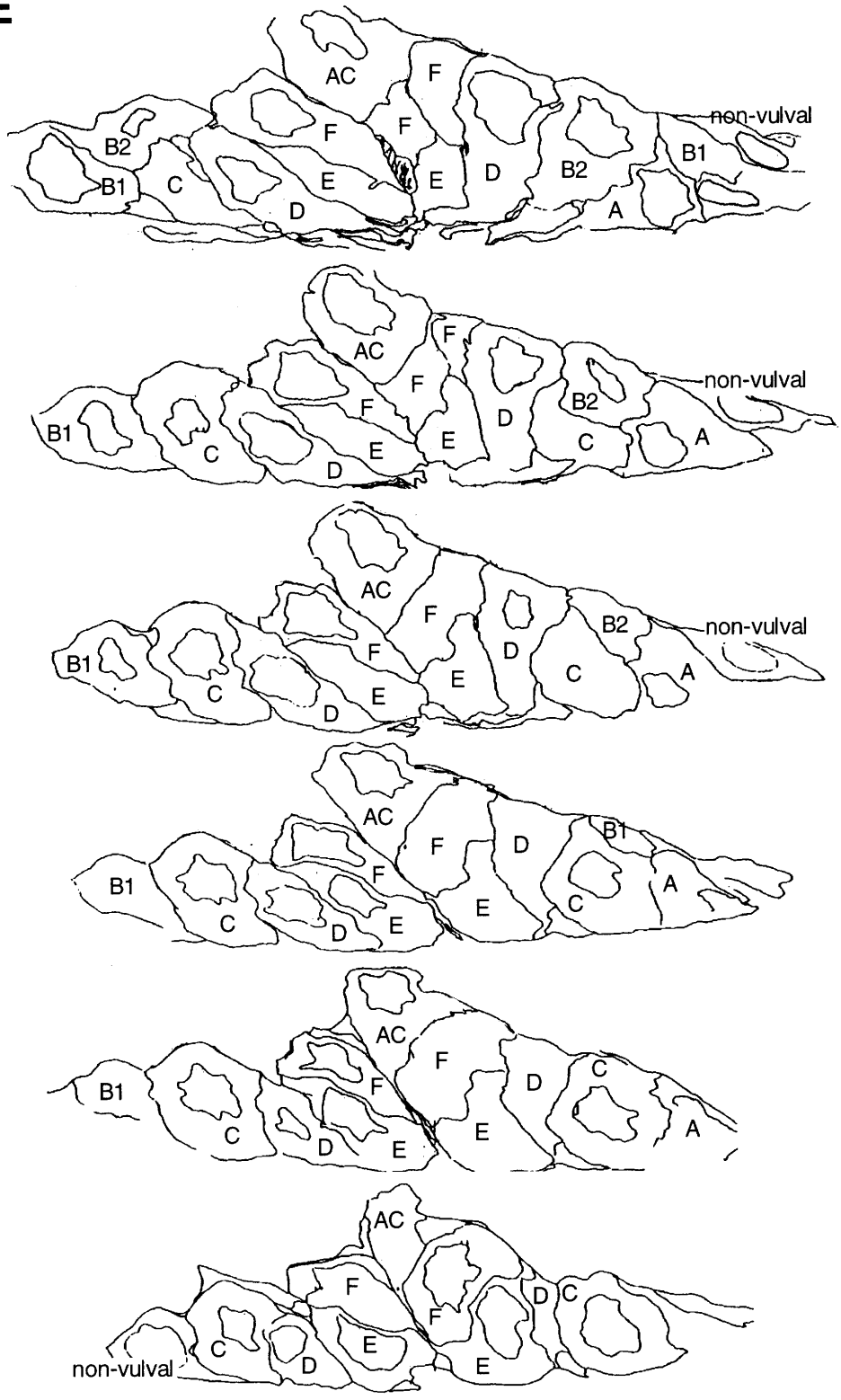
AC
F
F
F
B2
B1
C
E
E
D
D
B2
B1
A
non-vulval
AC
F
F
F
B1
C
D
E
E
D
B2
C
A
non-vulval
AC
F
F
D
B2
B1
C
D
E
E
C
A
non-vulval
AC
F
F
D
B1
B1
C
D
E
E
C
A
AC
F
F
D
C
B1
C
D
E
E
A
AC
F
F
D
C
C
D
E
E
non-vulval